

FINAL
CONTRACT REPORT
VTRC 09-CR8

**LIVE LOAD TEST
AND FAILURE ANALYSIS
FOR THE STEEL DECK TRUSS BRIDGE
OVER THE NEW RIVER
IN VIRGINIA**

LUCAS HICKEY
Graduate Research Engineer

CARIN ROBERTS-WOLLMANN, Ph.D., P.E.
Associate Professor

THOMAS COUSINS, Ph.D., P.E.
Professor

ELISA SOTELINO, Ph.D.
Professor

W. SAMUEL EASTERLING, Ph.D., P.E.
Professor

Via Department of Civil and Environmental Engineering
Virginia Polytechnic Institute & State University



Standard Title Page - Report on Federally Funded Project

1. Report No.: FHWA/VTRC 09-CR8	2. Government Accession No.:	3. Recipient's Catalog No.:	
4. Title and Subtitle: Live Load Test and Failure Analysis for the Steel Deck Truss Bridge Over the New River in Virginia		5. Report Date: May 2009	6. Performing Organization Code:
		8. Performing Organization Report No.: VTRC 09-CR8	
7. Author(s): Lucas Hickey, Carin Roberts-Wollmann, Thomas Cousins, Elisa Sotelino, and W. Samuel Easterling		10. Work Unit No. (TRAIS):	
9. Performing Organization and Address: Virginia Transportation Research Council 530 Edgemont Road Charlottesville, VA 22903		11. Contract or Grant No.: 87975	
		13. Type of Report and Period Covered: Final Contract	
12. Sponsoring Agencies' Name and Address: Virginia Department of Transportation Federal Highway Administration 1401 E. Broad Street 400 North 8th Street, Room 750 Richmond, VA 23219 Richmond, VA 23219-4825		14. Sponsoring Agency Code:	
15. Supplementary Notes: This project was financed with federal grant funds at an estimated cost of \$89,000.			
16. Abstract: <p>This report presents the methods used to model a steel deck truss bridge over the New River in Hillsville, Virginia. These methods were evaluated by comparing analytical results with data recorded from 14 members during live load testing. The research presented herein is part of a larger endeavor to understand the structural behavior and collapse mechanism of the erstwhile I-35W bridge in Minneapolis, Minnesota, that collapsed on August 1, 2007. Objectives accomplished toward this end include investigation of lacing effects on built-up member strain measurement, live load testing of a steel truss bridge, and evaluation of modeling techniques in comparison to recorded data. The most accurate model was used to conduct a failure analysis with the intent of then loading the steel truss bridge to failure.</p> <p>Before any live load testing could be performed, it was necessary to confirm an acceptable strain gage layout for measuring member strains. The effect of riveted lacing in built-up members was investigated by constructing a two-thirds mockup of a typical bridge member. The mockup was instrumented with strain gages and subjected to known loads to determine the most effective strain gage arrangement. The results of the testing analysis showed that for a built-up member consisting of laced channels, one strain gage installed on the middle of the extreme fiber of each channel's flanges was sufficient. Thus, laced members on the bridge were mounted with four strain gages each.</p> <p>Data from live loads were obtained by loading two trucks to 25 tons each. Trucks were positioned at eight locations on the bridge in four different relative truck positions. Data were recorded continuously and reduced to member forces for model validation comparisons. Deflections at selected truss nodes were also recorded for model validation purposes.</p> <p>The model validation process began by developing four simple truss models, each reflecting different expected restraint conditions, in the hopes of bracketing data from recorded results. The models included a simple truss model, a frame model with only the truss members, and a frame model that included the stringers. The final, most accurate model was selected and used for a failure analysis. This model showed where the minimum amount of load could be applied to learn about the bridge's failure behavior and was to be used for a test to be conducted at a later time. Unfortunately, the project was terminated because of a lack of funding before the actual test to failure of the steel truss bridge was conducted.</p> <p>Nevertheless, findings from the study led to two important recommendations:</p> <ol style="list-style-type: none"> 1. When instrumenting a steel truss bridge for load testing by placing strain gages on built-up members, four gages, one placed on each flange of each channel, should be used. 2. When modeling deck truss bridges, the system should be considered to be a frame and should include the stringers in the model. 			
17 Key Words: Steel deck truss bridge, live load tests, laced members		18. Distribution Statement: No restrictions. This document is available to the public through NTIS, Springfield, VA 22161.	
19. Security Classif. (of this report): Unclassified	20. Security Classif. (of this page): Unclassified	21. No. of Pages: 97	22. Price:

DISCLAIMER

The project that is the subject of this report was done under contract for the Virginia Department of Transportation, Virginia Transportation Research Council. The contents of this report reflect the views of the author(s), who is responsible for the facts and the accuracy of the data presented herein. The contents do not necessarily reflect the official views or policies of the Virginia Department of Transportation, the Commonwealth Transportation Board, or the Federal Highway Administration. This report does not constitute a standard, specification, or regulation. Any inclusion of manufacturer names, trade names, or trademarks is for identification purposes only and is not to be considered an endorsement.

Each contract report is peer reviewed and accepted for publication by Research Council staff with expertise in related technical areas. Final editing and proofreading of the report are performed by the contractor.

Copyright 2009 by the Commonwealth of Virginia.
All rights reserved.

ABSTRACT

This report presents the methods used to model a steel deck truss bridge over the New River in Hillsville, Virginia. These methods were evaluated by comparing analytical results with data recorded from 14 members during live load testing. The research presented herein is part of a larger endeavor to understand the structural behavior and collapse mechanism of the erstwhile I-35W bridge in Minneapolis, Minnesota, that collapsed on August 1, 2007. Objectives accomplished toward this end include investigation of lacing effects on built-up member strain measurement, live load testing of a steel truss bridge, and evaluation of modeling techniques in comparison to recorded data. The most accurate model was used to conduct a failure analysis with the intent of then loading the steel truss bridge to failure.

Before any live load testing could be performed, it was necessary to confirm an acceptable strain gage layout for measuring member strains. The effect of riveted lacing in built-up members was investigated by constructing a two-thirds mockup of a typical bridge member. The mockup was instrumented with strain gages and subjected to known loads to determine the most effective strain gage arrangement. The results of the testing analysis showed that for a built-up member consisting of laced channels, one strain gage installed on the middle of the extreme fiber of each channel's flanges was sufficient. Thus, laced members on the bridge were mounted with four strain gages each.

Data from live loads were obtained by loading two trucks to 25 tons each. Trucks were positioned at eight locations on the bridge in four different relative truck positions. Data were recorded continuously and reduced to member forces for model validation comparisons. Deflections at selected truss nodes were also recorded for model validation purposes.

The model validation process began by developing four simple truss models, each reflecting different expected restraint conditions, in the hopes of bracketing data from recorded results. The models included a simple truss model, a frame model with only the truss members, and a frame model that included the stringers. The final, most accurate model was selected and used for a failure analysis. This model showed where the minimum amount of load could be applied to learn about the bridge's failure behavior and was to be used for a test to be conducted at a later time. Unfortunately, the project was terminated because of a lack of funding before the actual test to failure of the steel truss bridge was conducted.

Nevertheless, findings from the study led to two important recommendations:

1. When instrumenting a steel truss bridge for load testing by placing strain gages on built-up members, four gages, one placed on each flange of each channel, should be used.
2. When modeling deck truss bridges, the system should be considered to be a frame and should include the stringers in the model.

FINAL CONTRACT REPORT

LIVE LOAD TEST AND FAILURE ANALYSIS FOR THE STEEL DECK TRUSS BRIDGE OVER THE NEW RIVER IN VIRGINIA

Lucas Hickey
Graduate Research Engineer

Carin Roberts-Wollmann, Ph.D., P.E.
Associate Professor

Thomas Cousins, Ph.D., P.E.
Professor

Elisa Sotelino, Ph.D.
Professor

W. Samuel Easterling, Ph.D., P.E.
Professor

**Via Department of Civil and Environmental Engineering
Virginia Polytechnic Institute & State University**

INTRODUCTION

On Wednesday, August 1, 2007, the I-35W bridge in Minneapolis, Minnesota, collapsed into the Mississippi River. The bridge was an eight-lane, arched deck truss bridge made of steel. It had opened in 1967 with a total length of 1,907 ft and a maximum span of 456 ft. Figure 1 shows the steel arch and concrete deck spanning the Mississippi. The collapse occurred while the bridge was carrying standard vehicular loads on a warm August afternoon. Steel deck truss bridges are abundant in the bridge inventories of almost all state departments of transportation; hence, it is important to understand the causes of this failure.

Virginia Route 100 crosses the New River between Pulaski and Hillsville. The bridge over the river is a steel deck truss bridge, constructed in 1941 with only two lanes. Its total length is 846 ft, 300 ft of which is spanned by the deck truss. Figure 2 shows the Hillsville truss. The Federal Highway Administration (FHWA) and the Virginia Department of Transportation (VDOT) believed that results from tests of this bridge would be useful for understanding the behavior of older steel deck truss bridges and would provide insight into the cause of the collapse of the I-35W bridge. The research presented herein is a concerted attempt to approximate mathematically the behavior of the Hillsdale Bridge under load so that a plan for a test to failure could be developed. This imposed failure was expected to provide valuable information to transportation authorities with regard to the evaluation and future design of steel deck truss bridges.



Figure 1. I-35W Truss



Figure 2. Hillsville Truss

PURPOSE AND SCOPE

The purpose of this study was to conduct a field test and detailed structural analysis of a steel truss bridge over the New River in Hillsville, Virginia, to allow a better understanding of the structural behavior and collapse mechanism of the I-35W Bridge in Minneapolis, Minnesota.

The results of the field test were used to calibrate structural models of the steel truss bridge. Once calibrated, the model was used to conduct a failure analysis. The objective was then to test the Hillsdale Bridge to failure; however, funding was not available and the research efforts were terminated. The scope of this report is limited to the field test results, model development and calibration, and failure analysis of the structural model.

To understand the bridge's behavior, the responses of the trusses to live load at various locations needed to be recorded and compared to mathematical models that could approximate the bridge's behavior. This was accomplished by parking loaded trucks of known weights and dimensions on the bridge and recording strains in selected members. The data obtained from live load testing were used to develop an accurate structural model. This model was then used to find the location and magnitude of load that must be applied to yield a truss member. All models investigated were two dimensional with linear-elastic constitutive laws. A non-linear, three-dimensional model was considered outside the scope of this research. Thus, the objectives of this research were the following:

1. Determine the best method to evaluate member forces in situ.
2. Perform live load tests and gather data.
3. Develop models for comparison to data.
4. Using the best model, determine the load and load position to cause failure.

METHODS

Laced Member Strain Gaging

Axial forces and nodal deflections were used to compare and evaluate structural models. In order to measure the axial force in a bridge member accurately, the average strain must be accurately determined. All the top chord, bottom chord, and diagonal members in the deck trusses are composed of built-up members. These are channel sections of known sizes and properties that are laced together, either singly or doubly, with bars of known size attached with hot rivets. As designed, the channels resist all axial forces while the lacing provides stability and maintains spacing between the channels. In reality, it is important to understand differences in strains read at lacing connection points compared to strains read between them.

Knowing which strain gage attachment location on the channels yields the most accurate average strain results is crucial to proper truss instrumentation and force calculation. To accomplish this objective, a two-thirds size mockup of a typical built-up section was tested in the Virginia Tech Structures Lab. It was built of two 4-ft sections of C8 by 13.75 channels doubly

laced at five spacings with bars measuring 2 in by $\frac{1}{4}$ in. The assembly was capped by welding a plate with the dimensions of 12 in by 16 in by $\frac{3}{4}$ in on each end.

Figure 3 presents the tested member and gage installation locations. The column was instrumented with an array of gages. One gage was installed at each web centroid at locations where bolts attached the lacing bars. At sections equidistant between the lacing connections, six gages were attached as shown in Figure 3, Sections A and C. Gages used in this setup were adhered to the steel with a cyanoacrylate adhesive. Gages used for live load testing in the field however, were welded to members, as this is a faster installation. Prior to gages being welded in the field, one was welded to the built-up column to confirm its accuracy. The column was then placed in a SATEC testing machine to apply load and monitor deflection.

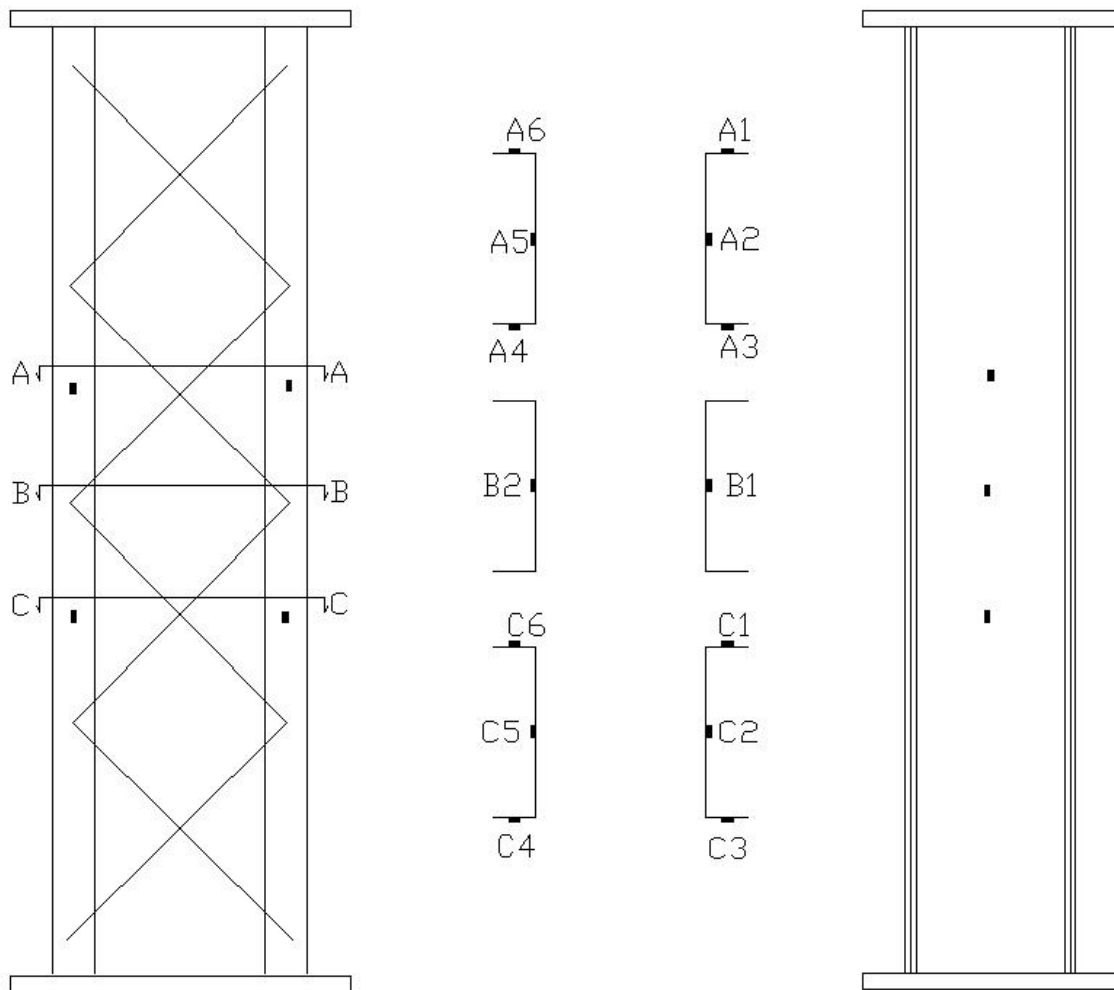


Figure 3. Column Gaging Diagram

Data gathered from column testing were used to investigate three issues associated with attaching strain gages to aging laced structural members:

1. The strain gages mounted to the webs of each section were compared to determine if lacing attachment points affected strain measurements.

2. The average strain value taken from the four flange gages in a section were compared to the average strain value of all six gages in a section to determine relative accuracies of the four flange gages to all six.
3. Both of these layouts were compared to the expected strain based on the SATEC load record to determine relative accuracies measured from the strain gages to expected values determined from the SATEC load cell.

Truss Instrumentation and Data Collection

The result of Item 1 in the preceding list was used to determine the necessary layout of strain gages to be used on each member. Once this was selected, the members to be monitored were chosen. Initial reports after the I-35W Bridge collapse indicated the second top chord truss connection out from the center pier was a crucial failure location. This was confirmed by a preliminary truss analysis. Thus, all members framing into Node U6 were selected for monitoring. On the truss designated “Far” (farther from the new replacement bridge, on the south/downstream side), seven members were instrumented with four strain gages each. Figure 4 presents a plan view of the old bridge and shows its position relative to its replacement structure. The New River and the bridge’s orientation between Pulaski and Hillsville are also shown.

Figure 5 shows the member instrumentation for the far truss; all highlighted members have four gages. On the truss designated “Near” (nearer to the new replacement bridge, on the north/upstream side), two members were instrumented with four gages each, and the remaining

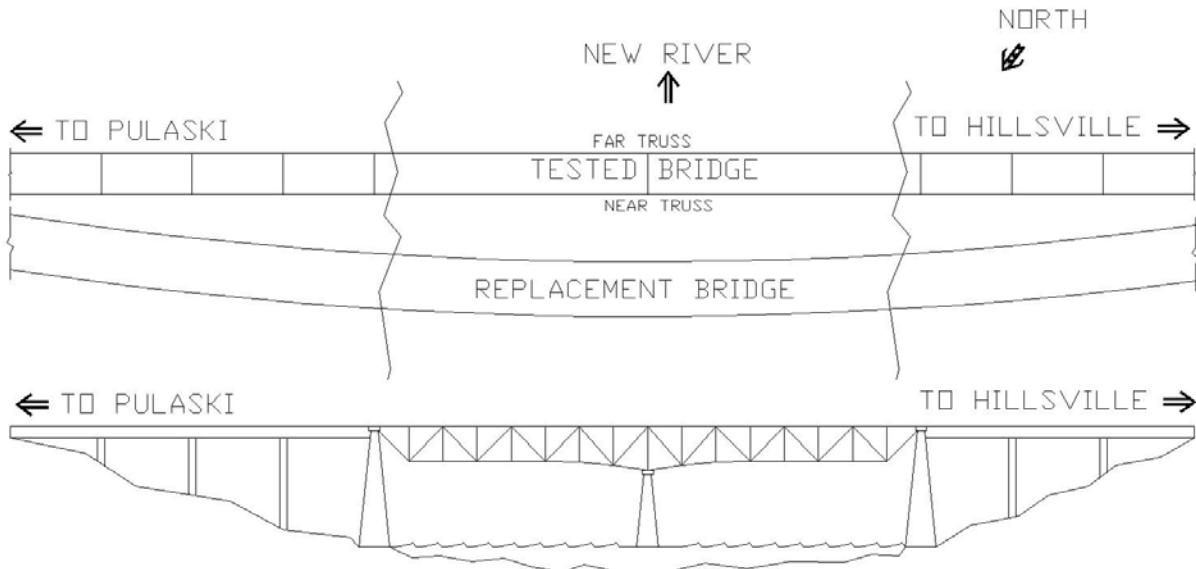


Figure 4. Plan and Profile View of Bridge

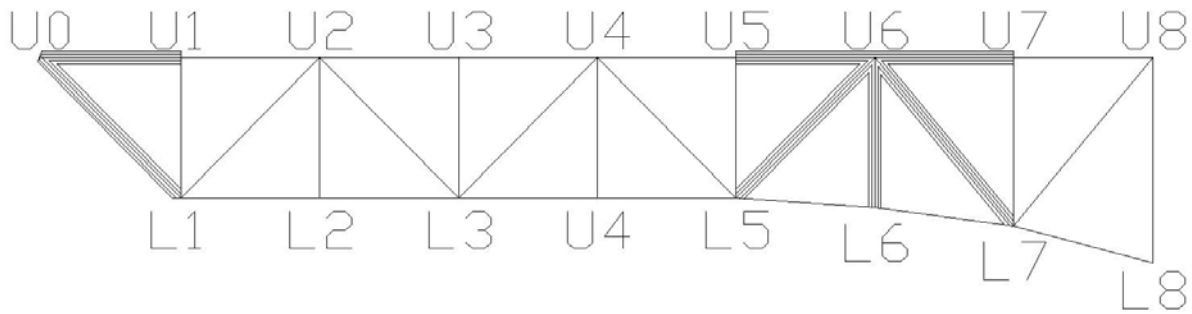


Figure 5. Instrumentation of Far Truss. All monitored members have 4 gages.

five members were instrumented with one gage each. Figure 6 shows the member instrumentation for the near truss. Boldly highlighted members have four gages each; faintly highlighted members have only one gage each. This was done to save time on gage installation but still provide rough data on the second truss for comparison. On each truss, only members on the Pulaski side of the central pier were instrumented. The assumption of perfect structural symmetry between the Pulaski and Hillsville truss halves was made. Models used to reflect bridge behavior were developed as complete, two-span trusses.

Deflectometers, referred to as twangers, were used to measure vertical deflection at Nodes L1 and L6 on each truss as well. These were calibrated at the Virginia Tech Structures Lab and were installed on the day of testing. Figure 7 shows the installation locations for twangers on both trusses.

After instrumentation, two trucks of known weights and dimensions were used to impose live load on the bridge. Four load regimes were imposed on the bridge, each moved incrementally from Nodes U1 to U8. The first regime was one truck traveling down the center; the second was one truck traveling down the left (far truss) lane; the third was two trucks side by side; and the fourth was two trucks rear to rear traveling down the left lane. Figures 8 and 9 illustrate the four load regimes.

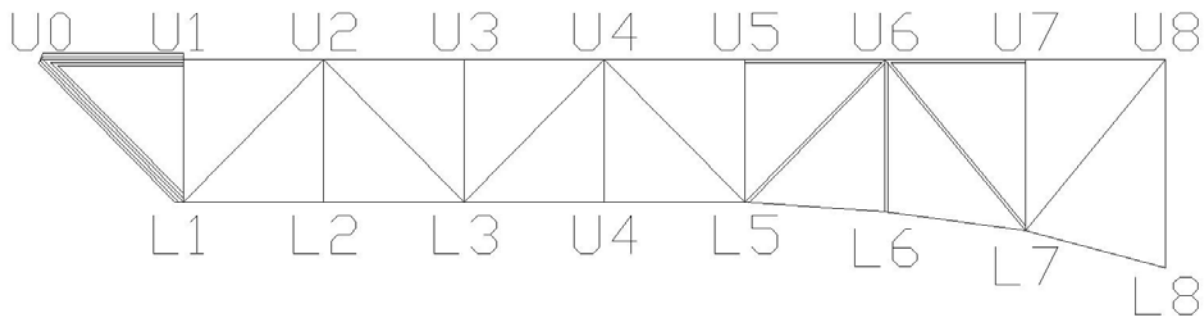


Figure 6. Instrumentation of Near Truss. Only end members have 4 gages.

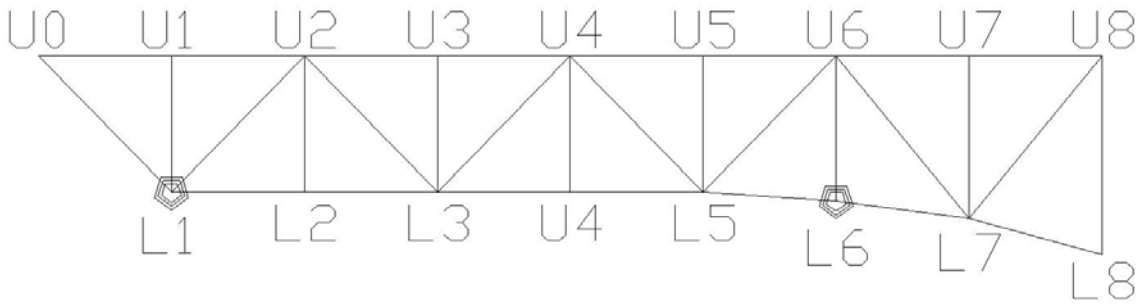


Figure 7. Twanger Installation on Near and Far Trusses

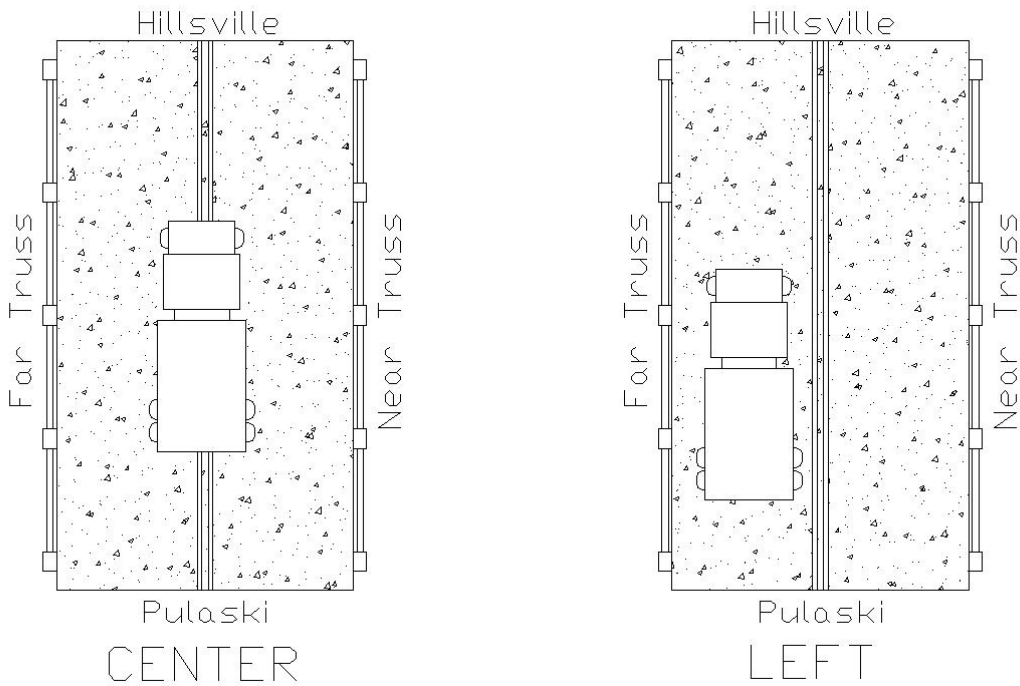


Figure 8. Center and Left Load Regimes

Gage Installation

Trusses were instrumented by spot welding gages to members of interest. An articulated arm “Snooper” truck was used to access the truss members. Gages were placed parallel to each member’s long axis in the center of the flanges. First, the location was sanded clean of paint and mill scale with an electric belt grinder. The sanded patches were then cleaned with alcohol. Gages were welded to the member and sealed against the weather (moisture) with waterproof butyl rubber and aluminum tape. Terminal blocks were installed with epoxy near the gages to install wiring. After wiring on the day of testing, the terminal blocks were sealed with butyl rubber and tape as well.

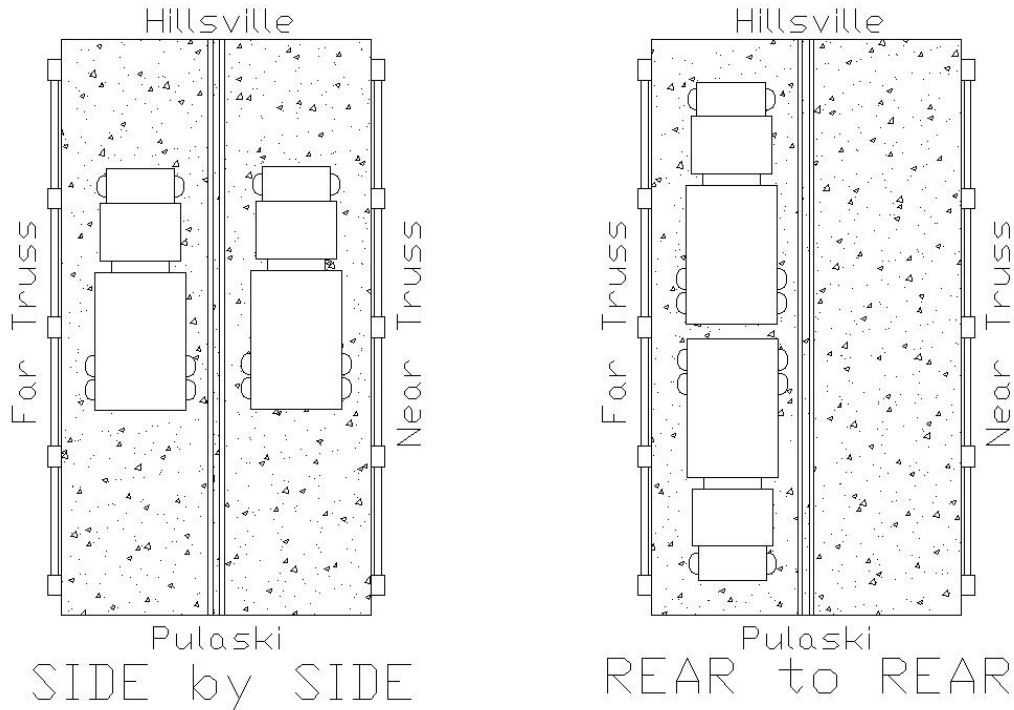


Figure 9. Side by Side and Rear to Rear Load Regimes

Data Collection Scheme

To begin a test, the trucks were moved completely off of the bridge. Then the data acquisitions system (DAS) was initiated at one sample per second per channel. Then the trucks were driven into their first position, typically above Node U1. The trucks' rear axles were positioned as directly above truss nodes as possible. Trucks were stationed at each load position for approximately 30 sec to allow enough data to be recorded to calculate a useful average strain. Strains were recorded to two decimal places of microstrain, and deflections were recorded to thousandths of an inch. The computer was powered by a grounded generator without power conditioning. This was tested at the Virginia Tech Structures Lab, and the difference between generator power and outlet power was negligible, within the gage's electronic noise range. One DAS file was recorded for each of the four load regimes. At each load position, truck axle locations relative to bridge and node centerlines were recorded for purposes of load distribution in the models.

Data Reduction Scheme

Proper identification of gage members and locations was necessary to calculate average strains at the load stages. Gage B on Member U0-U1 on the near truss malfunctioned because of damage at the terminal block and could not be used. The gage on Member U6-U5 on the near truss malfunctioned because of an unknown cause and could not be replaced. As a consequence, no data were available for this member on the near truss in any of the tests. Gage C on Member U0-U1 on the far truss was successfully balanced and zeroed but was reading strains approximately 10 times the amount expected. The suspected cause of this malfunction was

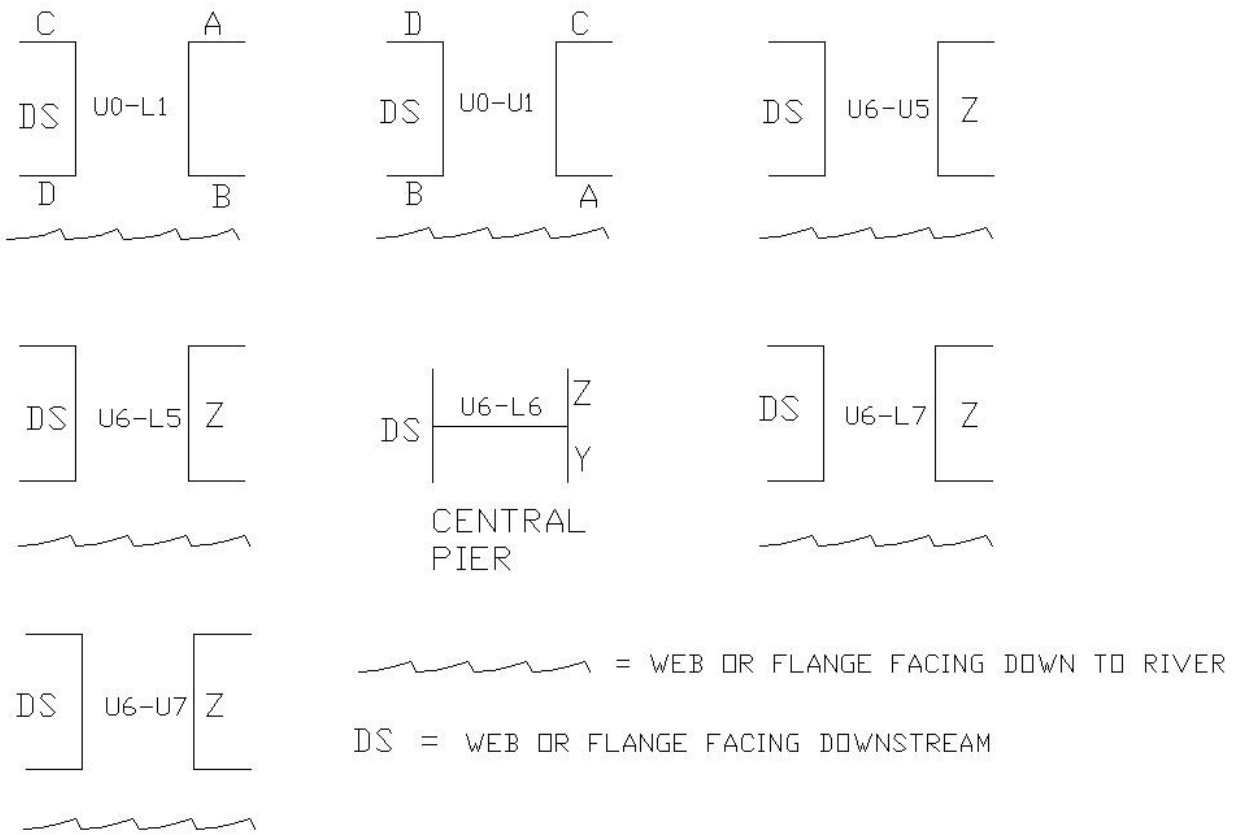


Figure 11. Gage Designations for Members on Near Truss

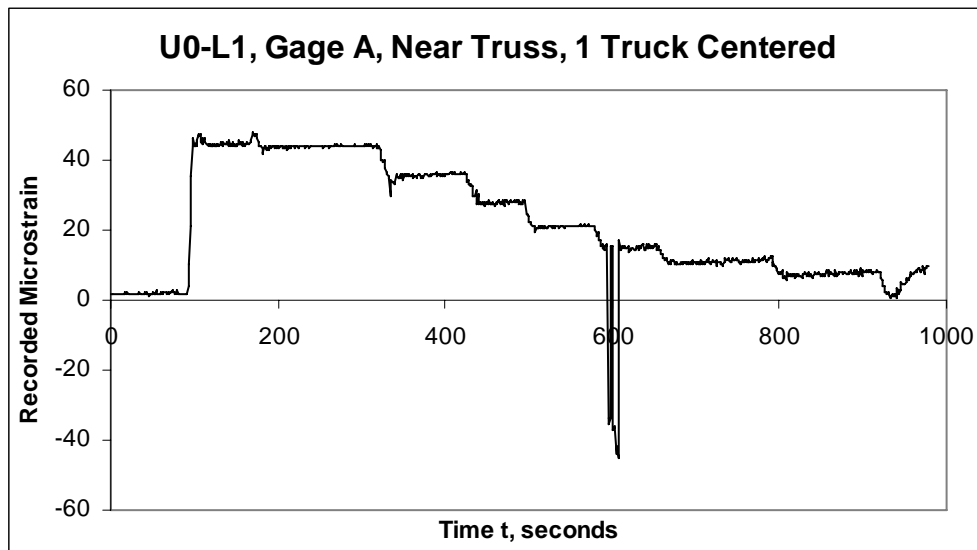


Figure 12. Full Strain Record in Gage A of U0-L1 on Near Truss, Single Centered Truck

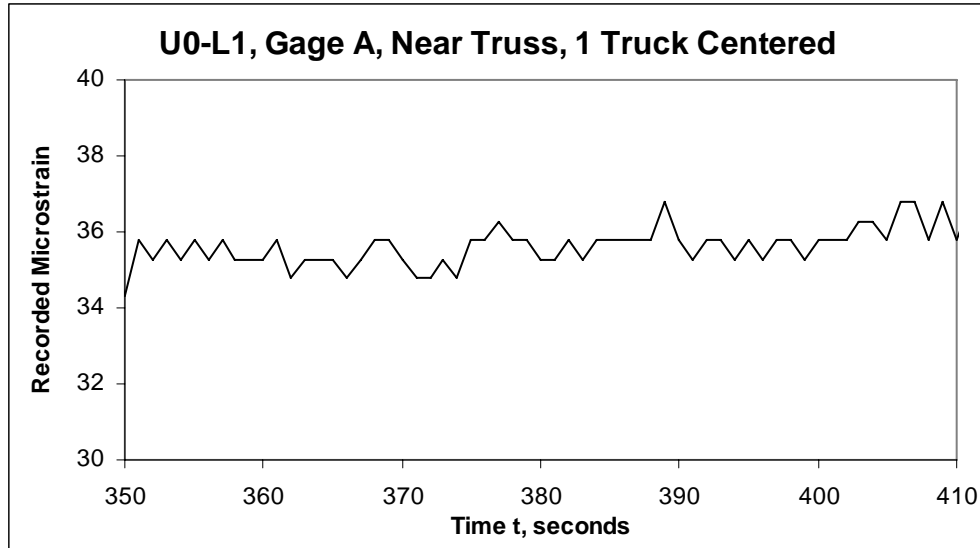


Figure 13. Third Load Position Enhanced

All channels in each load regime were inspected for plateau alignment so overall load position intervals could be determined. These intervals identify uniform start and stop times for all channels within one data file for a load regime. It is these data in these intervals that were used to calculate strains in the members for each load position. The lengths of the intervals were maximized in order to maximize the sample size on the plateau of data. Table 1 identifies the intervals used for each load position in each load regime. These same intervals were used to calculate average deflections recorded during the load position by the twangers.

Table 1. Data Intervals Per Load Regime and Load Position

Load Position	Center		Left		Side by Side		Rear to Rear	
	Start	Stop	Start	Stop	Start	Stop	Start	Stop
U1	120	160	35	65	160	190	55	95
U2	210	280	80	115	220	270	140	200
U3	370	410	135	180	300	320	290	340
U4	450	490	220	260	340	400	390	440
U5	520	560	290	330	600	620	480	510
U6	610	650	365	410	650	680	540	600
U7	710	770	450	500	730	770	660	710
U8	820	870	530	590	810	870	770	850

Member Force Calculations

Within the data intervals, the average strain in each channel for each load position during each load regime was calculated as the arithmetic mean. The accuracy of this method was confirmed by calculating the coefficient of variance, δ , as well. Typically, the values of δ were satisfactorily small, except when the calculated mean was near zero. The average strain in each member was calculated as the arithmetic mean of the strains in all the gages installed on that member. Nodal deflections were calculated in the same manner.

The simplest method of comparison between computer models and actual data was determined to be the difference of axial forces in each member. These data are easy to extract

from programs such as ANSYS, which was used for this analysis. Therefore, the average strains in the data recorded from live load testing were transformed into the member axial forces. These axial member forces were calculated as the member's cross-sectional area multiplied by Young's modulus of elasticity for steel (29,000 ksi was used for this research) multiplied by the average member strain. Table 2 presents the shape designations and cross sectional areas of the instrumented members.

Theoretically, bending moments could be calculated from the different strains on each side of a member's bending axis. Analysis of data from column testing was inconclusive, and these moments were ignored to simplify analysis. Although averaging strains of gages in a plane is accurate for approximating axial strain, the individual strains read in each flange were too variable to be indicative of significant bending moments. This could be attributed to initial warping of channel elements or load not being applied in an ideally concentric orientation. Tables 3 through 6 summarize the average axial forces calculated in each member for all four load regimes.

Table 2. Member Cross-Sectional Areas from Plans

Member	Shape	Area, in ²
U0-U1	2 x 12 in x 20.7# Channels	12.16
U0-L1	2 x 12 in x 30# Channels	17.62
U6-U5	2 x 12 in x 25# Channels	14.68
U6-L5	2 x 12 in x 35# Channels	20.60
U6-L6	10 in x 8 in x 41# I Section	12.07
U6-L7	2 x 15 in x 40# Channels	23.60
U6-U7	2 x 12 in x 40# Channels	23.60

Table 3. Average Member Forces with Truck Centered

	Member	CENTER Average Member Force @ Load Position [kips]							
		1	2	3	4	5	6	7	8
Near	U0-L1	19.22	17.89	14.11	10.52	7.77	5.45	4.36	3.03
	U0-U1	-5.91	-6.34	-4.55	-3.80	-2.96	-1.96	-0.96	0.19
	U6-L5	5.17	9.48	13.55	17.84	15.02	0.54	-2.10	-0.33
	U6-L6	0.07	0.02	0.14	0.57	1.07	1.69	0.86	0.50
	U6-L7	-5.45	-9.35	-12.74	-17.38	-20.98	-15.73	-0.59	2.49
	U6-U7	2.87	4.78	6.46	7.47	6.41	3.45	-0.77	-1.51
	U6-U5	5.17	9.48	13.55	17.84	15.02	0.54	-2.10	-0.33
Far	U0-L1	19.22	18.46	13.79	9.98	7.09	3.79	0.75	-0.27
	U0-U1	-4.27	-4.28	-3.76	-3.20	-2.64	-2.25	-1.84	-1.04
	U6-U5	-1.78	-3.04	-4.90	-7.38	-7.78	-4.44	-2.58	-2.15
	U6-L5	5.27	10.29	14.52	19.03	15.48	0.02	-1.27	0.33
	U6-L6	0.46	0.67	0.80	0.91	1.16	1.07	1.37	1.12
	U6-L7	-4.24	-8.59	-12.89	-16.43	-21.08	-17.51	-1.63	0.83
	U6-U7	1.73	3.80	5.37	6.97	6.33	2.21	-2.27	-2.75

Table 4. Average Member Forces with Truck in Left Lane

Member		LEFT Average Member Force @ Load Position [kips]							
ID		1	2	3	4	5	6	7	8
Near	U0-L1	-2.28	0.54	1.04	-0.36	-2.05	-3.51	-4.18	-4.51
	U0-U1	1.29	0.05	-0.30	0.37	0.84	1.23	1.61	2.35
	U6-L5	-13.84	-13.17	-10.41	-7.96	-5.62	-7.65	-14.58	-16.80
	U6-L6	0.00	0.01	0.10	0.57	0.99	1.77	2.30	1.42
	U6-L7	13.86	13.48	11.53	9.23	6.90	5.35	8.12	15.69
	U6-U7	-5.82	-5.65	-4.59	-3.68	-3.18	-3.83	-5.56	-7.73
Far	U0-L1	8.61	18.10	14.81	7.27	1.11	-3.89	-7.89	-10.59
	U0-U1	1.36	-1.98	-2.64	-0.55	0.35	0.93	1.48	2.34
	U6-U5	5.44	5.13	3.48	1.37	-2.25	-2.35	3.32	5.81
	U6-L5	-14.96	-11.89	-5.10	1.18	8.31	3.16	-20.47	-21.37
	U6-L6	0.23	0.28	0.37	0.42	0.55	0.53	0.20	0.86
	U6-L7	14.91	11.92	5.45	-0.40	-6.49	-14.00	-10.33	16.06
	U6-U7	-5.48	-3.57	-0.71	2.07	4.59	3.61	0.05	-5.88

Table 5. Average Member Forces with Trucks Side by Side

Member		SbS Average Member Force @ Load Position [kips]							
ID		1	2	3	4	5	6	7	8
Near	U0-L1	28.71	38.16	36.31	35.89	13.65	8.75	6.03	3.76
	U0-U1	-8.08	-11.93	-13.41	-13.60	-6.21	-4.58	-2.71	-0.73
	U6-L5	6.86	9.76	15.06	17.27	30.28	1.21	-2.61	0.11
	U6-L6	0.69	0.78	0.78	0.88	2.38	3.46	2.37	1.39
	U6-L7	-5.28	-6.86	-11.53	-13.43	-40.61	-32.16	-2.10	3.21
	U6-U7	3.37	4.60	7.19	8.11	13.57	8.26	0.24	-0.52
Far	U0-L1	13.07	41.11	41.74	39.29	12.94	7.97	5.04	2.96
	U0-U1	-2.69	-7.13	-7.25	-7.19	-1.33	-0.49	1.12	2.84
	U6-U5	2.40	1.71	0.96	-0.11	-8.20	-0.67	3.89	6.04
	U6-L5	4.04	11.52	15.01	20.31	31.55	-0.09	-2.81	0.10
	U6-L6	1.19	1.31	1.43	1.55	2.41	2.05	2.44	1.72
	U6-L7	-4.40	-11.22	-14.97	-19.87	-47.83	-41.79	-6.12	-1.16
	U6-U7	5.89	9.30	10.59	13.31	20.46	14.35	6.67	7.54

Table 6. Average Member Forces with Trucks Rear to Rear

Member		R2R Average Member Force @ Load Position [kips]							
ID		1	2	3	4	5	6	7	8
Near	U0-L1	6.95	13.10	16.81	12.67	10.57	7.94	3.49	0.26
	U0-U1	-2.62	-4.45	-6.51	-5.20	-4.60	-3.85	-2.68	-1.29
	U6-L5	-8.15	-6.97	-0.53	5.57	7.47	10.71	7.58	-4.77
	U6-L6	-0.46	-0.35	-0.20	0.14	0.59	0.94	2.17	2.88
	U6-L7	7.86	7.15	2.49	-3.77	-7.21	-9.83	-12.43	-6.95
	U6-U7	-2.68	-2.09	0.88	3.63	3.91	5.26	4.38	0.81
	Far	U0-L1	16.64	31.03	36.51	25.97	21.10	15.18	6.35
U0-U1		-4.37	-5.21	-7.37	-4.92	-4.07	-2.23	-0.61	0.63
U6-U5		7.28	7.26	5.28	1.50	-0.87	-2.76	-2.81	3.48
U6-L5		-16.86	-14.16	-2.36	10.05	13.72	19.59	10.51	-17.28
U6-L6		0.13	0.20	0.51	0.70	0.78	0.73	0.61	0.65
U6-L7		16.23	13.33	2.35	-8.81	-14.82	-20.39	-31.07	-22.82
U6-U7		-5.95	-4.17	1.49	7.41	9.45	12.33	12.68	5.67

Raw Deflection Data

Although twanger devices were installed at Nodes L1 and L6 on each truss, only data on the near truss were able to be used. All twangers were tested and calibrated the night prior to installation, but the twangers on the far truss did not yield any data outside of their electronic noise ranges. There was likely damage incurred or moisture infiltration along their lead wires during installation. The same data sampling intervals used to calculate the mean member strains were used to calculate the mean nodal deflections. Average vertical nodal deflections at each load position during each load interval were calculated from continuous data in the same way as member strains were. Tables 7 through 10 present these mean deflections.

Table 7. Average Nodal Deflections, Truck Centered

Node		CENTER Average Vertical Node Deflection @ Load Stage [in.]							
ID		1	2	3	4	5	6	7	8
Near	L1	-0.033	-0.049	-0.042	-0.042	-0.034	-0.024	-0.017	-0.004
	L6	-0.017	-0.037	-0.050	-0.056	-0.062	-0.059	-0.035	-0.013

Table 8. Average Nodal Deflections, Truck in Left Lane

Node		LEFT Average Vertical Node Deflection @ Load Stage [in.]							
ID		1	2	3	4	5	6	7	8
Near	L1	0.021	0.010	-0.002	-0.006	-0.003	0.004	0.015	0.023
	L6	0.038	0.035	0.024	0.012	0.002	0.001	0.009	0.026

Table 9. Average Nodal Deflections, Trucks Side by Side

Node		SbS Average Vertical Node Deflection @ Load Stage [in.]							
ID		1	2	3	4	5	6	7	8
Near	L1	-0.050	-0.076	-0.092	-0.097	-0.064	-0.046	-0.023	-0.006
	L6	-0.028	-0.043	-0.056	-0.068	-0.120	-0.106	-0.056	-0.011

Table 10. Average Nodal Deflections, Trucks Rear to Rear

Node		R2R Average Vertical Node Deflection @ Load Stage [in.]							
ID		1	2	3	4	5	6	7	8
Near	L1	-0.002	-0.015	-0.042	-0.041	-0.040	-0.037	-0.027	-0.002
	L6	0.025	0.020	-0.007	-0.028	-0.035	-0.047	-0.055	-0.044

Summary

The data contained in the preceding eight tables were used to evaluate the structural models. Analytical data were compared to these recorded “actual” values. Center and side by side load regimes exhibit symmetry in the data between the trusses, as there is relatively equal load distributed to each side.

Data Analysis and Model Validation

The continuously recorded data were organized into discreet data points measuring structural response. Using strain data provided by the gages and section properties from bridge plans and inspection, member forces were calculated at all eight load positions for each of the four load regimes. It is these data that the structural models were compared against.

It was not expected that the data recorded would match an idealized model perfectly. Although designed as a truss, most connections have large, rigid gusset plates that prevent some rotation (ideal truss connections may freely rotate). Differences in conditions of connection, restraint, and material properties also affect the model's validity. For this reason, four different models were created in order to determine the best modeling techniques. The first model had a pin at the middle support, and rollers on the right and left ends. The second model's supports, from left to right, were pin-roller-roller. The supports of the third model were roller-roller-pin. All supports in the fourth model were pins. All restraints were assumed to be able to freely rotate (no bearing seizure) based on inspection at the site. Table 11 summarizes these conditions and Figure 14 illustrates the models.

Since the truss models proved inaccurate, even with the four restraint options, other changes were implemented to improve results. Because greater truss stiffness was observed in node deflections, the truss was modeled as a frame instead, possessing rigid joints and members that experience bending, not just axial forces. Another modification was the inclusion of the steel stringers and floor beams that support the deck. The deck's resistance was not included in any models, as inspection revealed substantial cracking across the deck. All models were two dimensional trusses, with truck loads apportioned at nodes according to statics.

Table 11. Model Restraint Conditions

Model ID	Left Support	Middle Support	Right Support
M	Roller	Pin	Roller
L	Pin	Pin	Roller
R	Roller	Pin	Pin
A	Pin	Pin	Pin

Truss Model

The first structural model whose response was compared to the recorded data was a simple truss. Only the actual truss members from the plans were included, stringers, floor beams, and bracing were omitted. The deck was neglected as well. The included members could resist load and deflect only along their long axes and loads could be applied only at their end nodes. ANSYS input consisted of node locations and member areas determined from the bridge plans. All elements were 2D spars. Free rotations were permitted at nodes. Four models were prepared as described previously. These models were identical except for their support conditions.

Model designations M, L, R, and A correspond to the location of resistance to translation along the bridge's longitudinal axis. These designations are summarized in Table 11. Truck loads were first apportioned to the near and far trusses by statics, treating the deck as a simply

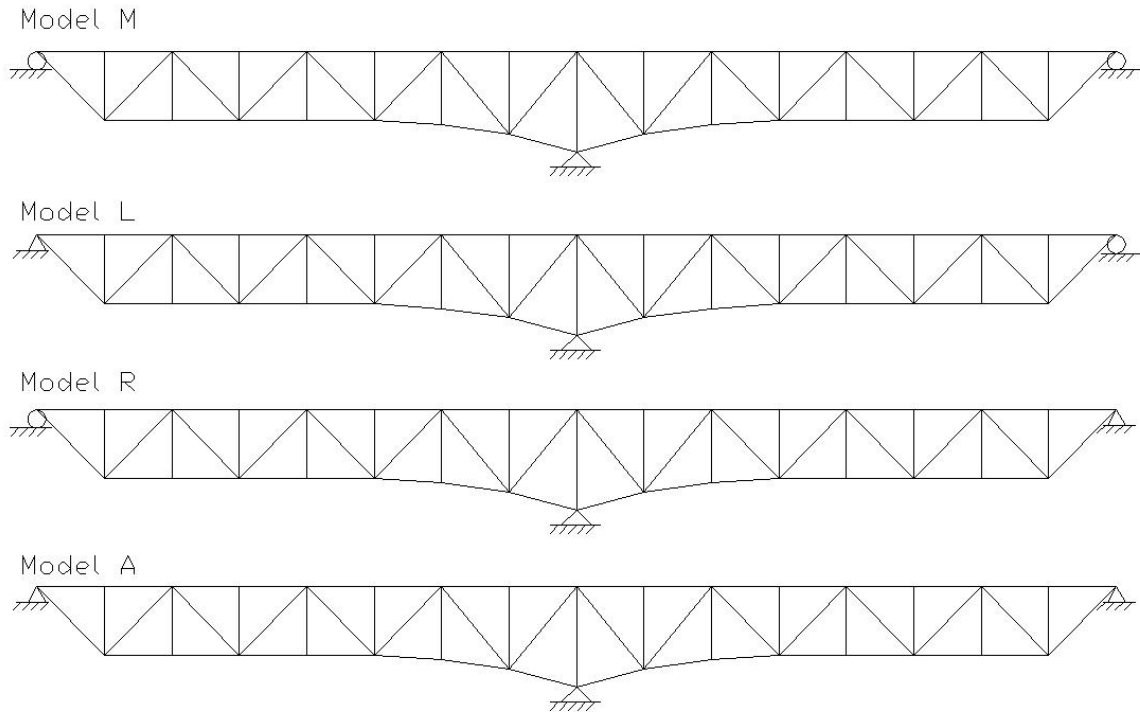


Figure 14. Truss Models

supported beam. Rear axle loads were assumed to act directly at the nodes over which the trucks were parked. Front axle loads were apportioned to two nodes at the ends of the member on which the truck was parked, treating the deck also as a simply supported beam.

These loads were input into the models created in ANSYS and the response of each truss was recorded. Deflections at Nodes L1 and L6 were used for comparison, as well as axial forces in the members whose strains were recorded during live load testing.

Frame Model

Initial results from the simple truss model were unsatisfactory for all tested restraint conditions. Since the truss was observed to be stiffer than expected according to deflections, the model was modified to act as a frame. Only the actual truss members from the plans were included, the stringers, floor beams, and bracing were omitted again. The deck was neglected as well. All elements were 2D beams. The included members could resist axial forces and bending moments. Built-up member moments of inertia were calculated using the parallel axis theorem, geometric section properties, and back to back distances listed in the plans. Loads were still only applied at member end nodes. No rotations were permitted between members, as almost all the connections on the truss contain stout gusset plates. Four models were prepared as described previously. Truck loads were first apportioned to the near and far trusses by statics, treating the deck as a simply supported beam. Rear axle loads were assumed to act directly at the nodes at which the trucks were parked. Front axle loads were apportioned to two nodes at the ends of the member on which the truck was parked, treating the deck also as a simply supported beam.

Frame Model Including Floor Beams and Stringers

The frame model was an improvement on the truss but further refinement was needed. The third structural model tested against the recorded data was a frame that included the resistance from the steel floor beams and stringers that support the concrete deck. Again, all elements were 2D beams. Stringers support the deck directly and the floor beams support the stringers, spanning between the two main trusses. The deck is supported by six evenly spaced stringers. Figure 15 presents a cross section of the bridge and the orientations of the floor beams and stringers.

To include these in the analysis, three stringers were apportioned to each truss. The section parameters were entered as one member having area and moment of inertia values exactly three times that of a single specified stringer. The stringers were entered as rigid vertical links separating the floor beams from the truss members. The deck itself was still excluded, as it was substantially cracked and weakened. The included members could resist axial load and bending moments. Rear axle loads were applied at member end nodes. No rotations were permitted between members, as almost all the connections on the truss contain stout gusset plates. Four models were prepared as described previously. Truck loads were first apportioned to the near and far trusses by statics, treating the deck as a beam whose ends were fixed. Rear axle loads were assumed to act directly at the nodes at which the trucks were parked. Front axle loads were treated as point loads within the span of the floor beams they acted upon. Figure 16 presents the new models including the extra members.

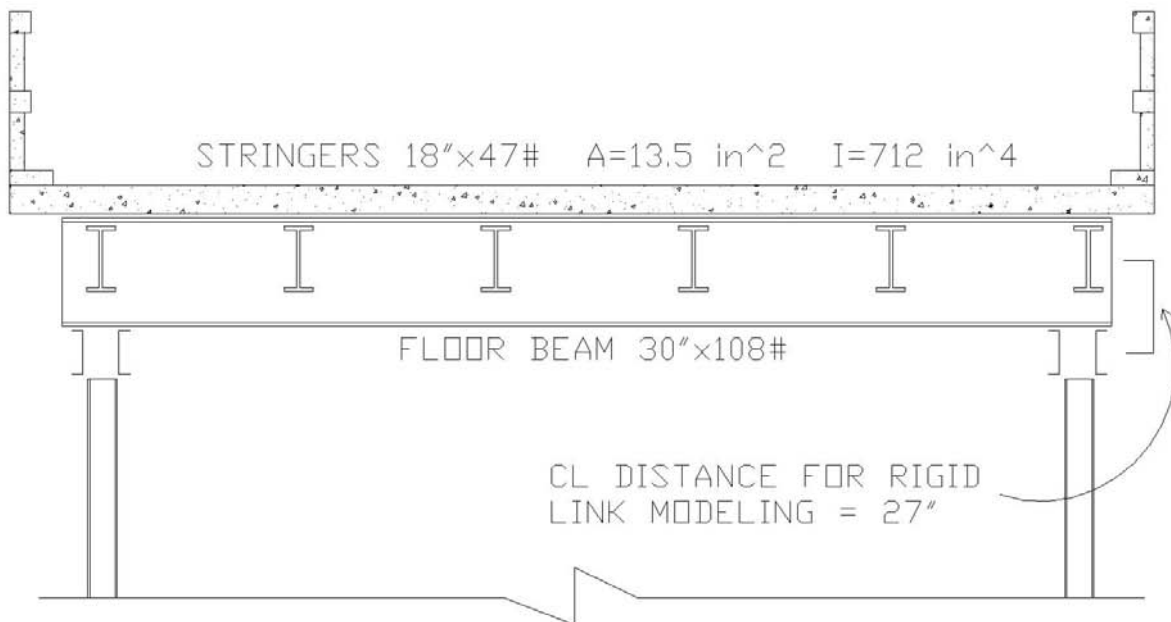


Figure 15. Bridge Cross Section

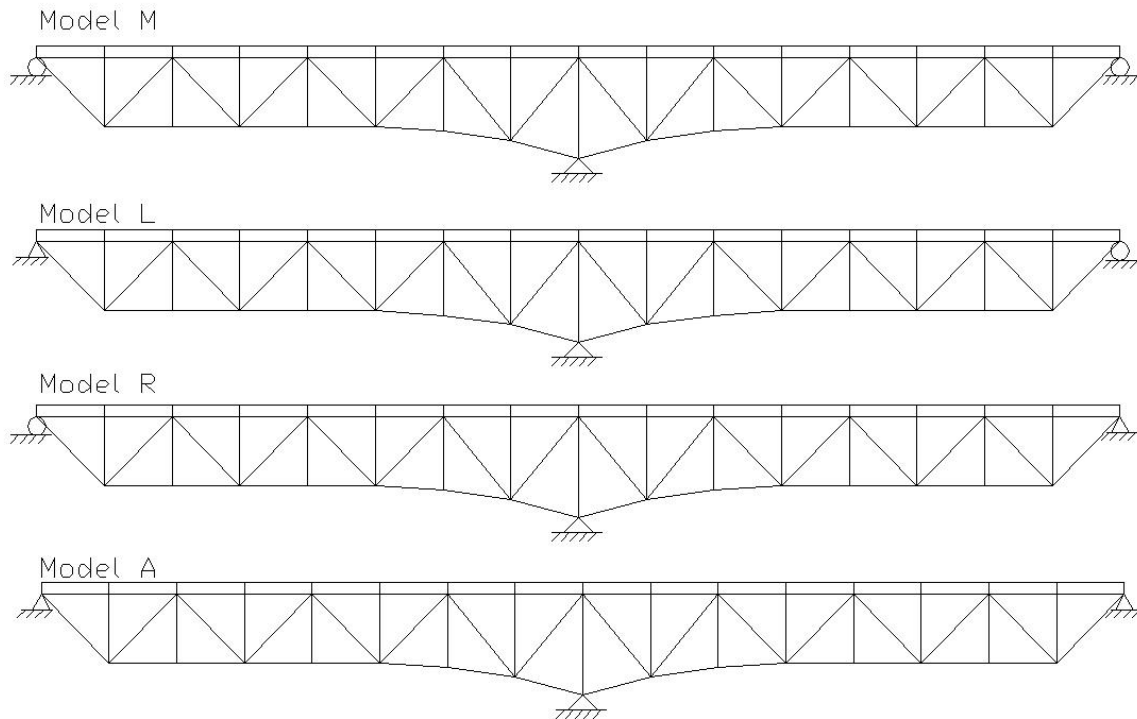


Figure 16. Frame Models Including Floor Beams

Failure Load Prediction

Once a structural model was validated, a failure load for a given location was predicted. That is, by imposing a point load at each node on the top chord of the truss, the structure's response was measured. From these responses, the member closest to its yield point was determined. To design a test to failure, which would approximate the failure mode of the Minnesota bridge, the researchers needed to know the required load and load position to cause the desired failure.

In this research, "failure" of the bridge is defined as the yielding or buckling of a primary structural member, not complete collapse. Preliminary analyses predicted the easiest member to fail would be a truss member connected to Node U6, and thus all five members connecting there were monitored during live load testing. This node is also a suspected failure initiation point in the collapse of Minnesota's I-35W Bridge. To accomplish this objective, it was necessary to calculate the strain induced in members by the bridge's dead load. From these values, the remaining strain to yield could be calculated. A sensitivity analysis of the monitored members would then determine which member could reach this strain first with a point load positioned above a given node.

Dead Load Strain Analysis

To calculate the dead load strain in the monitored members, each member's self-weight was distributed evenly to its end nodes. Bracing and deck weights were distributed the same

way. Connection weights were calculated based on shapes and plate sizes as specified in the bridge plans, these weights were added as nodal loads. The sum of these dead loads was found to roughly approximate the dead loads shown on the plans. Table 12 summarizes the dead loads and strains in each member.

Some of the calculated values are substantially less than those from the plans. This has been attributed to accounting for rivet weight. It also appears that the truss may have been originally analyzed as having no self-weight, and all dead loads were distributed to the nodes along the top chord. The analysis performed for this research, in which all self-weights were carefully distributed to all nodes, is considered to be more accurate.

Table 12. Dead Load Axial Forces and Strains in Monitored Members

Member ID	Calculated Dead Load [kips]	Dead Load from Plans [kips]	Dead Load Axial Microstrain [kips]
U0-L1	81.4	100.3	0.159
U0-U1	115.9	142.2	0.23
U6-U5	60.7	66.4	0.143
U6-L5	129.5	162.0	0.217
U6-L6	0.93	0	0.003
U6-L7	164.6	204	0.24
U6-U7	134.9	181	0.197

Sensitivity Analysis

To determine which member would be easiest to fail, unit loads were applied successively to nodes on one side of the truss using the previously-validated stringer frame model. The responses in each monitored member were recorded and divided by those members' calculated yield loads. Member yield loads were taken as the product of member cross sectional areas (section losses ignored) and the yield stress, 36 ksi. The member showing the greatest calculated fraction was identified as the most probable member to fail, resulting in the least amount of load to be applied to observe yielding in the truss. Table 13 presents each member's sensitivity to failure according to unit loads applied along the top chord.

Table 13. Member Sensitivities

Unit Load @ node	Axial Force In Member Due To Unit Load / Yield Load (x1000)						
	U0-L1	U0-U1	U6-U5	U6-L5	U6-L6	U6-L7	U6-U7
U1	2.405	0.538	0.135	0.288	0.005	0.231	0.110
U2	2.032	0.522	0.283	0.577	0.010	0.462	0.218
U3	1.566	0.367	0.446	0.854	0.022	0.689	0.308
U4	1.130	0.263	0.675	1.148	0.034	0.915	0.389
U5	0.757	0.172	0.850	1.321	0.071	1.154	0.393
U6	0.418	0.094	0.387	0.151	0.097	1.360	0.239
U7	0.191	0.043	0.147	0.092	0.055	0.025	0.079
U8	0.005	0.001	0.003	0.002	0.001	0.002	0.008

The maximum value in Table 13 is 2.405, in Member U0-L1 when a unit load is applied at Node U1. There is a disparity between recorded data and this value, however, likely attributable to unknown end effects. Therefore Member U0-L1 is not preferred as a member to fail, as doing so would not reveal as much about the truss's actual behavior. In this case, the remaining maximum value in the table is 1.36, in Member U6-L7, when the unit load is applied at Node U6. By this reasoning, Member U6-L7 will be the first member to fail when enough load is applied at Node U6. This is in accordance with the earlier prediction made in preliminary truss analysis and observations made during the Minnesota bridge collapse.

RESULTS

Laced Member Strain Gaging

A 20 kip test load was selected for evaluating the gage arrays. This load was selected because it would cause strains in the column (approximately $80 \mu\epsilon$) similar to the maximum strains expected to be observed on bridge members during load testing. The use of linearly variable displacement transducers (LVDTs), also known as wire pots, was considered, but loads required to measure deflections larger than the devices' electronic noise range would have been unrealistically large. The wire pots could have been used to confirm the strains measured on the gages.

There were two plane sections on the column on which six gages were mounted. In these locations, there was one gage in the middle of the extreme fiber on each column flange and in the middle of the web of each channel (see Figure 3). Although there was substantial difference in the strains measured in each gage, the averages taken in a plane were very similar. In each plane section, the average of the four flange-mounted gages was compared to the average of the entire array of six gages. These averages were compared throughout the entire load range. Figure 17 presents the raw strain data from section A, prior to averaging for comparisons. This was typical of all column sections analyzed.

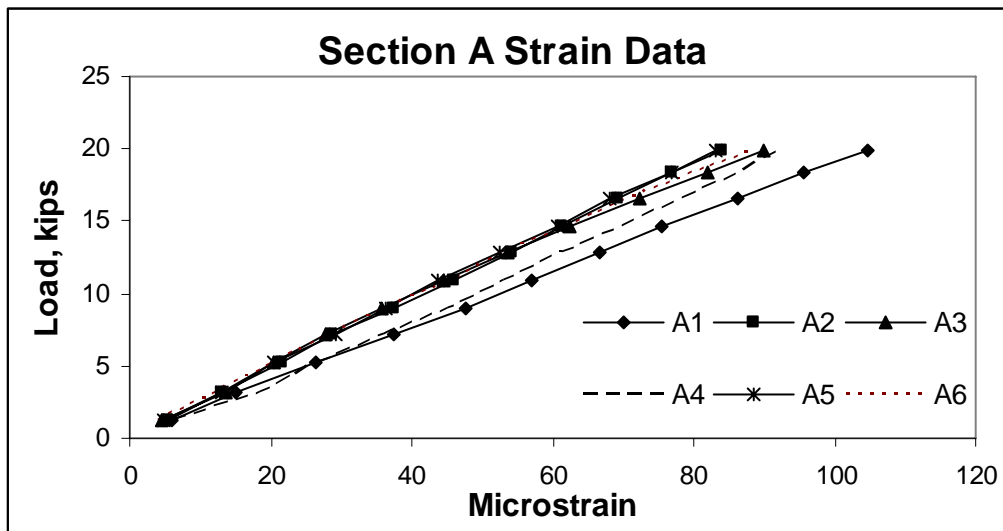


Figure 17. Section A Raw Strain Data

Except where very low strains were recorded at the lower end of the load range, the difference between the four and six gage averages was typically less than 2%. These results diverged somewhat as strains increased. This is accurate for use in bridge instrumentation; an error on the order of magnitude of a few microstrain is acceptable.

Figure 18 shows that the six gage layout (4F+2W) is marginally more accurate than the four gage, flange-only layout (4F). Both are consistently below the expected strain reading, with some divergence as load increases. The four gage layout is not so inaccurate, however, as to demerit its use considering it is 33% (four gages instead of six) faster to install.

Figure 19 presents the average readings taken on strain gages located in the webs at column sections A, B, and C (see Figure 3). Although web strain in section C diverges from the other sections somewhat, this may be attributed to imperfect end conditions in the testing machine. The figure does demonstrate that there is no substantial difference between strains measured at section B, where no lacing is attached, and strains measured at section A, where lacing is bolted to the channels. Thus it is conclusive that the lacing does not have a significant effect on axial strain measurements.

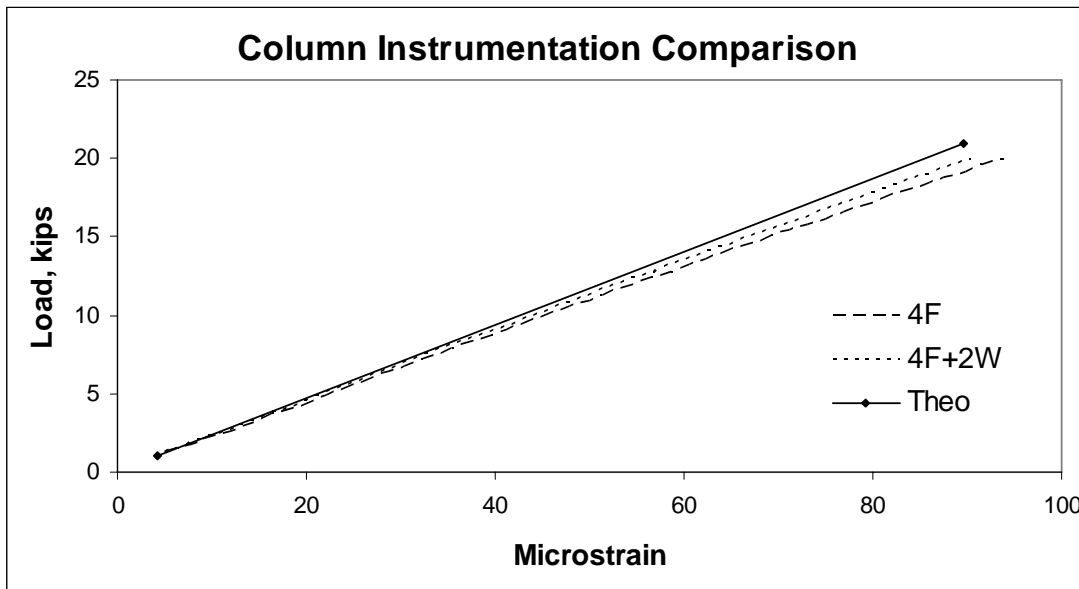


Figure 18. Instrumentation Comparison Between 4 and 6 Gage Layouts

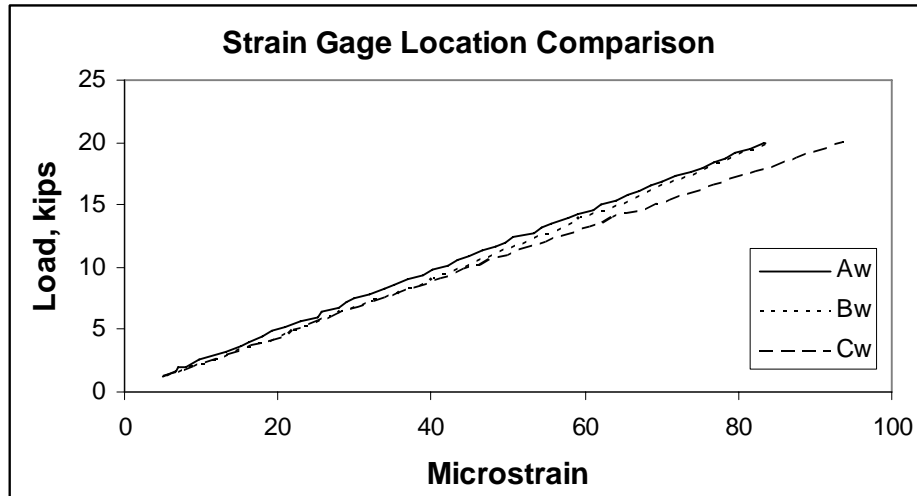


Figure 19. Strain Gage Location Comparison

Selected Strain Gage Layout

There was no substantial difference between strains measured in the channels at locations of lacing attachment or points between them. From the column test data, it is concluded that riveted lacing does not affect average axial strain measurement. Since there was negligible difference between averages of four or six gages in the same plane, the simpler arrangement was chosen for application in the field. Thus, it was decided that the more heavily instrumented bridge members would have one strain gage mounted in the middle of the extreme fiber of each channel flange at the middle of the member to minimize error caused by imperfect end conditions. Some monitored members were I sections, and these were instrumented similarly, with one strain gage on each side of each flange.

Comparisons of Live Load Test Data to Model Predictions

Axial Force per Monitored Member per Truss

There was marked improvement in the performance of models with progression from the simpler models to more complex and inclusive ones. In general, as the model complexity grew, trends in the calculated response within a load regime matched the recorded data more accurately. Likewise, the possibility of bracketing recorded data between some of the expected results according to various restraint conditions improved with more complex modeling. Some members, such as U6-L7, modeled virtually identically for all models. Simple to complex progression for this member did not show a noticeable increase in accuracy. Other members, such as U6-L6, could not be accurately modeled at all, regardless of the complexity of the model being used. The left loading regime, in which the truck is in the lane closer to the far truss, could not be modeled well at all, regardless of model complexity or even how loads were distributed. Figures 20 through 28 demonstrate the general improvement between models on various members, trusses, and load regimes. These sequences of plots are the best examples of the described model progression; however, they are by no means the only proof. The entire modeling record for all members is included in the appendix.

Figure 20 shows that the truss model does not match the data very well, especially when load is far from the central pier beneath Node U8.

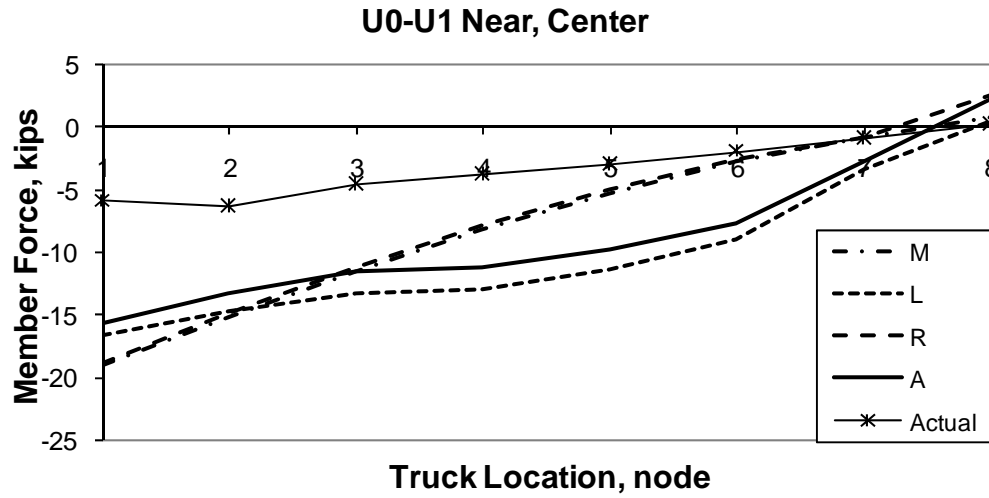


Figure 20. Member U0-U1, Near Truss, Truck Centered, Truss Model

Figure 21, the frame model results, shows some improvement over the results from the truss model, although these results would still not be useful for behavior predictions.

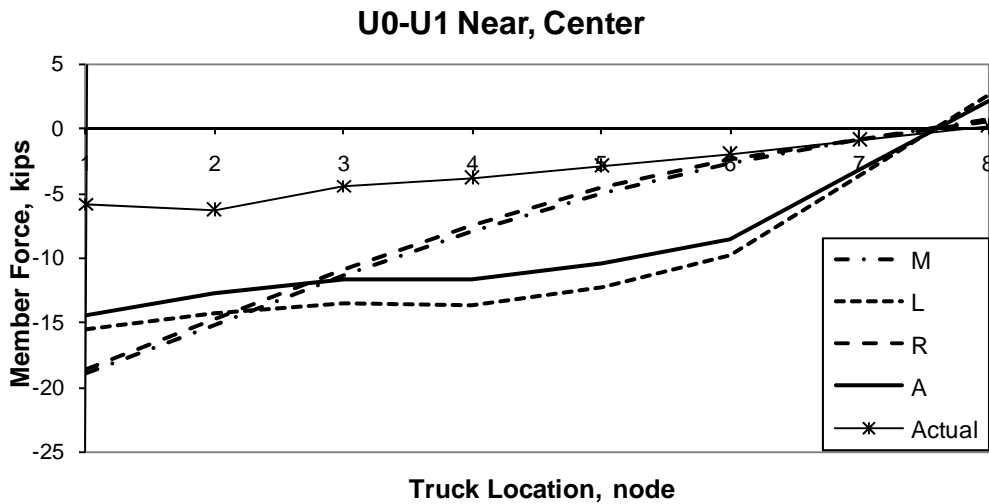


Figure 21. Member U0-U1, Near Truss, Truck Centered, Frame Model

Figure 22, the stringer frame model results, matches the data very well and bracketing between some end conditions is evident over the entire truss span.

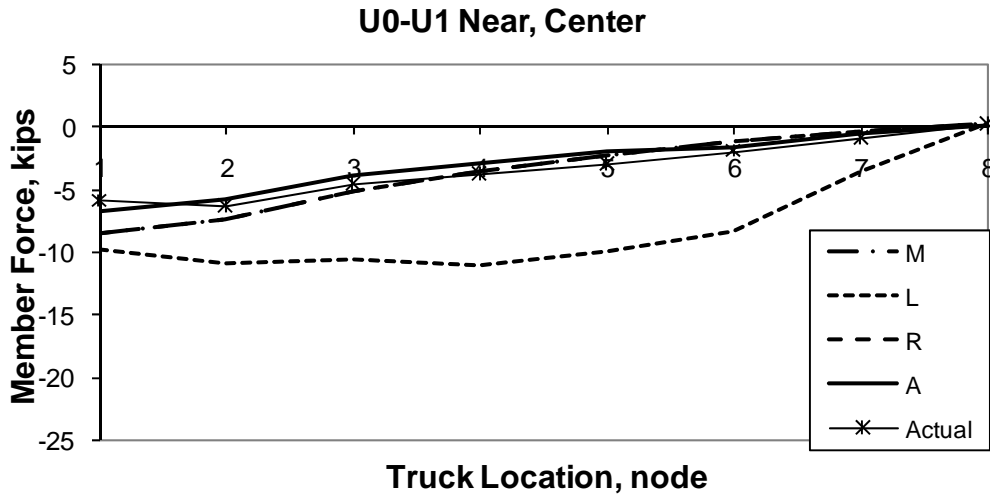


Figure 22. Member U0-U1, Near Truss, Truck Centered, Stringer Frame Model

Figure 23 shows that the truss model does a poor job of replicating the bridge's behavior, especially when load is far from the central pier.

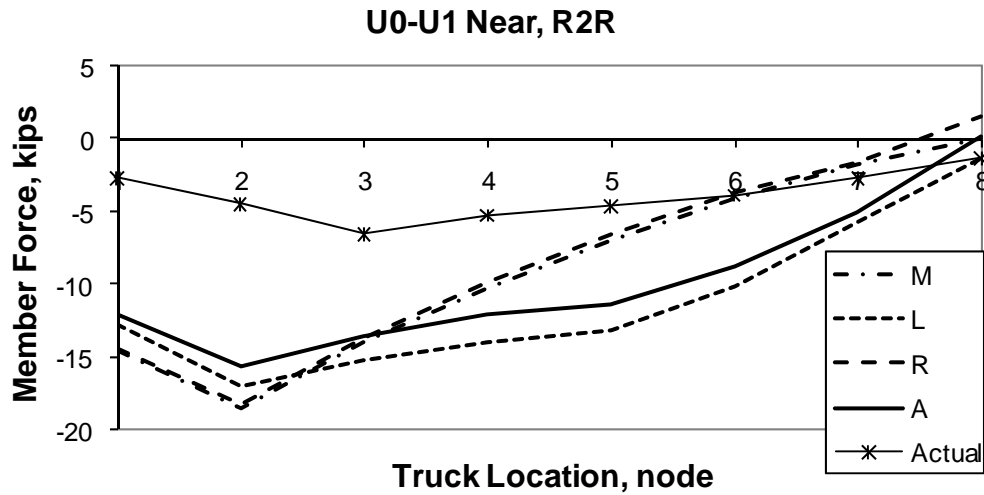


Figure 23. Member U0-U1 on the Near Truss, Trucks Rear to Rear, Truss Model

Figure 24, the frame model, shows some improvement over the truss model, although these results would still not be useful for behavior predictions.

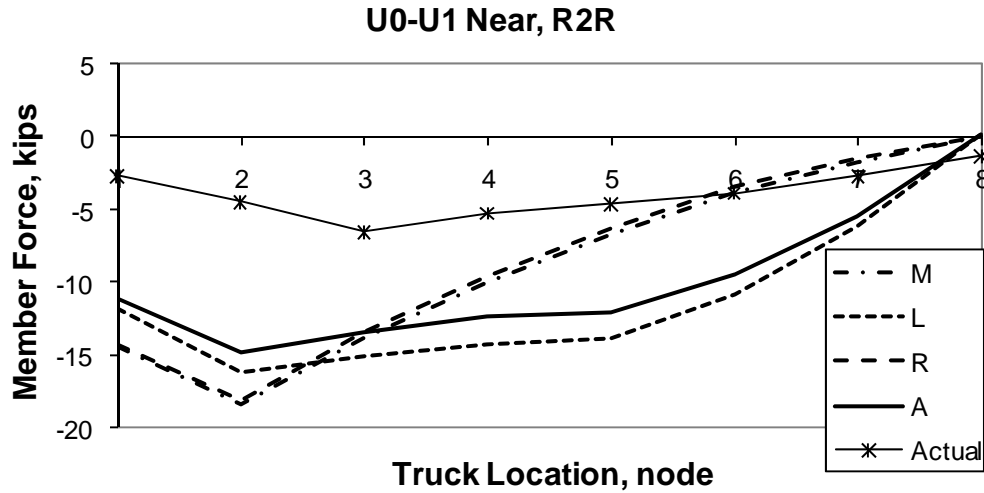


Figure 24. Member U0-U1 on the Near Truss, Trucks Rear to Rear, Frame Model

Figure 25, the stringer frame model results, demonstrates that this model matches the recorded data most accurately. The recorded data are bracketed by different end conditions in more than 75% of the truss span.

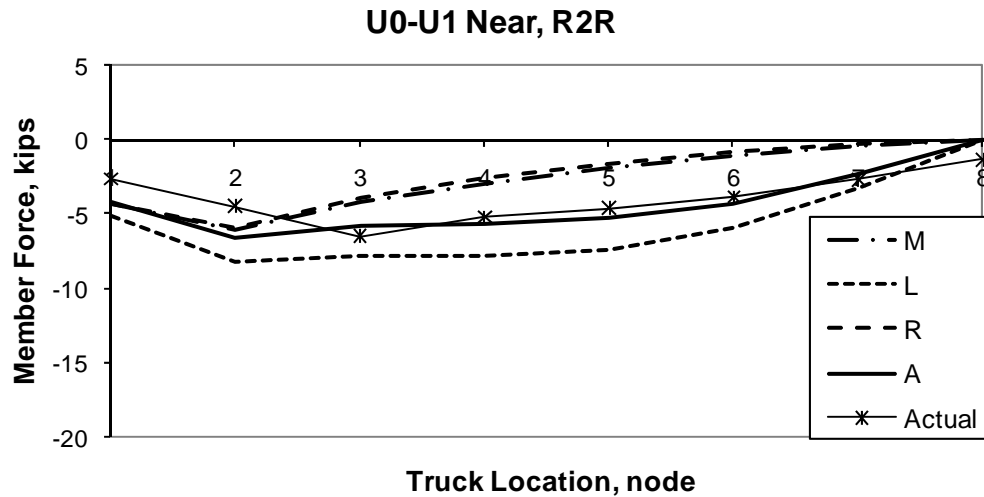


Figure 25. Member U0-U1 on the Near Truss, Trucks Rear to Rear, Stringer Frame Model

Figure 26 shows that there is a great gulf between the bridge's actual behavior and the truss model's expectations.

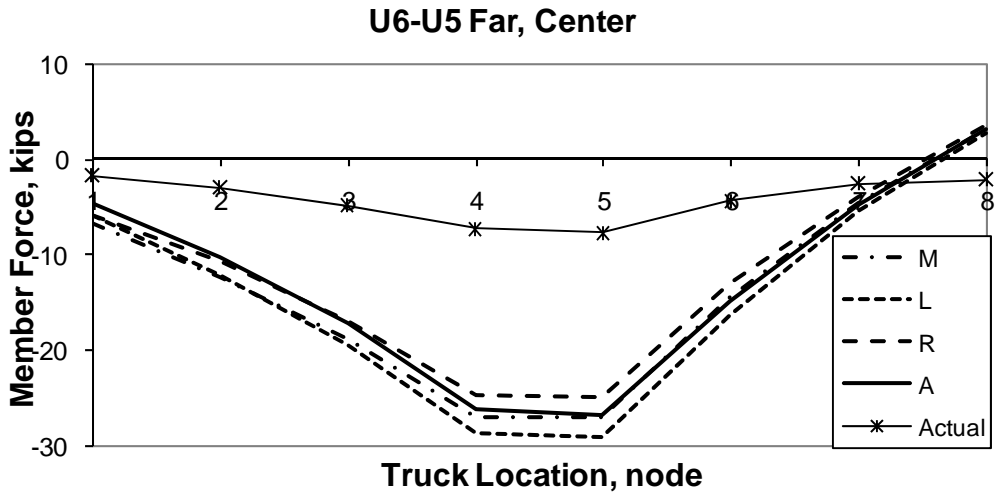


Figure 26. Member U6-U5 on the Far Truss, Truck Centered, Truss Model

Figure 27 shows that the frame model is only a small improvement over the truss model for this member in this load regime.

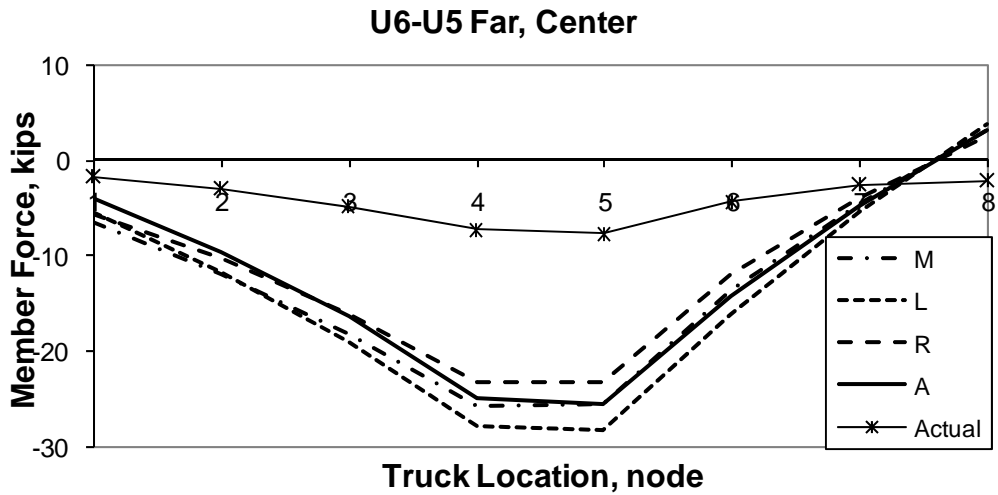


Figure 27. Member U6-U5 on the Far Truss, Truck Centered, Frame Model

Figure 28 shows that the stringer frame model comes very close to replicating the data recorded from live load testing. Member forces could be predicted with other loads using this model.

These three examples illustrate that the stringer frame model predicts the member forces far more accurately than the basic truss model or the basic frame model. It is difficult to determine, however, which of the four boundary conditions is most accurate.

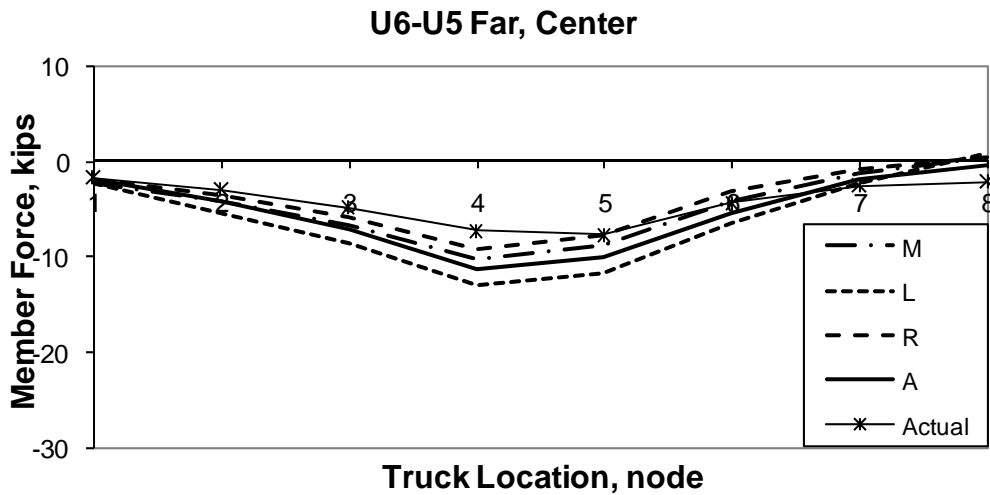


Figure 28. Member U6-U5 on the Far Truss, Truck Centered, Stringer Frame Model

Deflections per Monitored Node per Truss

Model improvement can be demonstrated with comparison of expected and recorded nodal deflections as well. Once again, trends in the calculated response within a load regime matched recorded data more accurately as models progressed in complexity. The prevalence of bracketed results increased with model complexity again as well. The following sequences of plots demonstrate the improvement of accuracy with increasing model complexity. From top to bottom, the truss, frame, and floor beam frame models are represented. Once again the Left lane loading regime proved difficult to model accurately, regardless of load distribution used. Figures 29 through 37 present the general accuracy progression. These sequences of plots are the best examples of the described model progression; they are by no means the only proof. The entire modeling record for all deflections is included in the appendix.

Figure 29 shows that there is a vast difference in the data recorded and the expectation of the truss model.

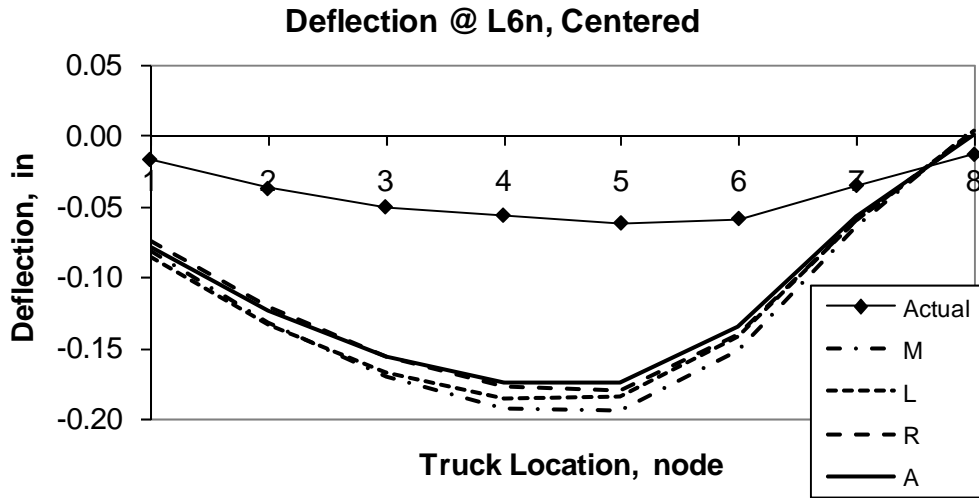


Figure 29. Node L6, Near Truss, Truck Centered, Truss Model

Figure 30 shows that the frame model is a great improvement on the truss model for this node in this load regime.

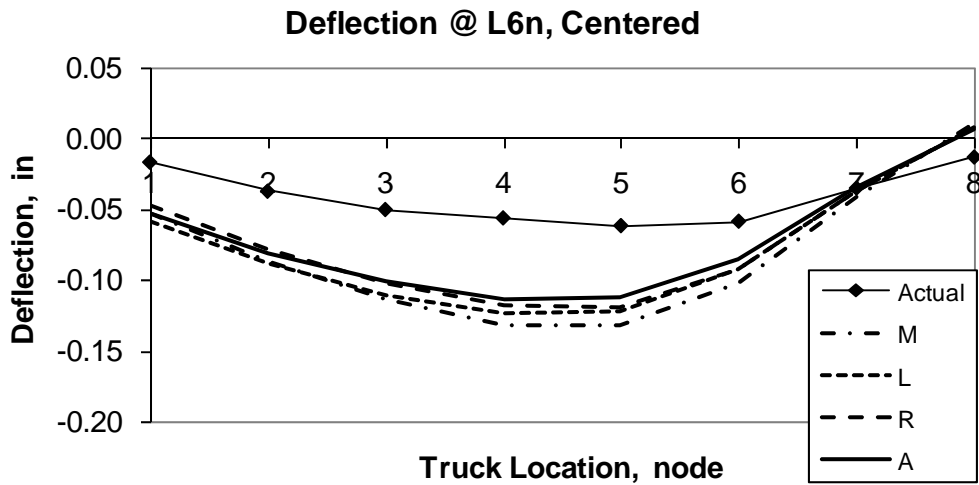


Figure 30. Node L6, Near Truss, Truck Centered, Frame Model

Figure 31 shows that the stringer frame matches the recorded data best and would be useful for predicting deflections due to other loads.

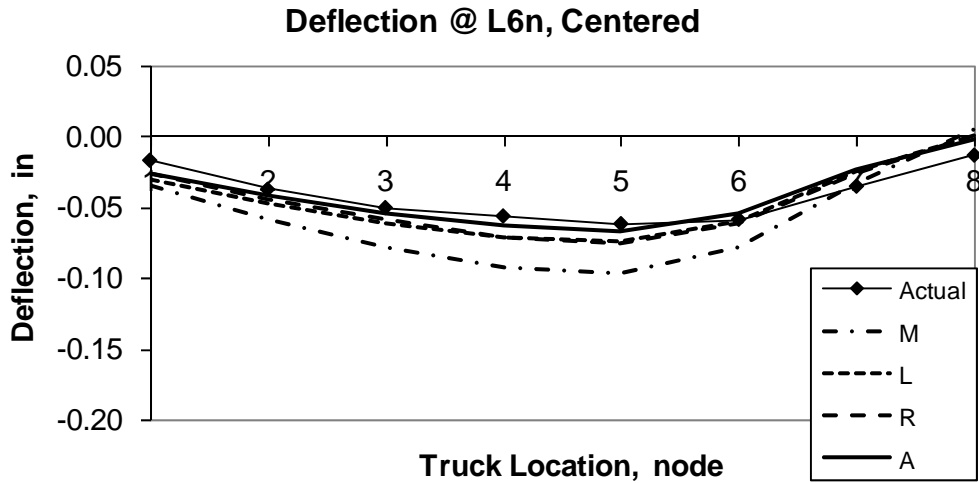


Figure 31. Node L6, Near Truss, Truck Centered, Stringer Frame Model

Figure 32 shows that once again, the truss model does a poor job of matching recorded data. It is observed that there are no data points in the recorded data at load positions 3 and 4. The van containing the DAS was parked on the bridge between these nodes. As the bridge is only two lanes wide, it was impossible to fit the two trucks side by side at these locations. Thus their load position data were omitted.

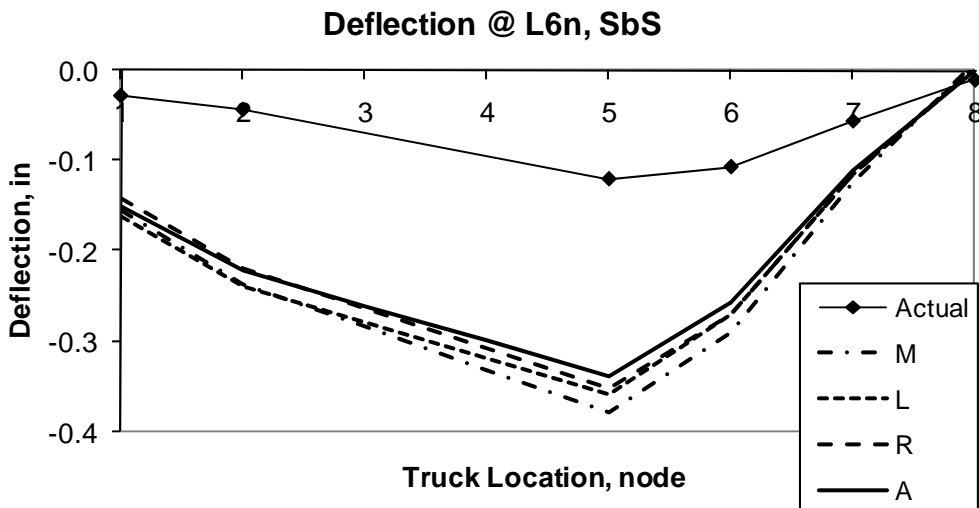


Figure 32. Node L6 on Near Truss, Trucks Side by Side, Truss Model

Figure 33 shows that the frame model is a great improvement on the truss model for deflection prediction for this node in this load regime.

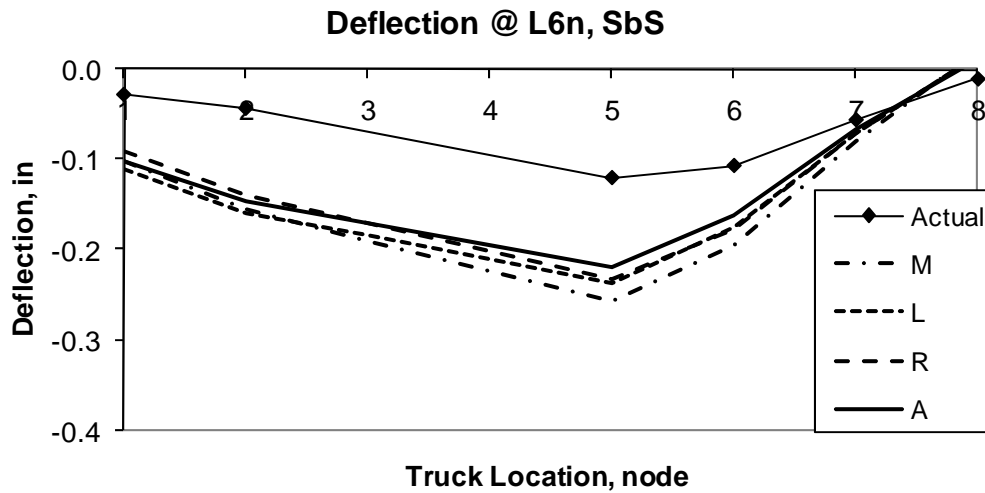


Figure 33. Node L6 on Near Truss, Trucks Side by Side, Frame Model

Figure 34 shows that once again, the stringer frame model best matches the live load data. It is especially accurate (with bracketed data) as the load is placed closer to the central pier.

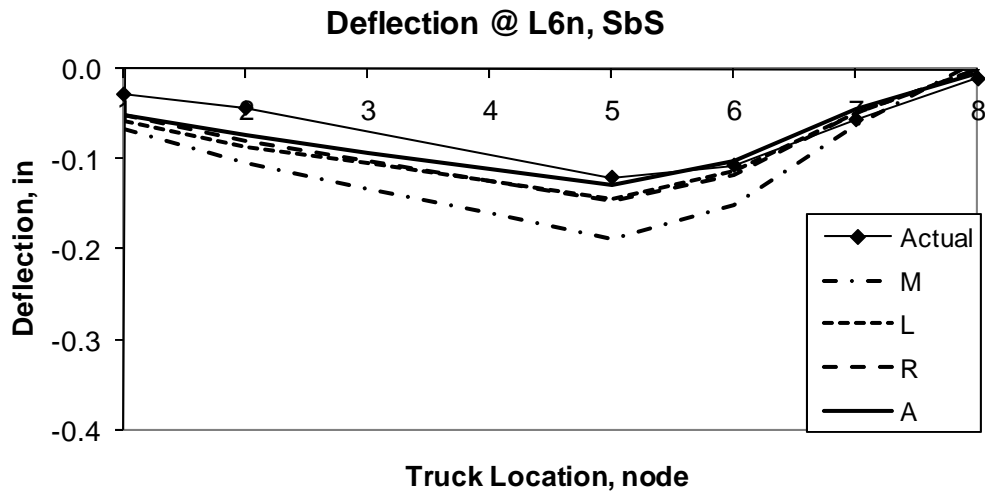


Figure 34. Node L6 on Near Truss, Trucks Side by Side, Stringer Frame Model

Figure 35 shows that the truss model is accurate only for load position U7. Otherwise it poorly approximates the bridge's behavior.

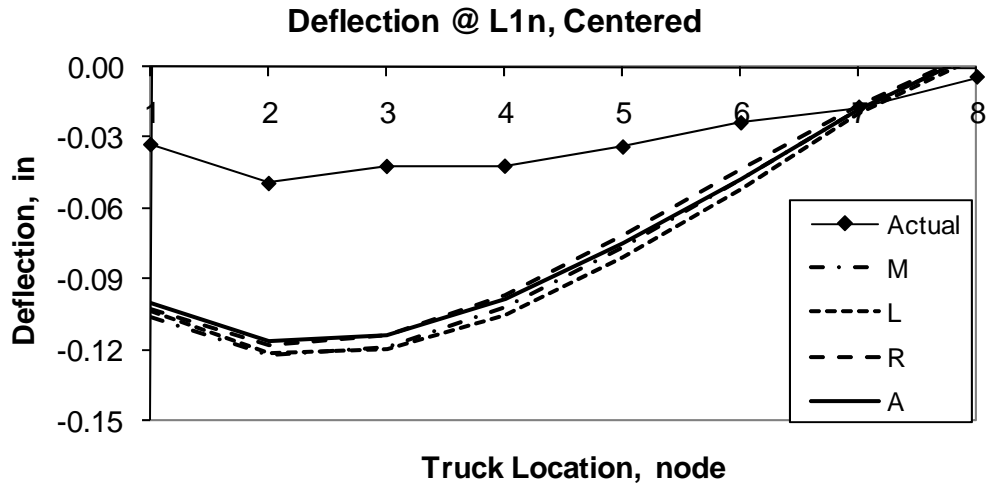


Figure 35. Node L1 on Near Truss, Truck Centered, Truss Model

Figure 36 shows that the frame model comes much closer to predicting the actual truss behavior than the original truss model. It would still not be useful enough for future use, however.

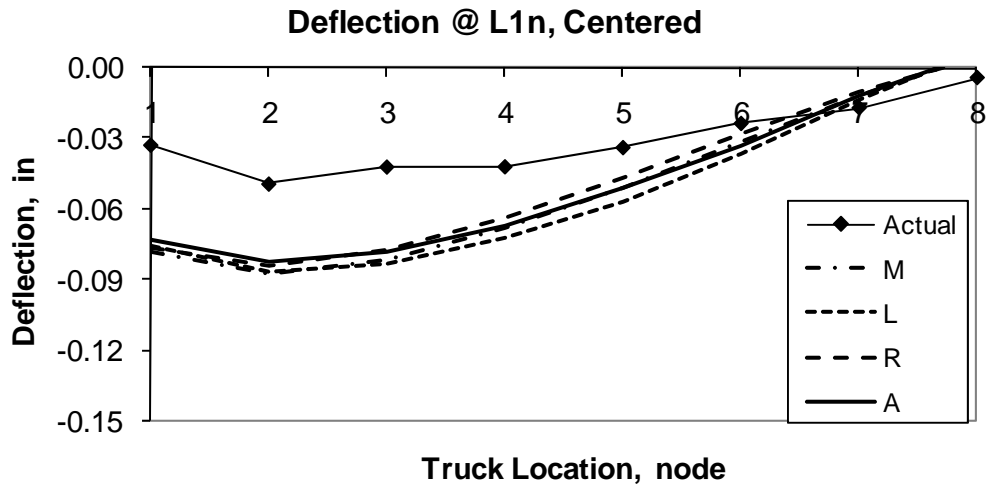


Figure 36. Node L1 on Near Truss, Truck Centered, Frame Model

Figure 37 shows that the stringer frame model performs best at approximating the bridge's actual behavior for this node in this load regime.

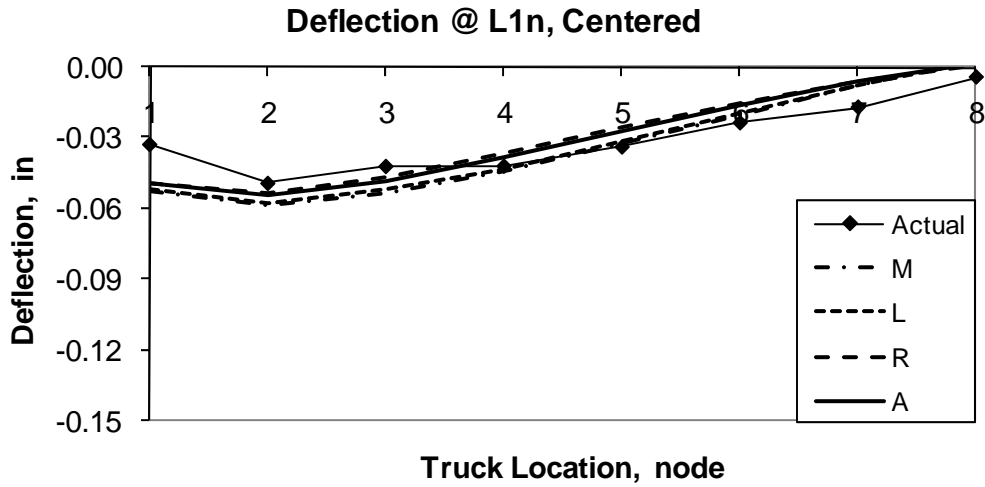


Figure 37. Node L1 on Near Truss, Truck Centered, Stringer Frame Model

Data Observation

According to the data recorded for deflections on the near truss with one truck in the left lane, the nodes actually deflected upward for much of the load regime. This seems to indicate that the deck and bracing provide enough stiffness between the trusses that the entire structure acts like a rigid member experiencing torsion about its center. In this case, load in the left lane causes downward deflection in the far truss and upward deflection in the near truss. Figure 38 illustrates this trend. This effect would best be investigated with a three dimensional model.

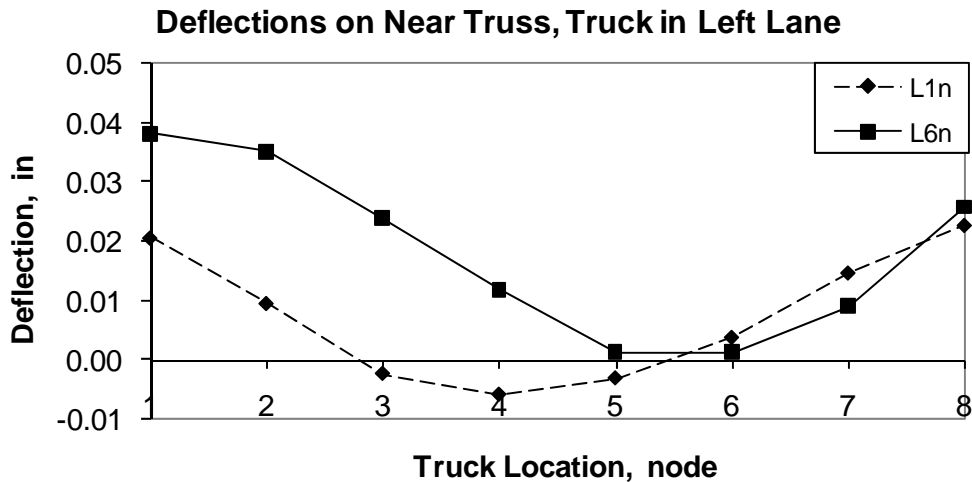


Figure 38. Near Truss Deflections, Truck in Left Lane

Results of Failure Prediction

Based on the stringer frame model, a load of 1 kip applied at Node U6 causes a 1.16 kip compression response in Member U6-L7. This indicates 1.70×10^{-6} strain is caused in Member U6-L7 by a unit load applied at Node U6. The yield strain for all members in the truss is the ratio of the yield stress to the modulus of elasticity, 36 ksi / 29000 ksi, or 0.0012 ϵ . Subtracting the previously calculated dead load strain of 0.00024 ϵ results in 0.00096 ϵ is required to yield the member. Thus the load required to fail Member U6-L7 is 0.00096 ϵ divided by 1.70×10^{-6} ϵ per kip applied at Node U6, which equals 565 kips. This is 565 kips per truss. If load is applied symmetrically, in order to ensure a stable and safe load rig, this indicates the bridge will need to be loaded with 1130 kips at Node U6. This value is certainly an upper bound, as U6-L7 is a compression member and far more likely to buckle before then.

CONCLUSIONS

Instrumentation and Data Analysis When Placing Strain Gages on Steel Bridges

- Gages welded to the steel were just as accurate as those affixed to steel by chemical adhesion.
- The arithmetic mean of strains measured on gages in a plane matches the expected strain according to the load within ~2%.
- The average of four flange gages in a plane was slightly less accurate than using all six but still an adequate approximation.
- Average axial strain measured at locations of lacing attachment was equal to the average axial strain measured at locations between lacing attachments.
- Continuously recorded strain and deflection data were successfully reduced to discreet data points per member or node per load position per regime.
- The arithmetic mean of data over a load position interval was used because there was negligible drift within these data intervals. These discreet data points were the ordinates of comparison between the structural models.

Live Load Testing and Comparisons of Results to the Analytical Models

- All models are especially competent at predicting the bridge's response when loadings are relatively symmetric to either truss, as in the case of the centered truck and side by side truck loading regimes.
- Despite being nominally designed as a truss, the bridge's structural response to static vertical loads proved to be more characteristic of a frame that included the floor beam and stringer elements.

- The stringer frame model is observed to be the most accurate at predicting this bridge's response to static, vertical loads.

Failure Load Analysis

- Member U6-L7 was most susceptible to first yield stress. It was calculated to yield first with 565 kips applied vertically at Node U6. This is the load to fail one member in one truss.
- To fail both simultaneously would require 1130 kips across this node on the bridge. It is likely that, since it is a compression member, U6-L7 would buckle long before the full yield load is applied.

RECOMMENDATIONS

1. *When instrumenting a steel truss bridge for load testing by placing strain gages on built-up members, researchers from VDOT or the Virginia Transportation Research Council (VTRC) should use four gages, one placed on each flange of each channel.*
2. *When modeling deck truss bridges, VDOT or VTRC engineers should consider the system to be a frame and should include the stringers in the model.*

SUGGESTIONS FOR FUTURE RESEARCH

Greater model validation could be accomplished by instrumenting more members for strain measurement and more nodes for deflection measurement prior to the application of live load. Members framing into the central pier would be of interest. It could be also be valuable to instrument identical members on the opposite side of the pier and apply load there as well to see if the full truss behaves as symmetrically as expected. Percent difference between recorded and expected data could be calculated at all load positions and averaged to show quantitatively how accuracy changes between models.

The structural models in this study were also somewhat rudimentary. More accurate finite element models could be developed and compared to those used in this research. Actual built-up members and connections could be modeled exactly as they appear in the VDOT plans. A three-dimensional and non-linear model could possibly answer some of the questions raised from the analysis of data gathered in this research.

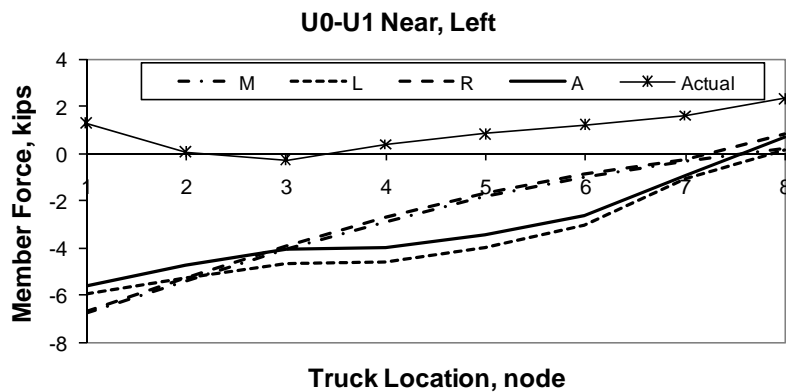
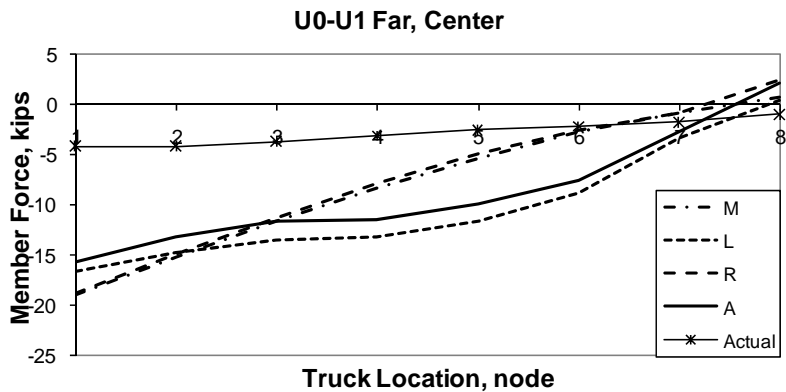
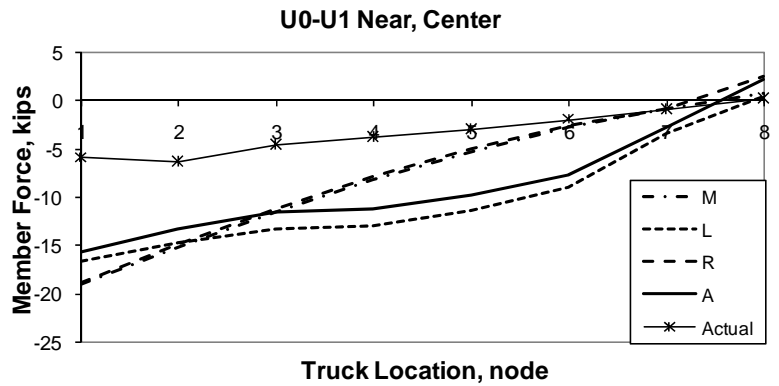
ACKNOWLEDGMENTS

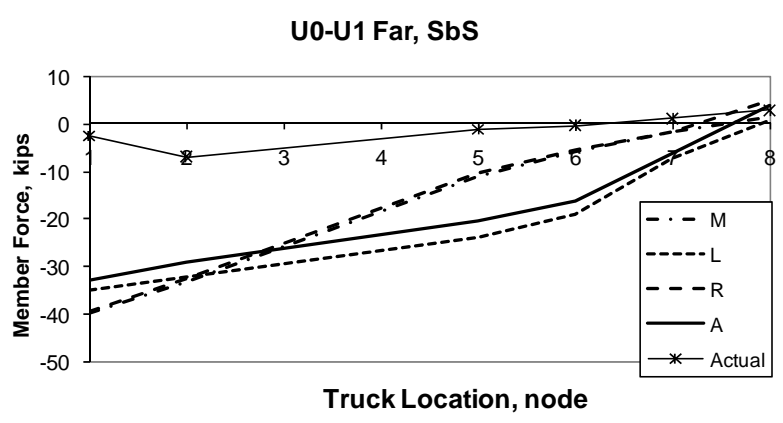
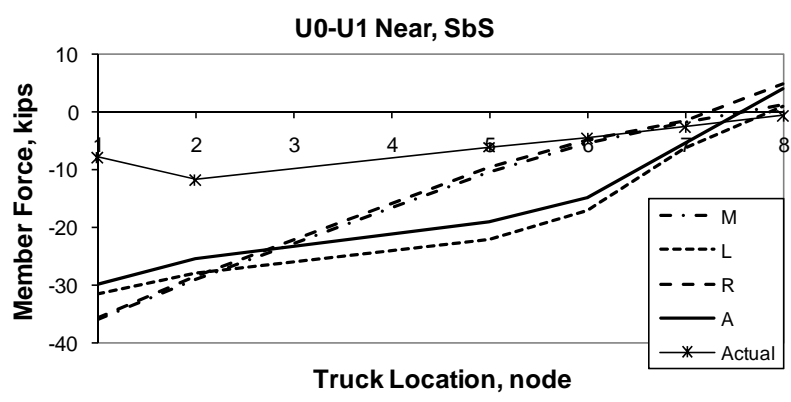
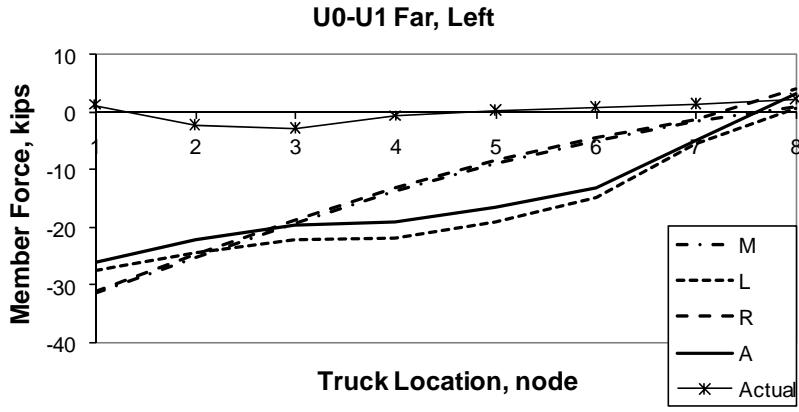
This project was funded by the Federal Highway Administration and the Virginia Department of Transportation. The authors gratefully acknowledge the assistance of researchers at the Virginia Transportation Research Council and the engineers and field personnel of VDOT's Bristol District.

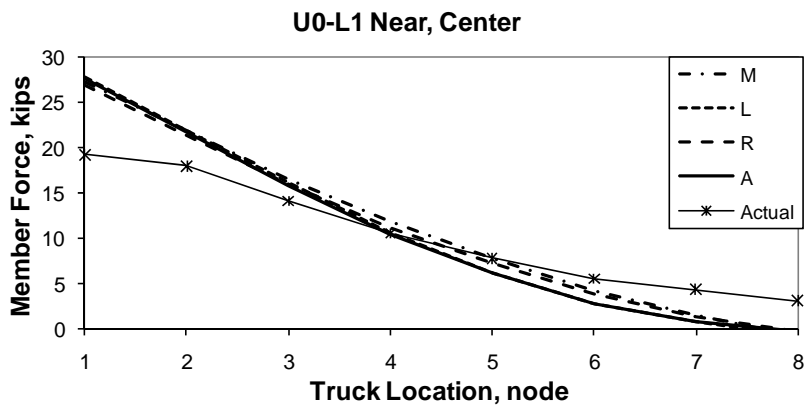
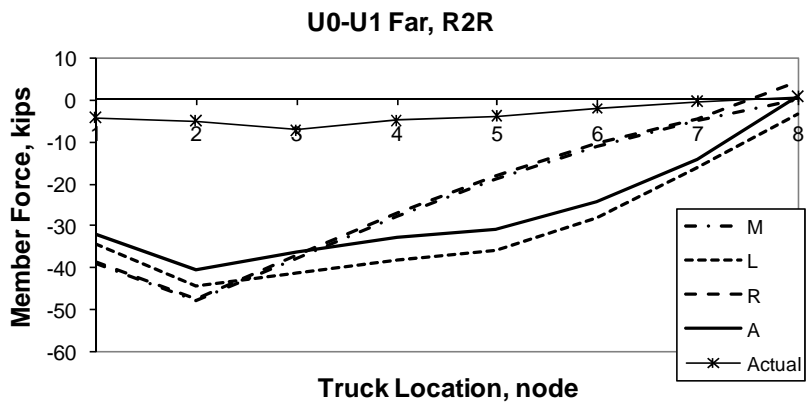
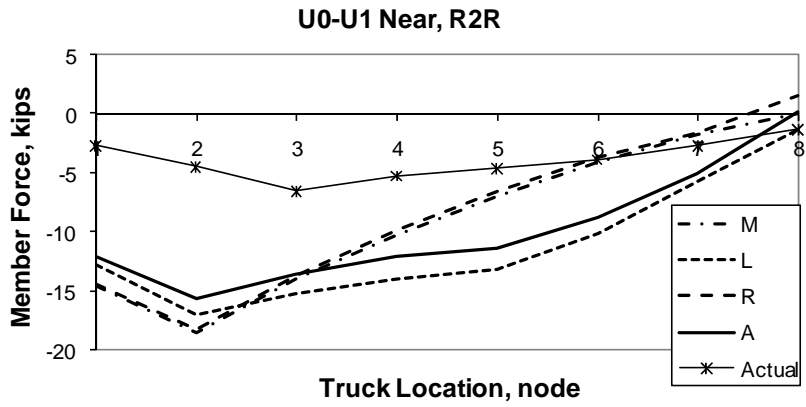
APPENDIX

MEMBER FORCE PLOTS FOR ALL MONITORED MEMBERS AND THE MEMBER FORCES PREDICTED BY THE TRUSS MODEL FOR ALL FOUR LOAD REGIMES

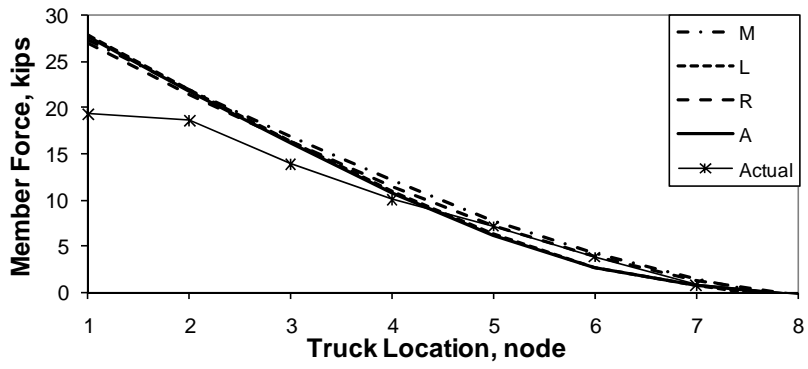
This appendix contain the member force plots for all monitored members and the member forces predicted by the truss model for all four load regimes. These are organized by member. Node deflection plots are included, and the deflections predicted by the truss model for all four load regimes follow. These are organized by node.



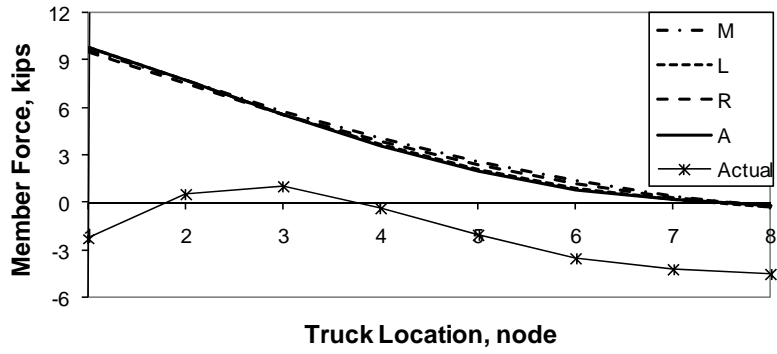




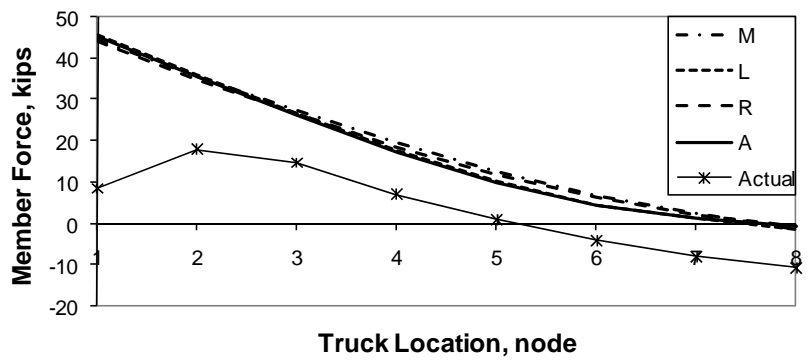
U0-L1 Far, Center



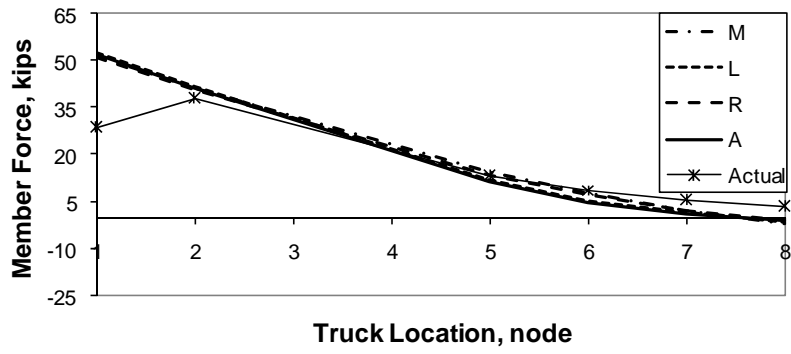
U0-L1 Near, Left



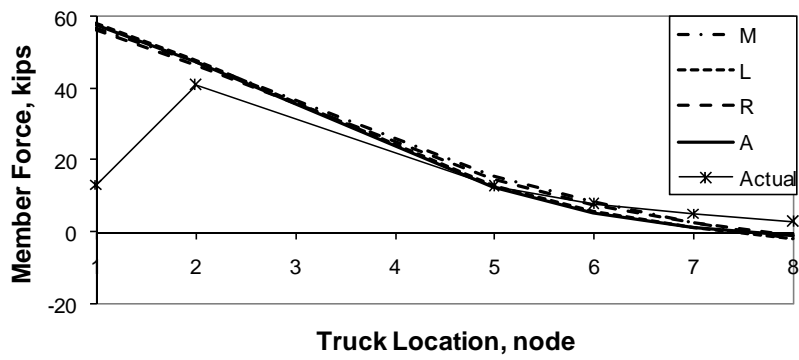
U0-L1 Far, Left



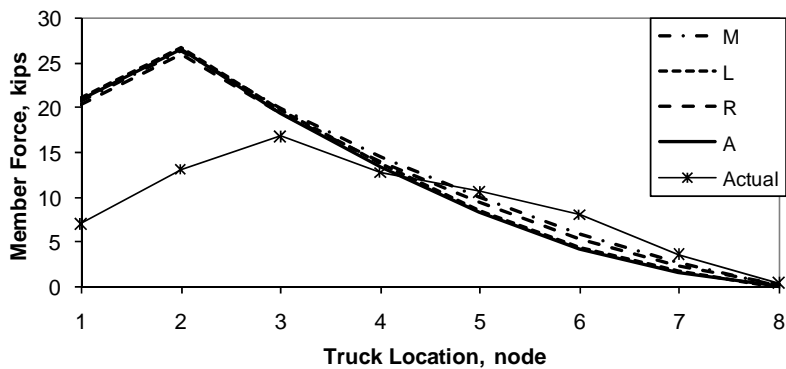
U0-L1 Near, SbS



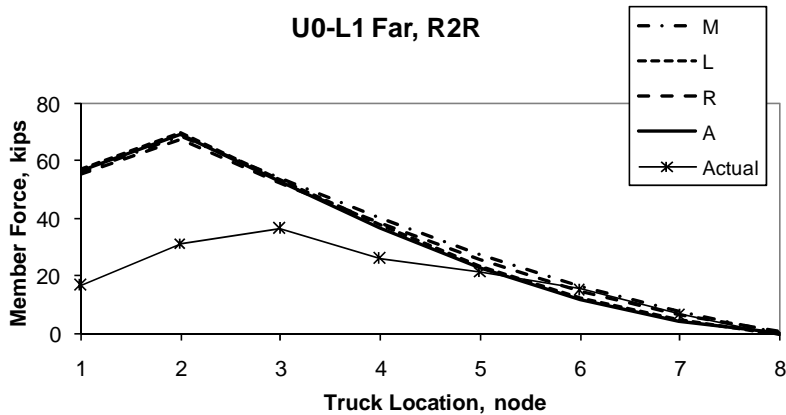
U0-L1 Far, SbS



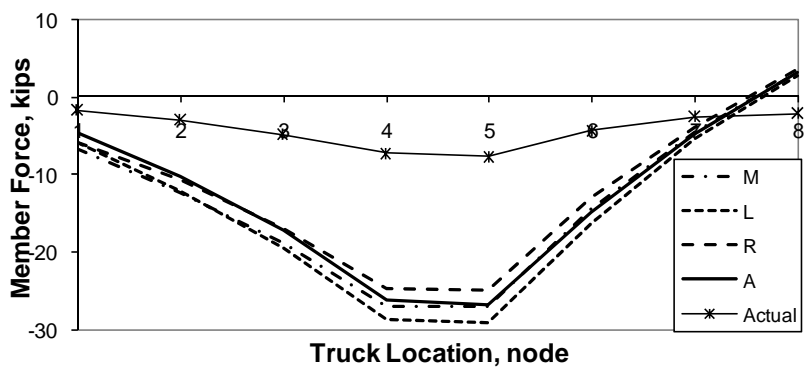
U0-L1 Near, R2R



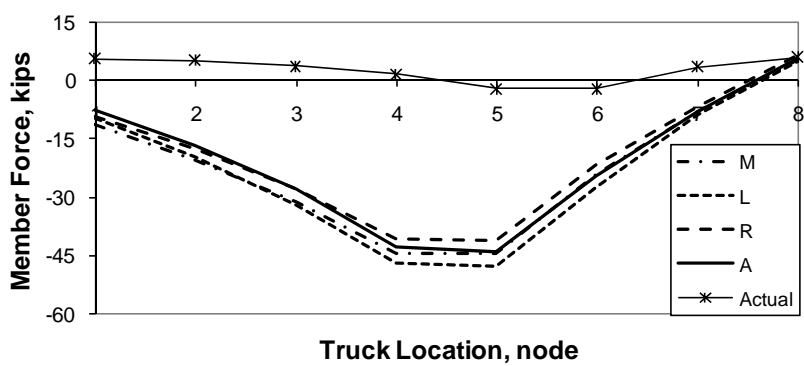
U0-L1 Far, R2R



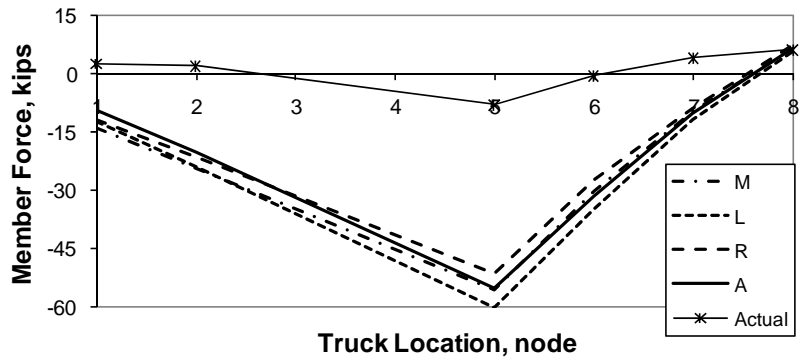
U6-U5 Far, Center



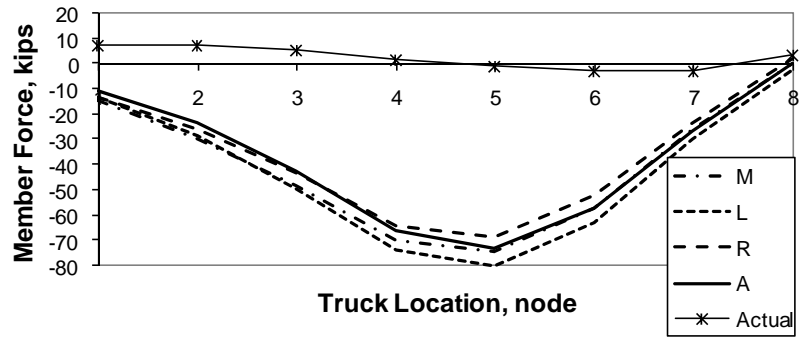
U5-U5 Far, Left



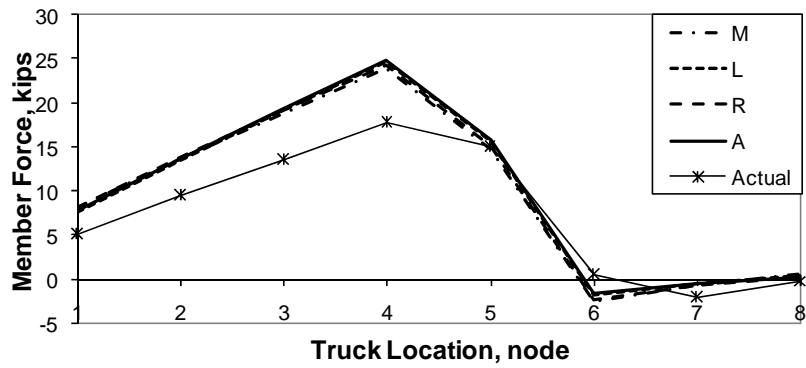
U6-U5 Far, SbS

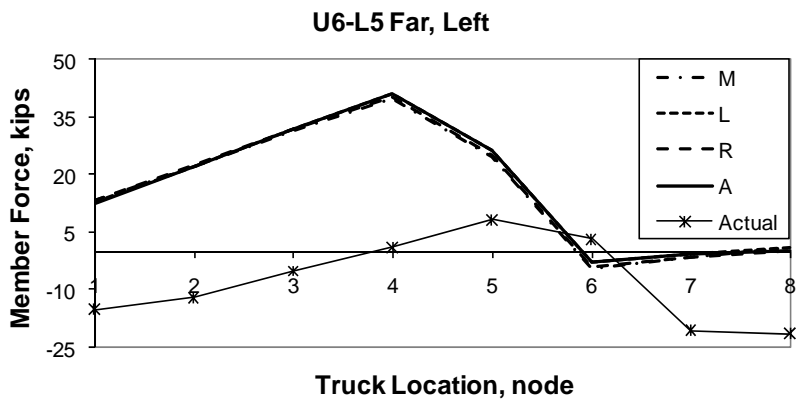
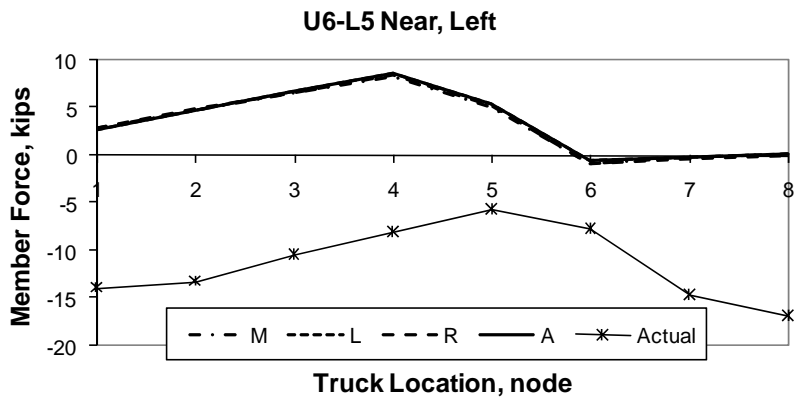
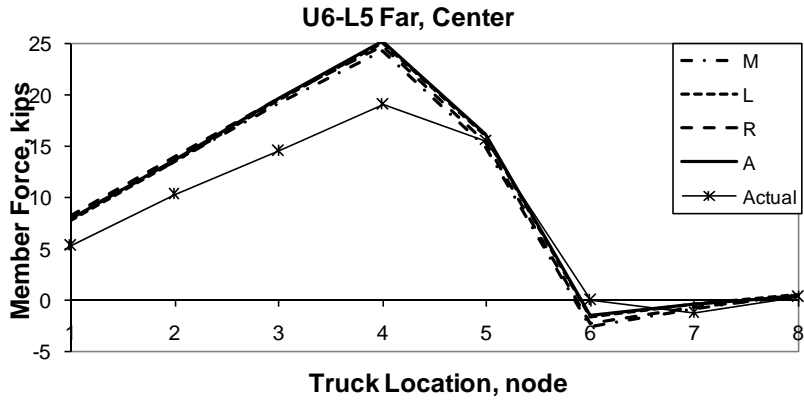


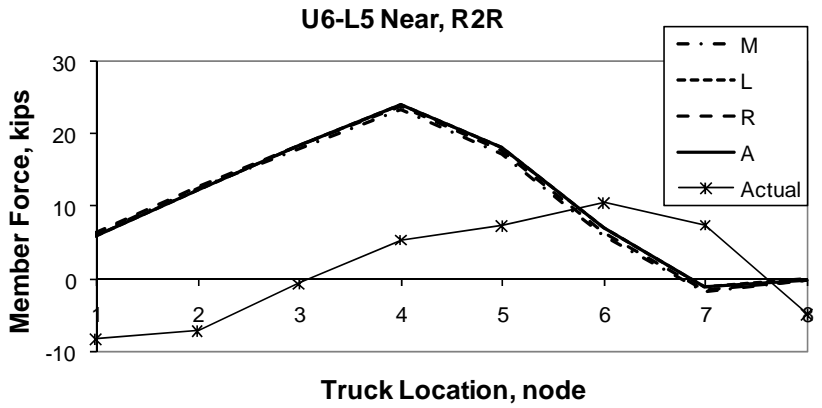
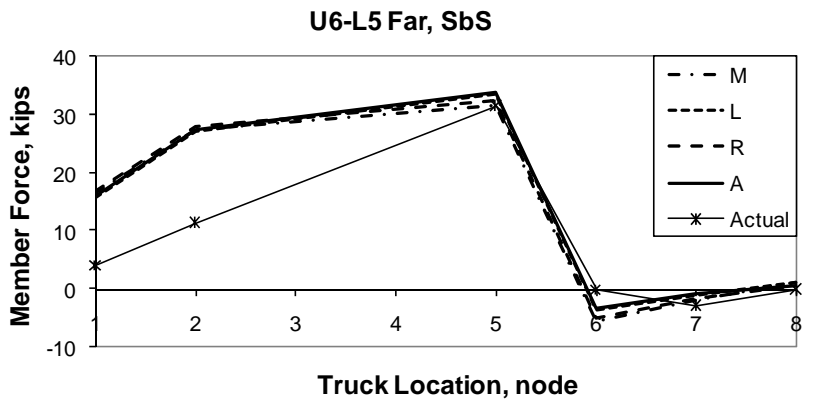
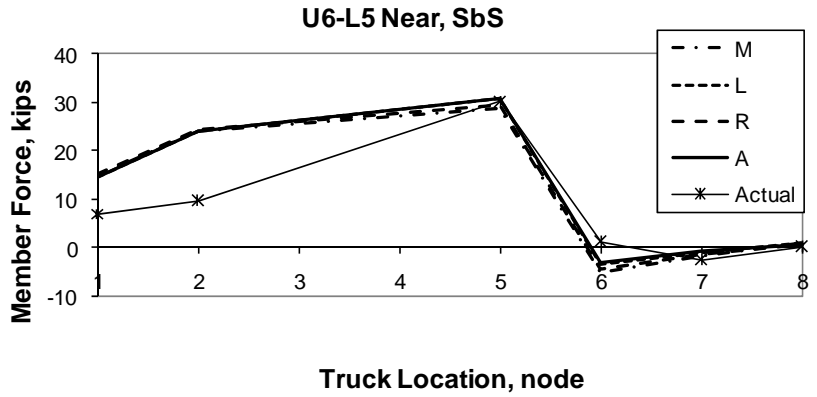
U6-U5 Far, R2R

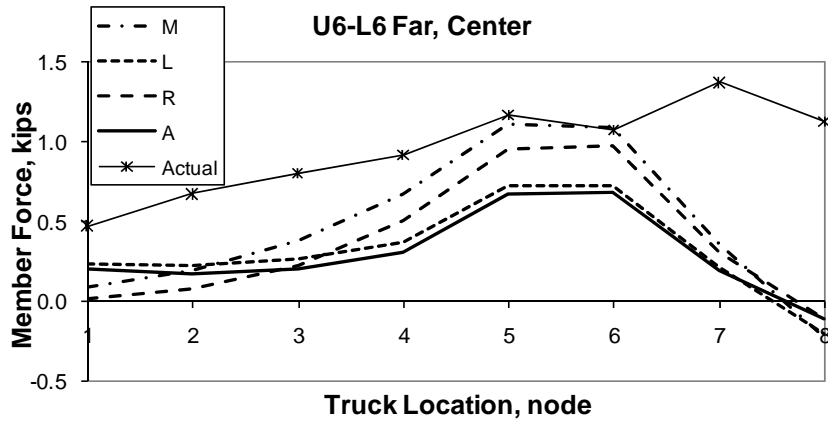
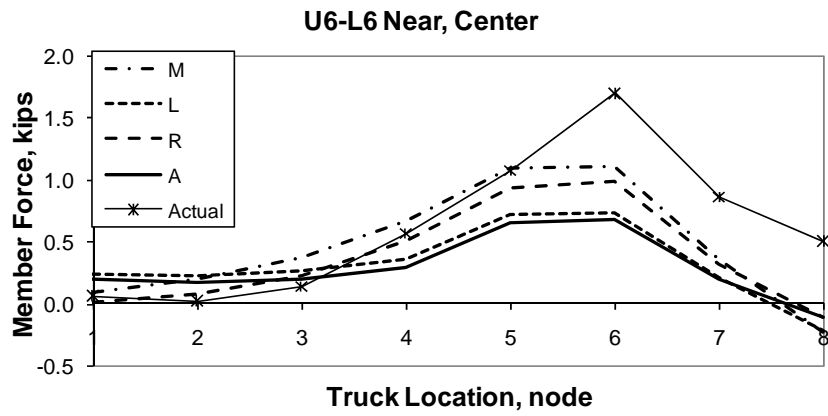
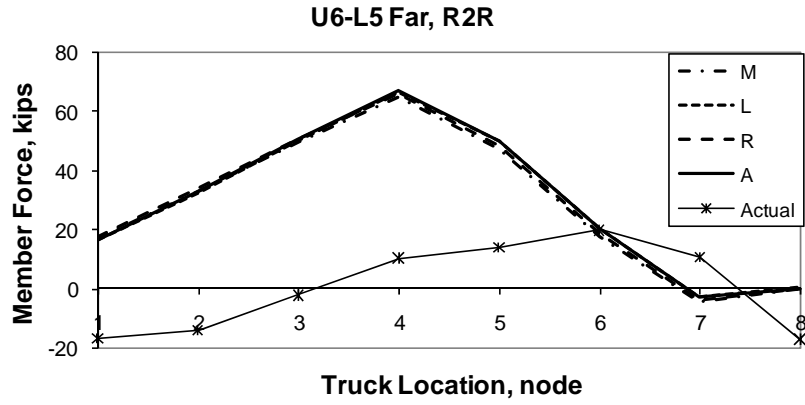


U6-L5 Near, Center

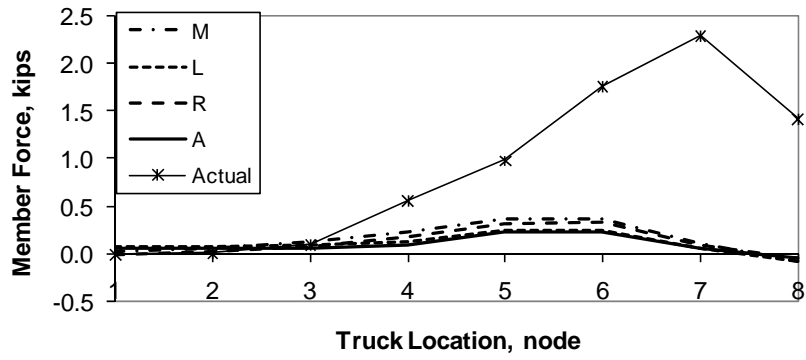




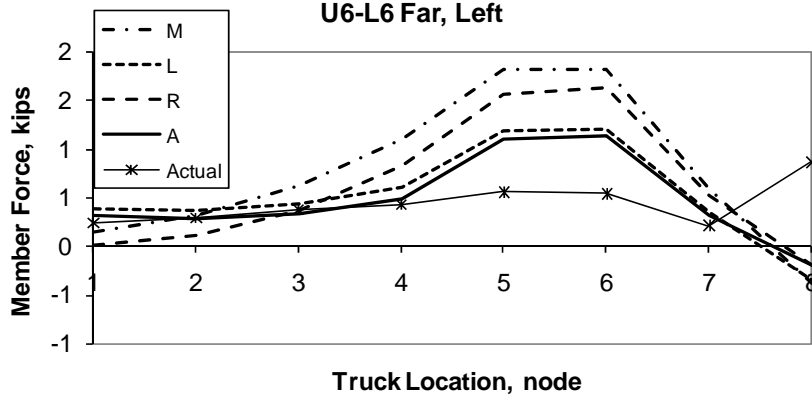




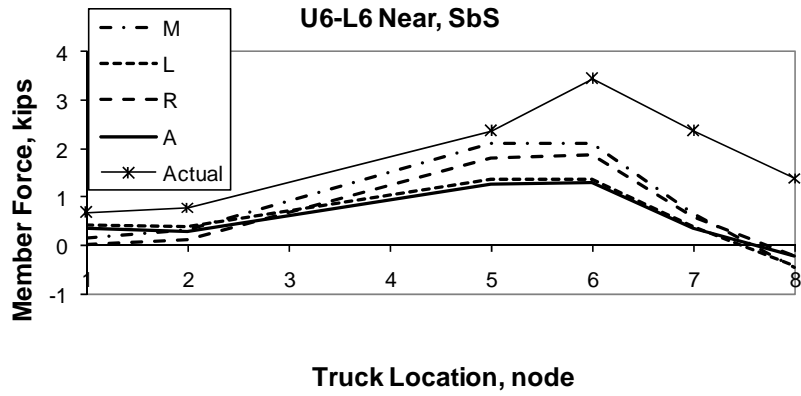
U6-L6 Near, Left

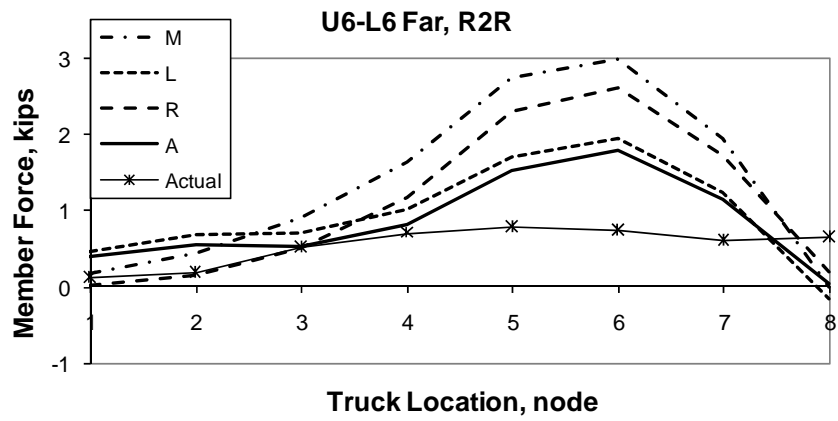
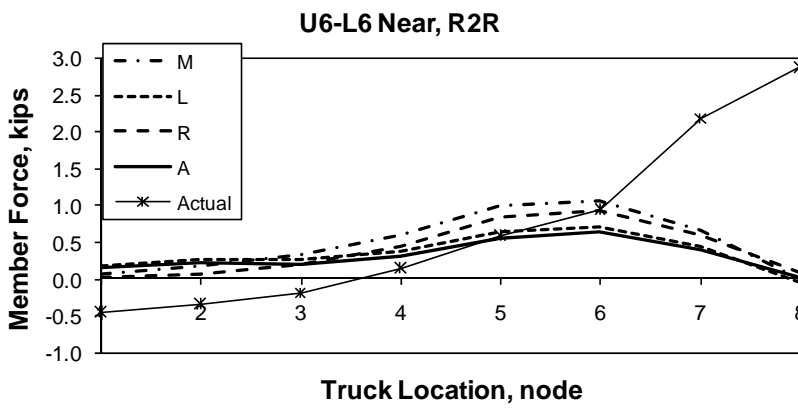
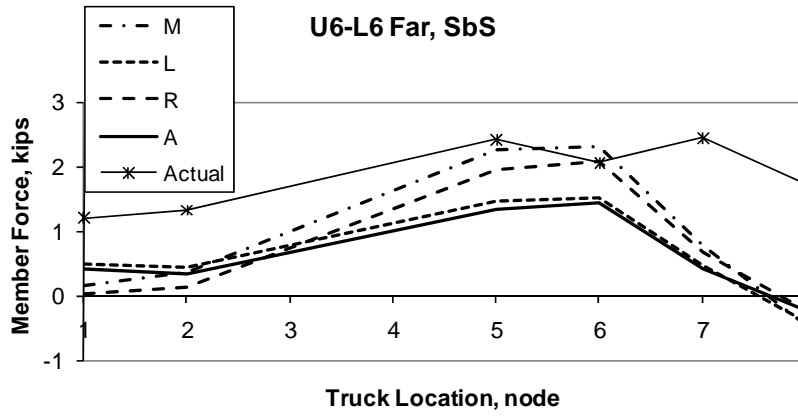


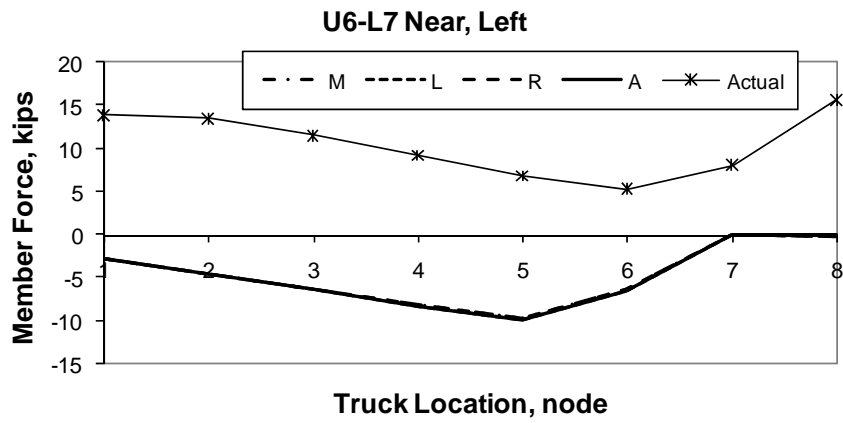
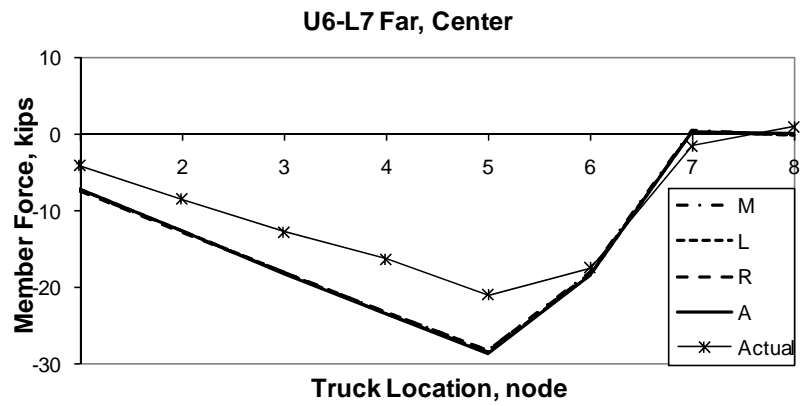
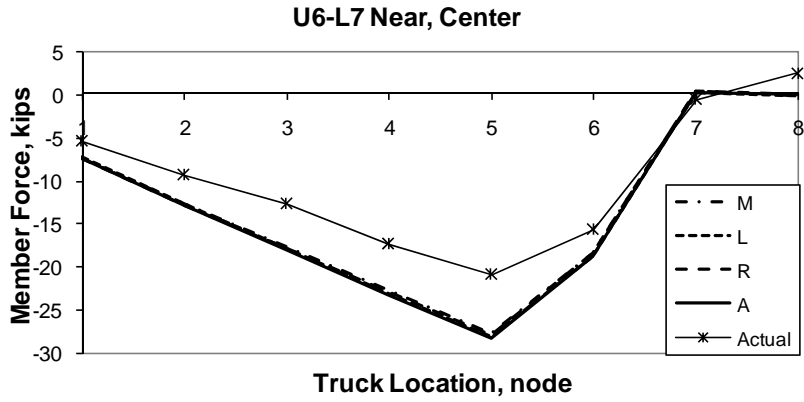
U6-L6 Far, Left

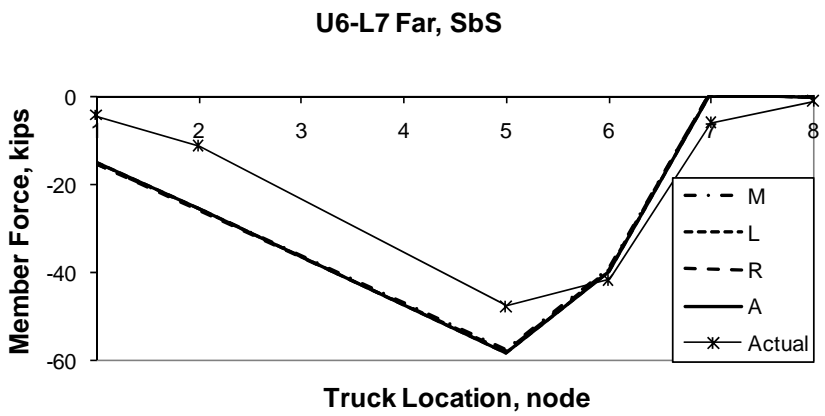
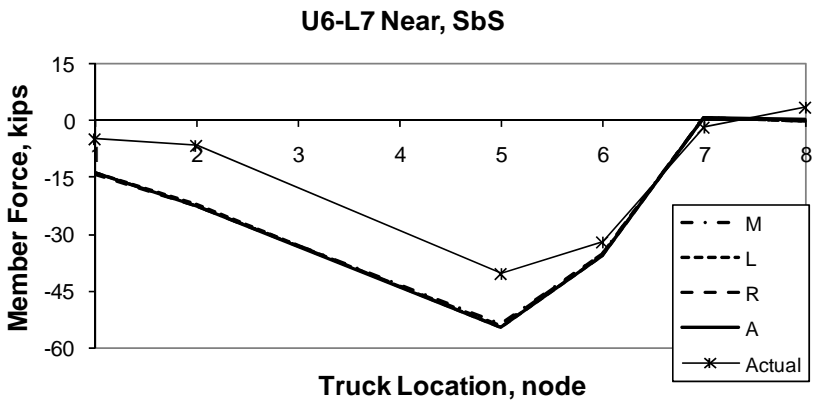
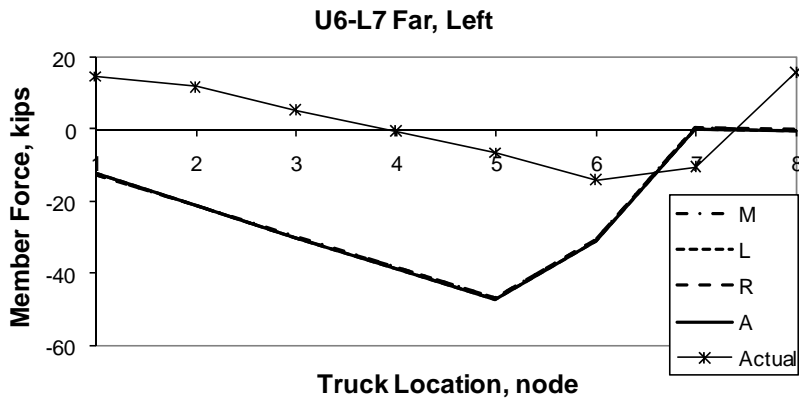


U6-L6 Near, SbS

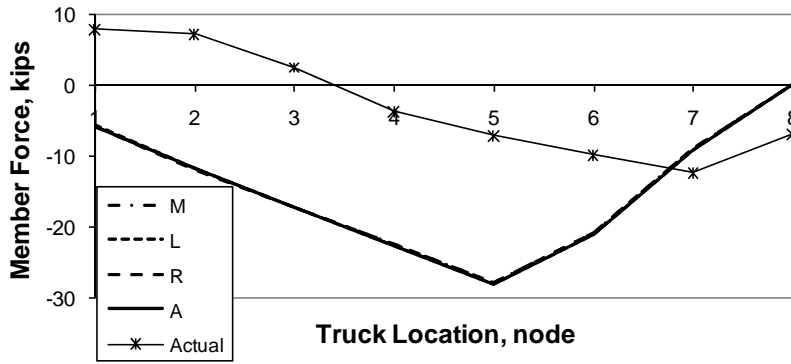




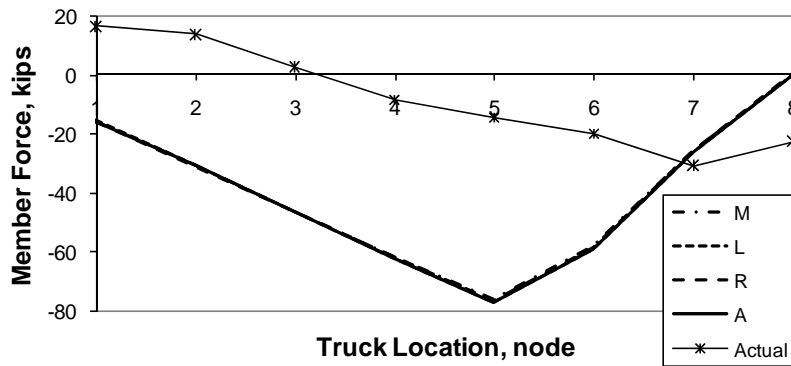




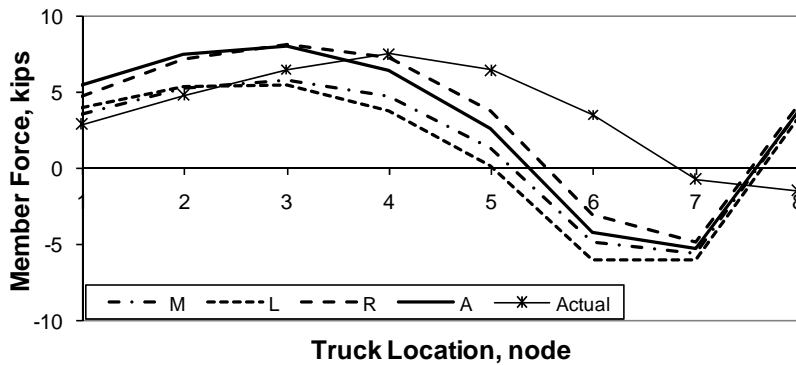
U6-L7 Near, R2R

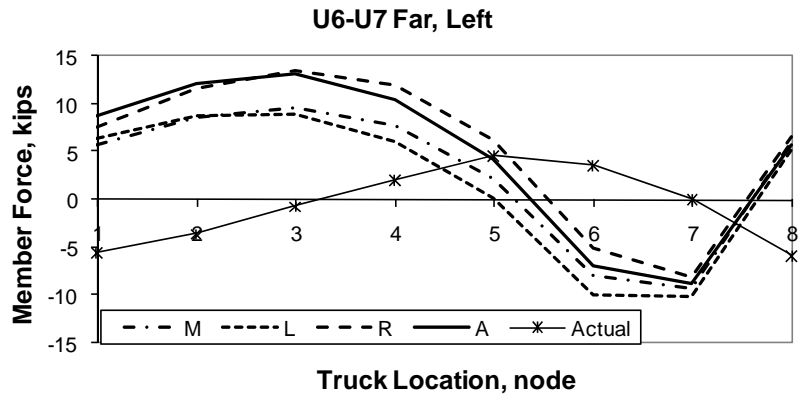
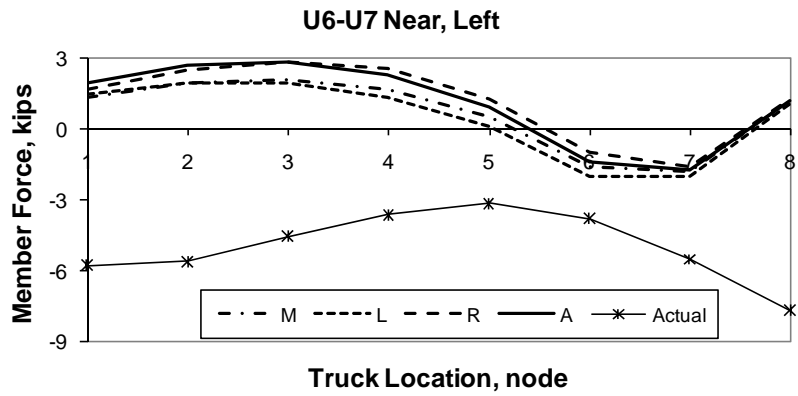
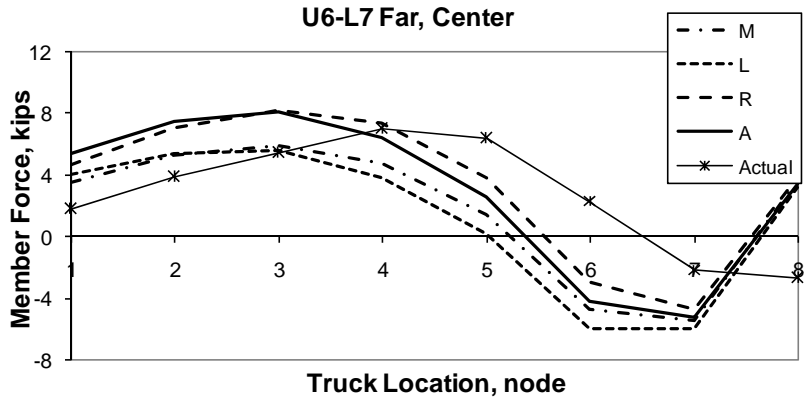


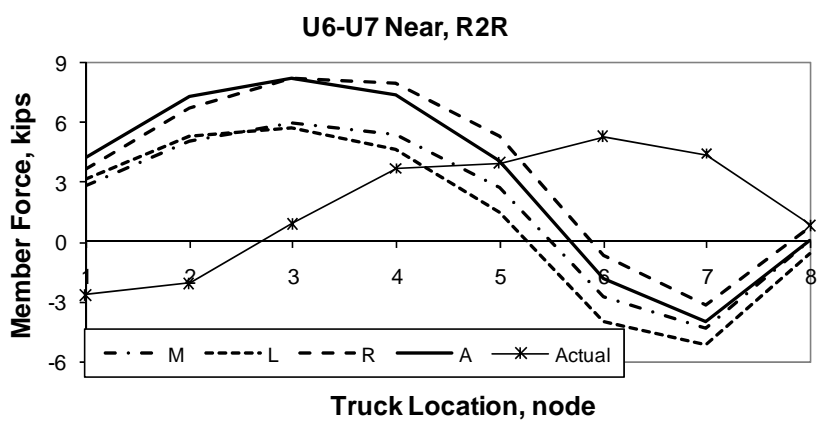
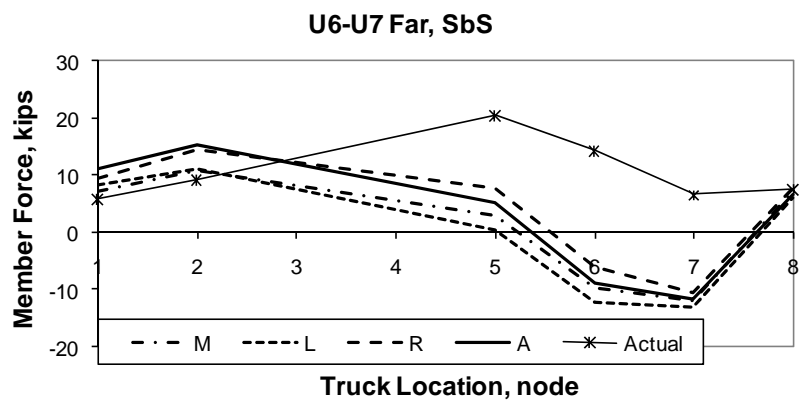
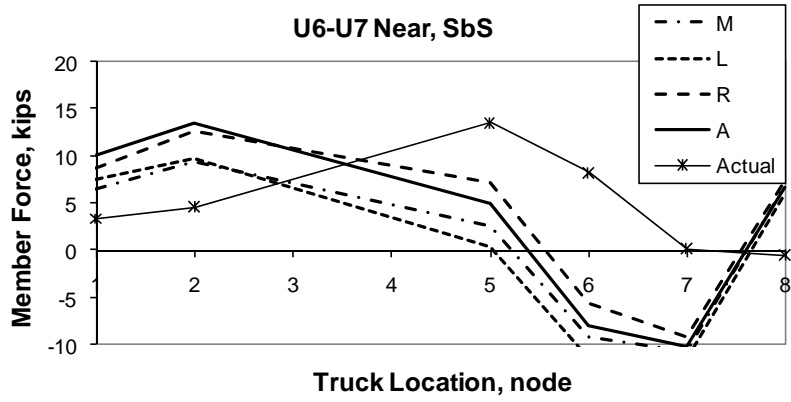
U6-L7 Far, R2R

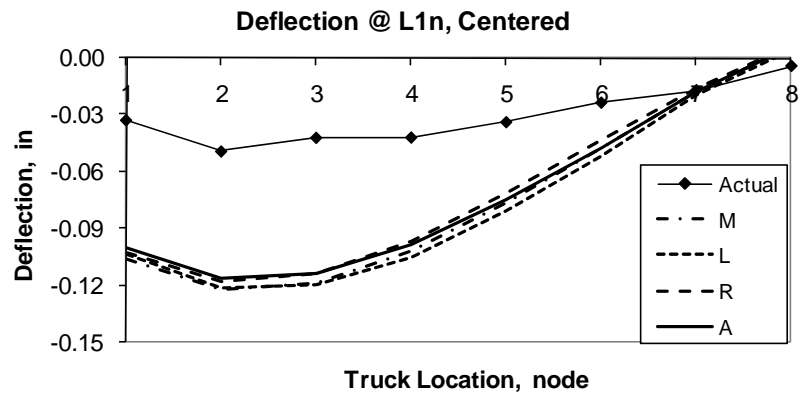
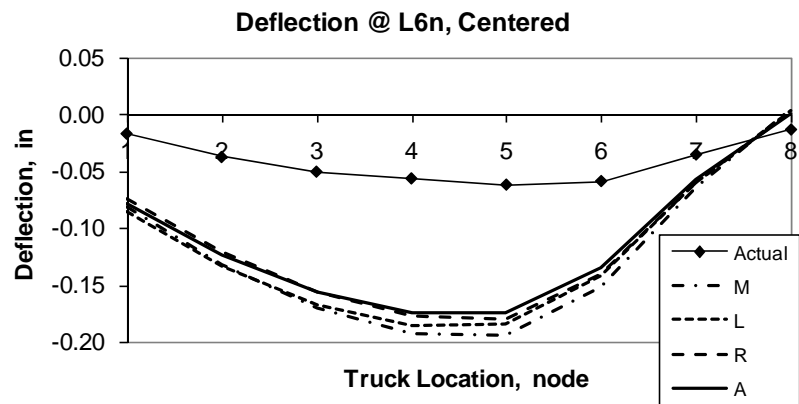
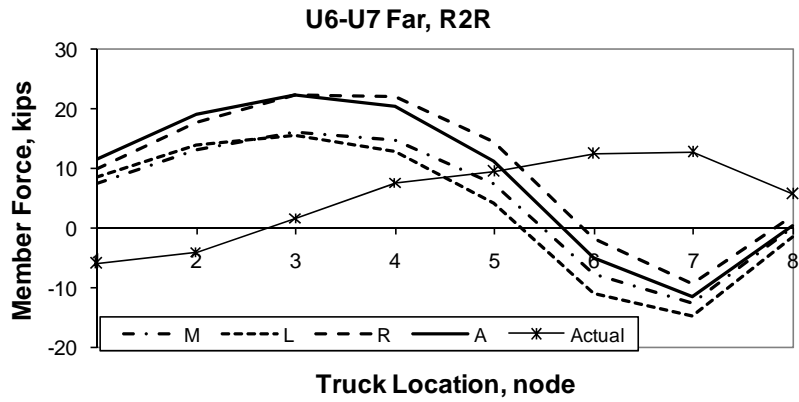


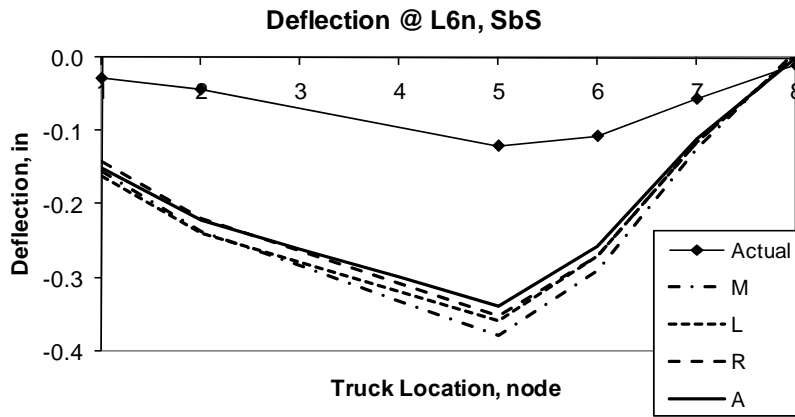
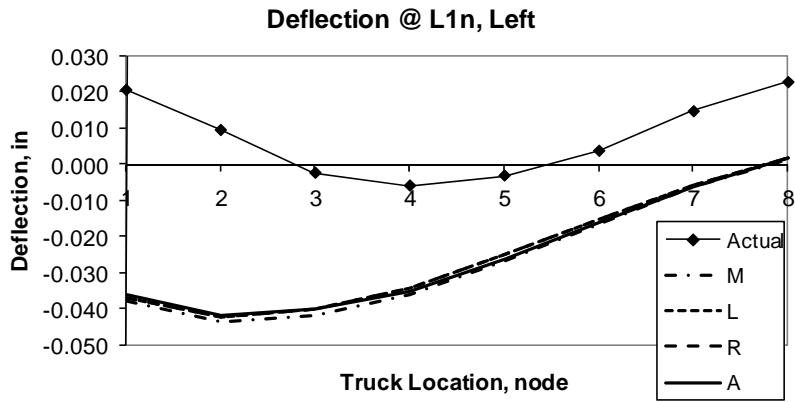
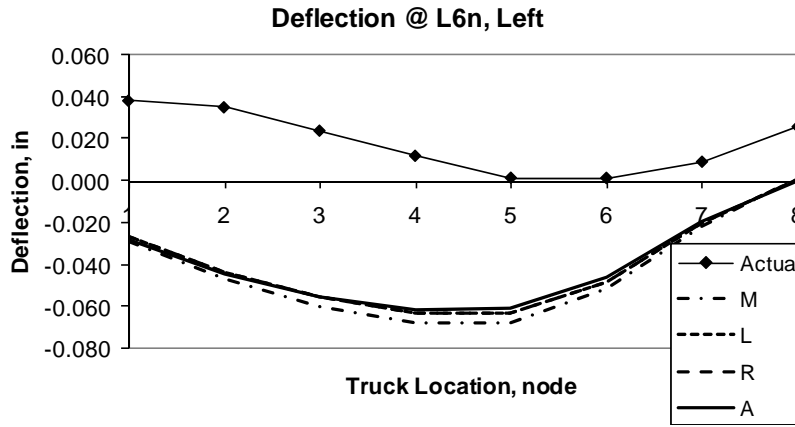
U6-U7 Near, Center

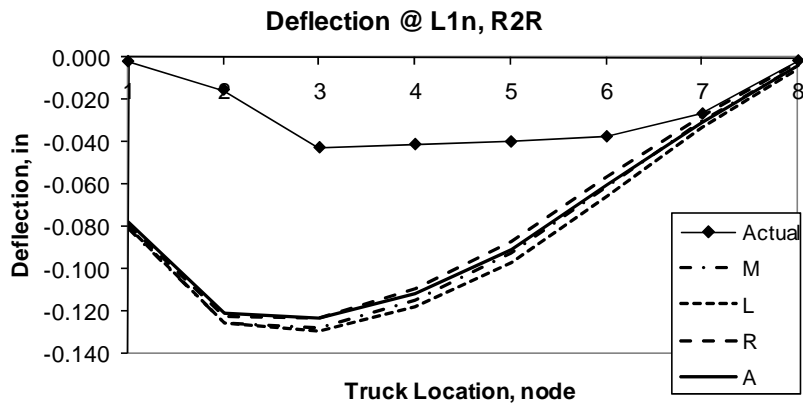
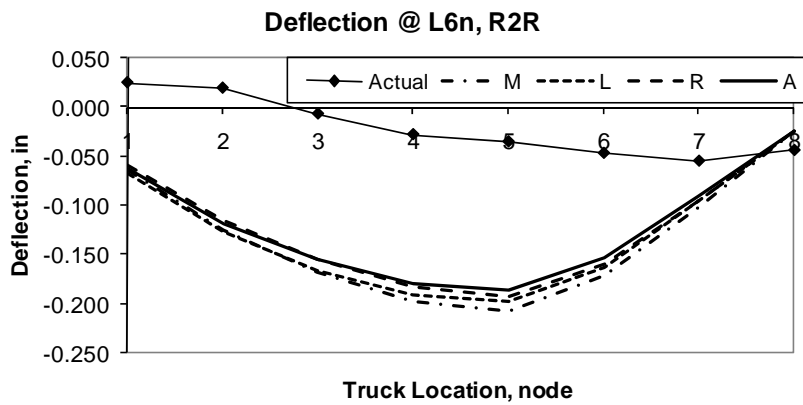
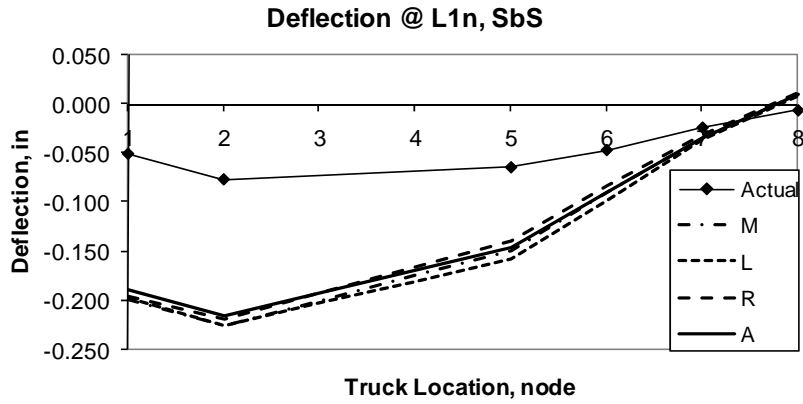




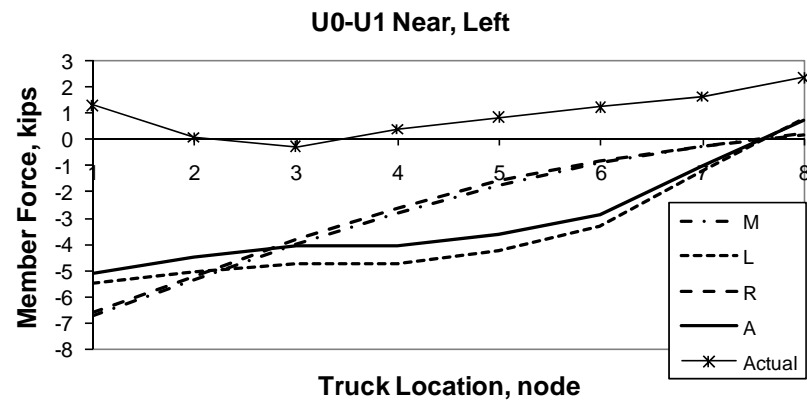
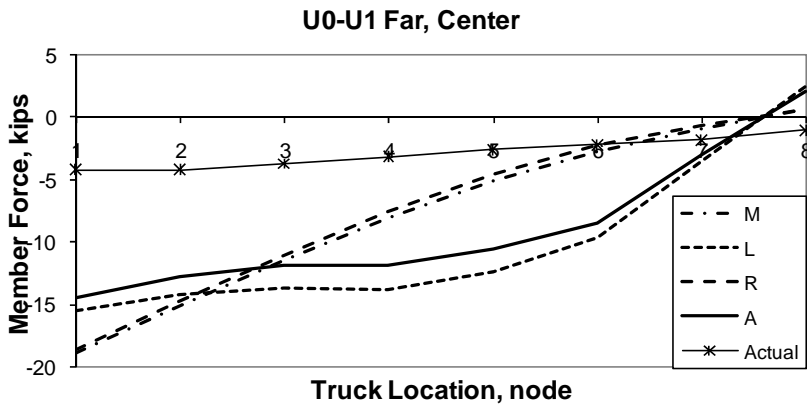
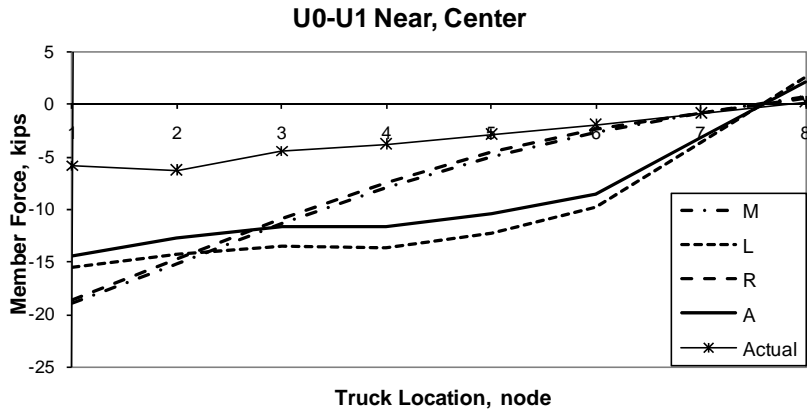




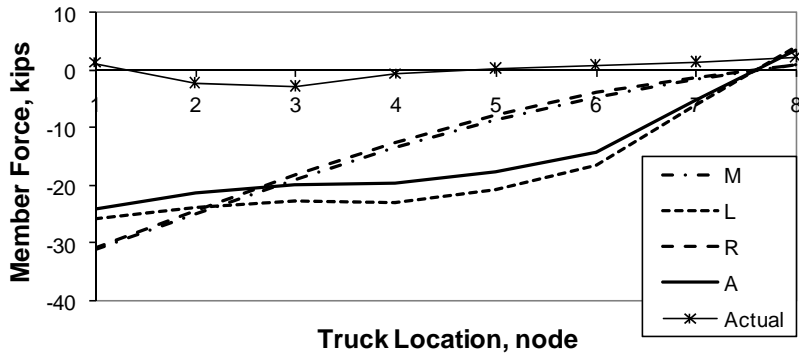




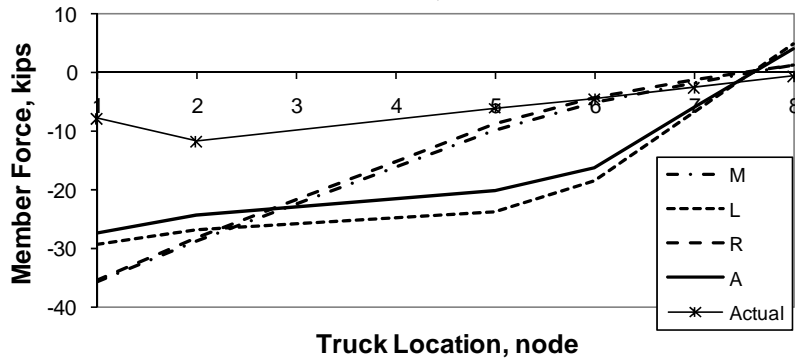
The following pages contain the member force plots for all monitored members and the member forces predicted by the frame model for all four load regimes. They are organized by member. Node deflection plots are included, and the deflections predicted by the frame model for all four load regimes follow. They are organized by node.



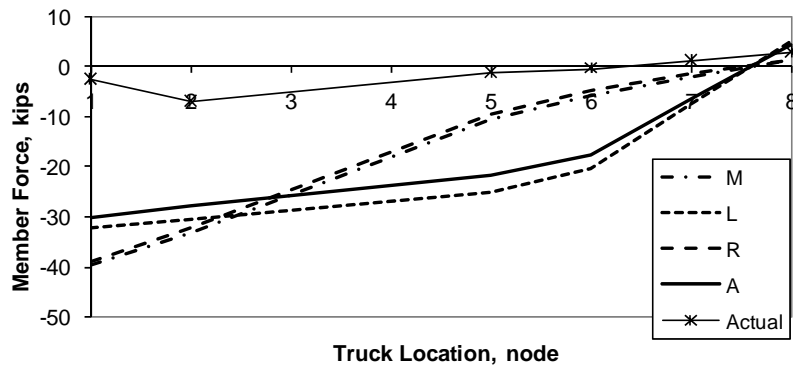
U0-U1 Far, Left

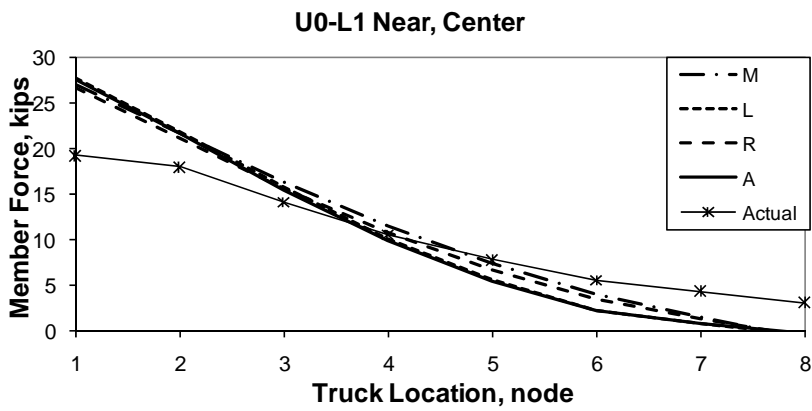
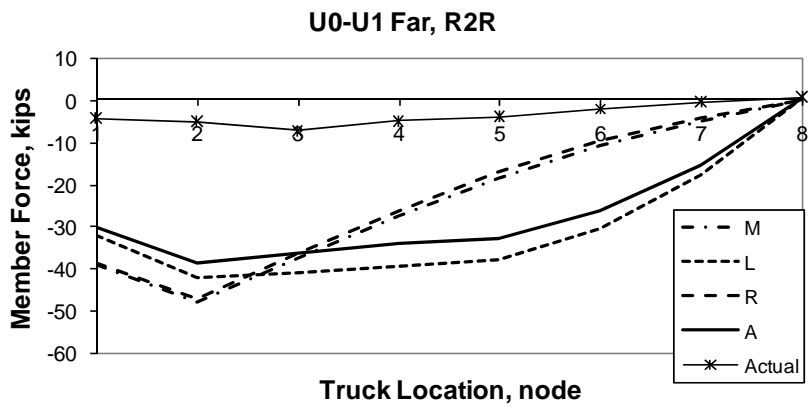
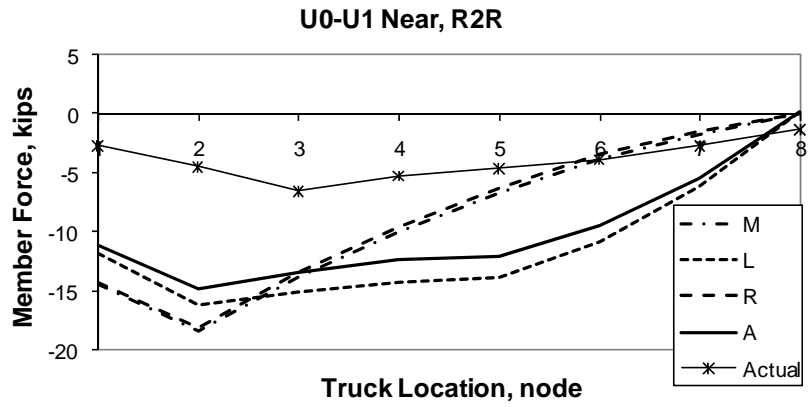


U0-U1 Near, SbS

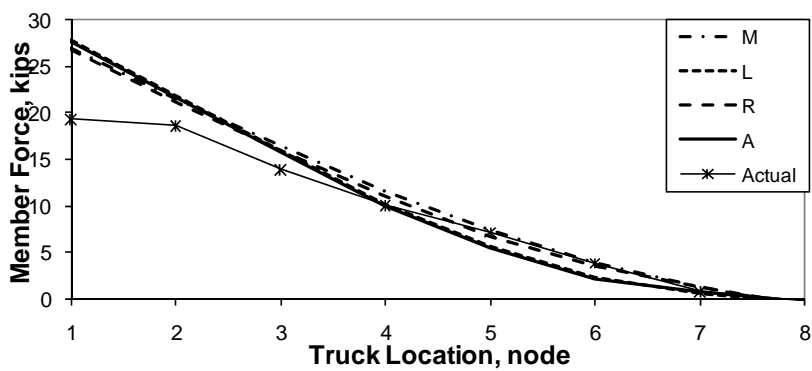


U0-U1 Far, SbS

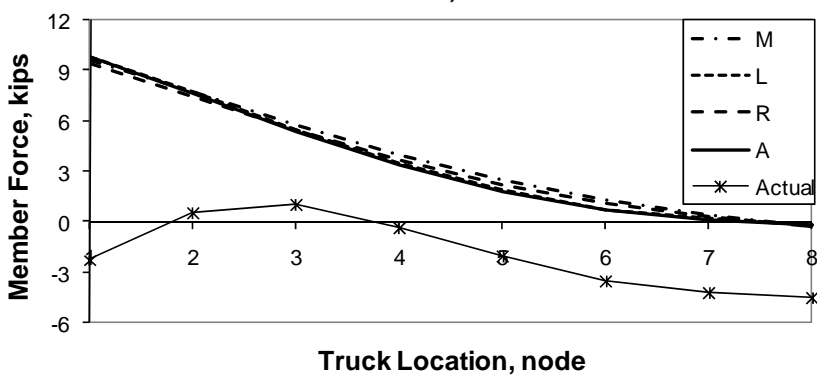




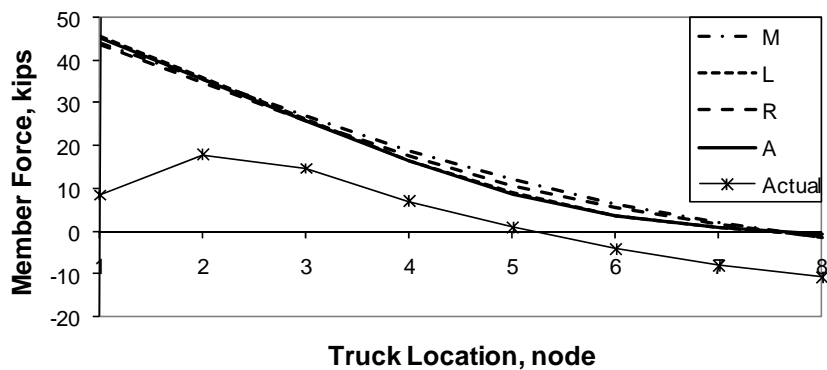
U0-L1 Far, Center



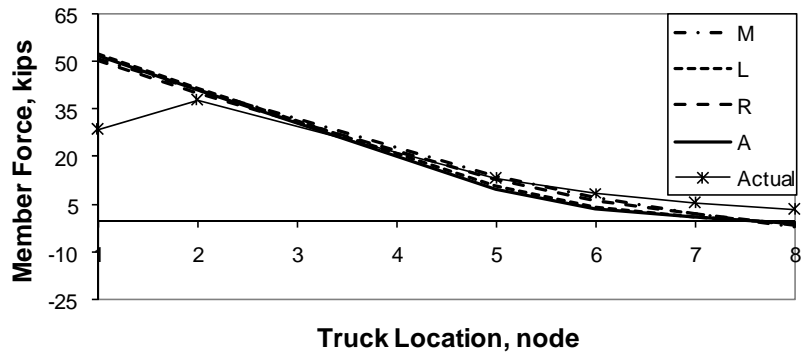
U0-L1 Near, Left



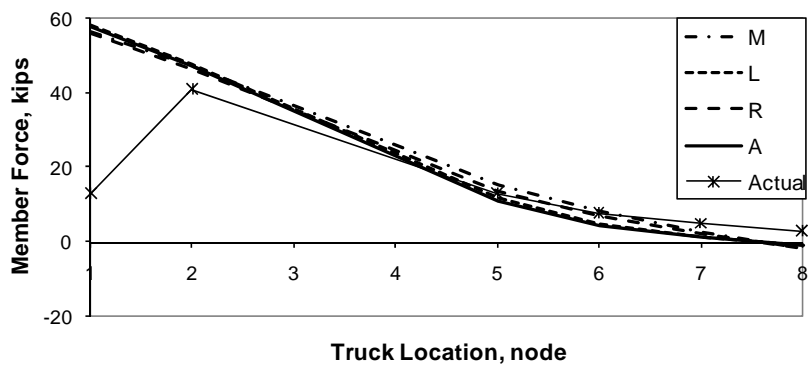
U0-L1 Far, Left



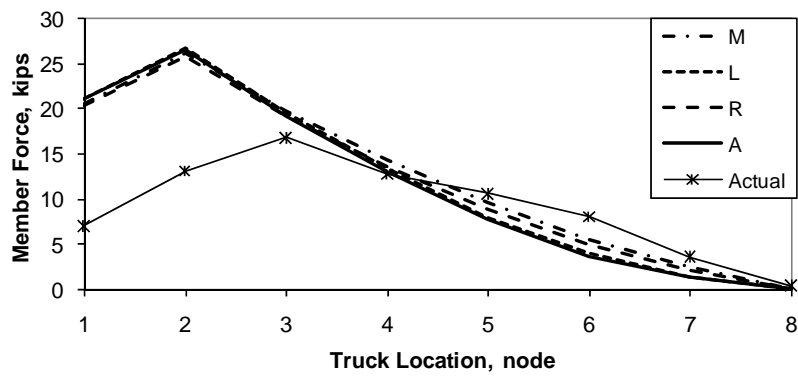
U0-L1 Near, SbS

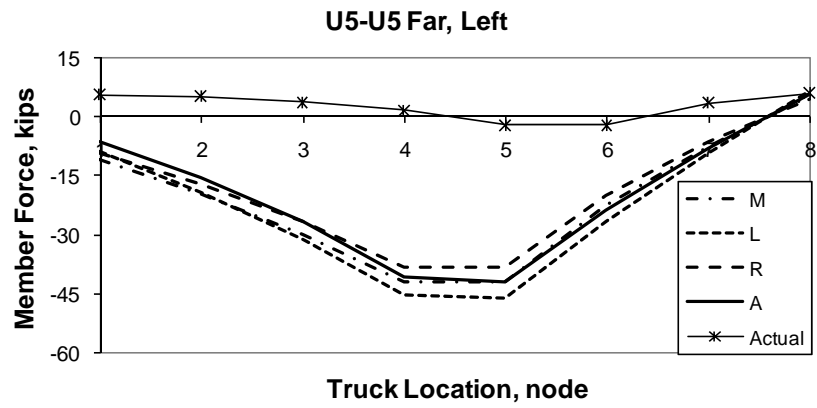
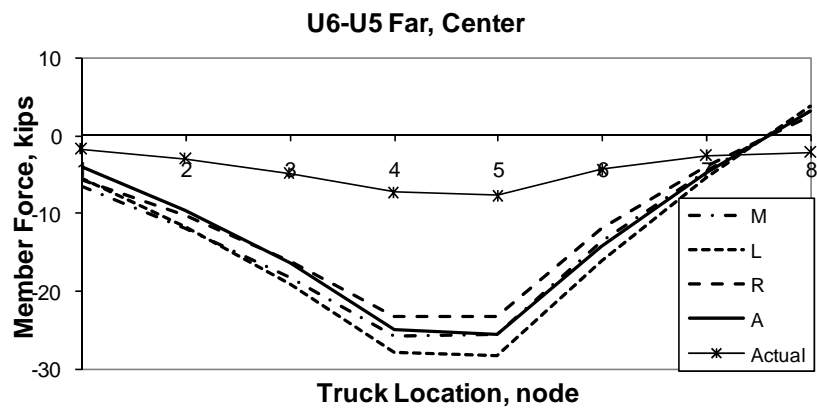
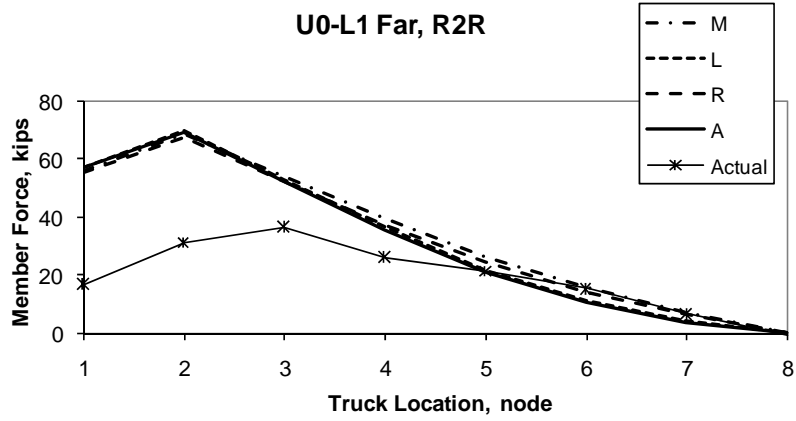


U0-L1 Far, SbS

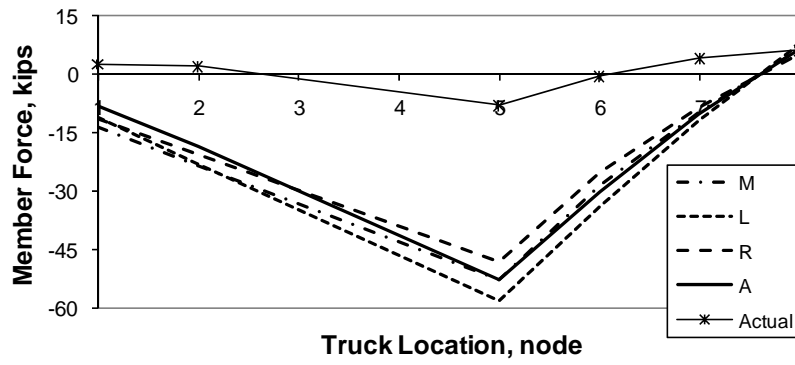


U0-L1 Near, R2R

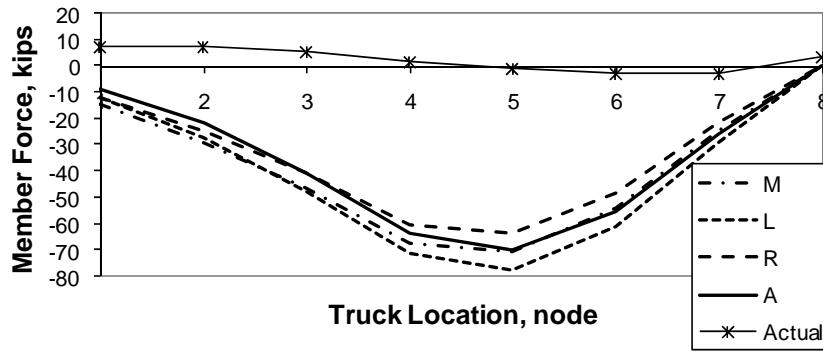




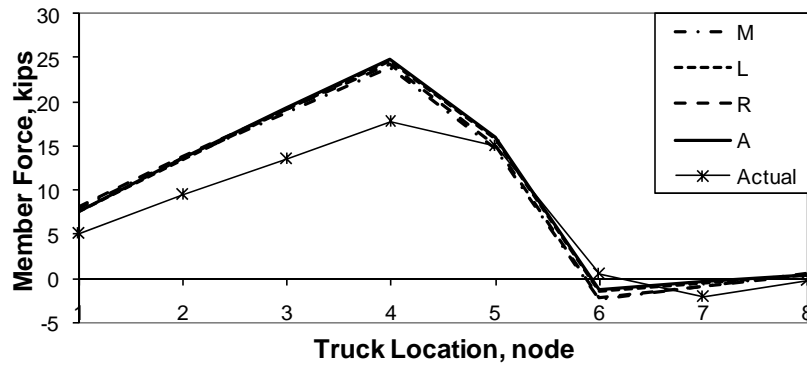
U6-U5 Far, SbS

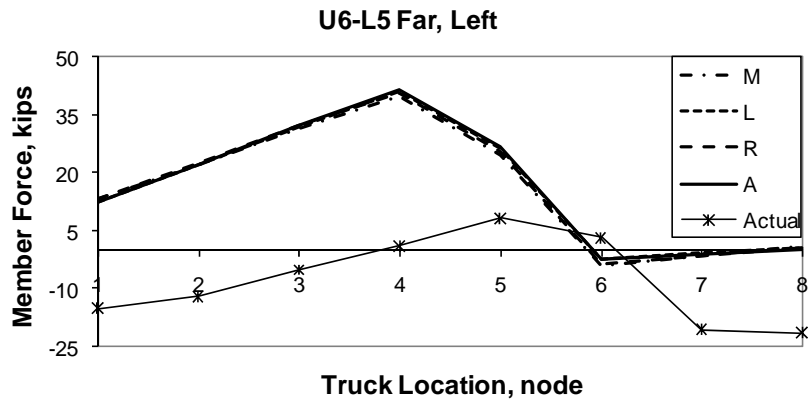
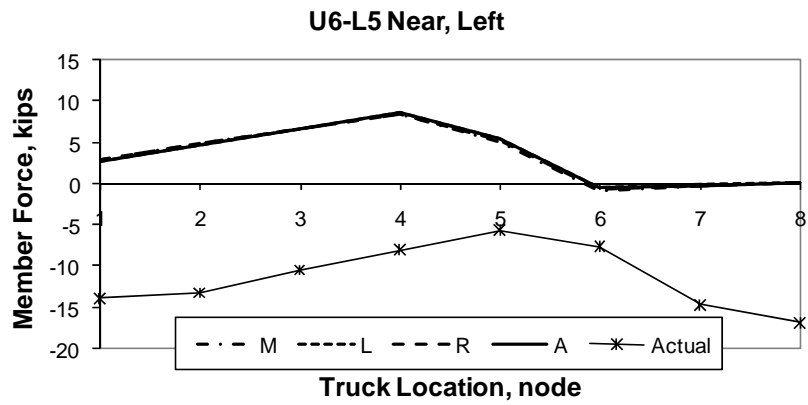
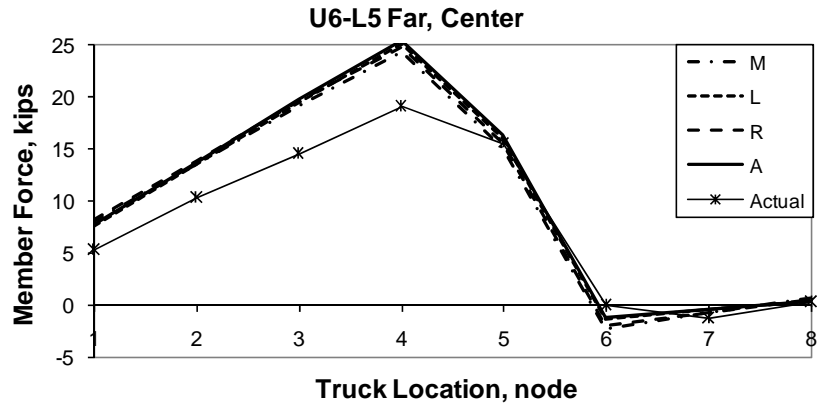


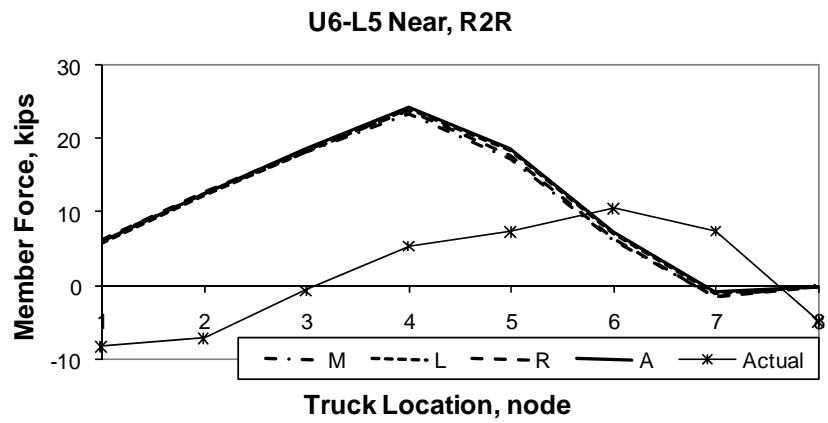
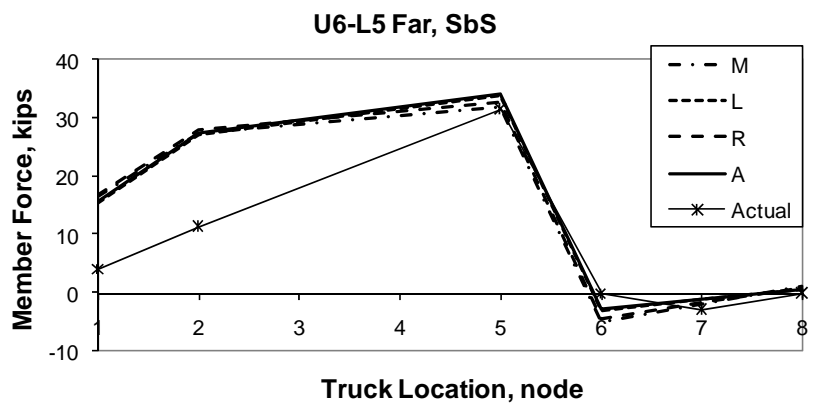
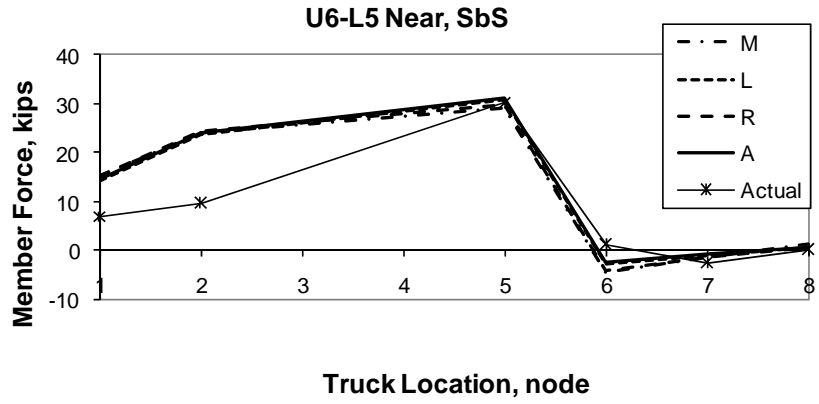
U6-U5 Far, R2R



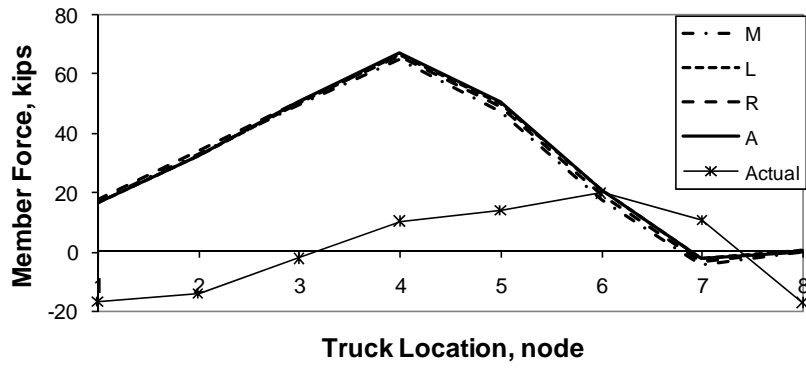
U6-L5 Near, Center



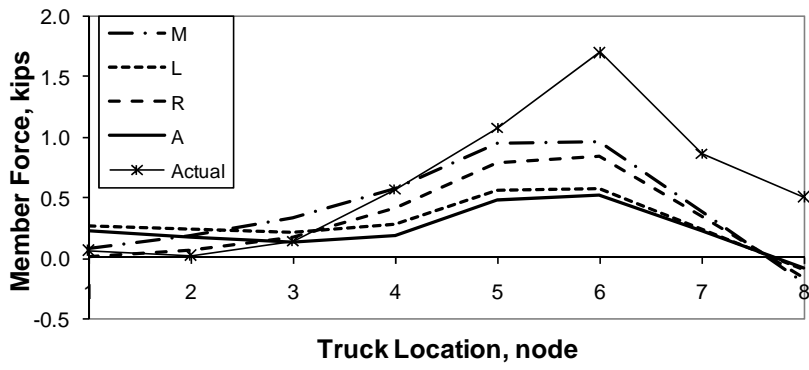




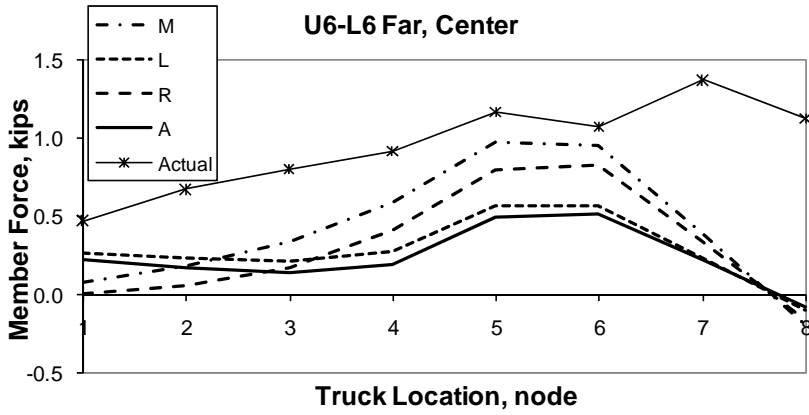
U6-L5 Far, R2R



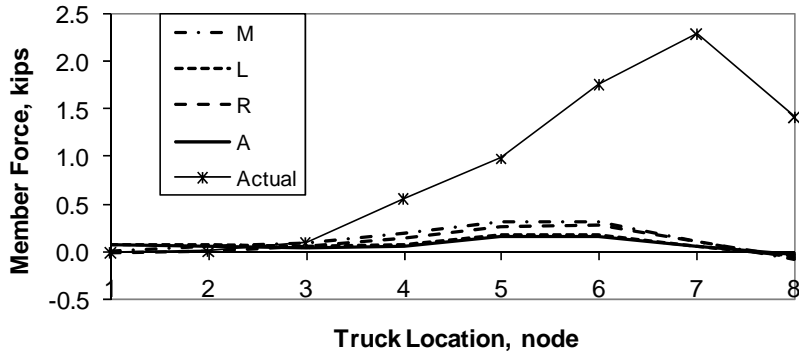
U6-L6 Near, Center



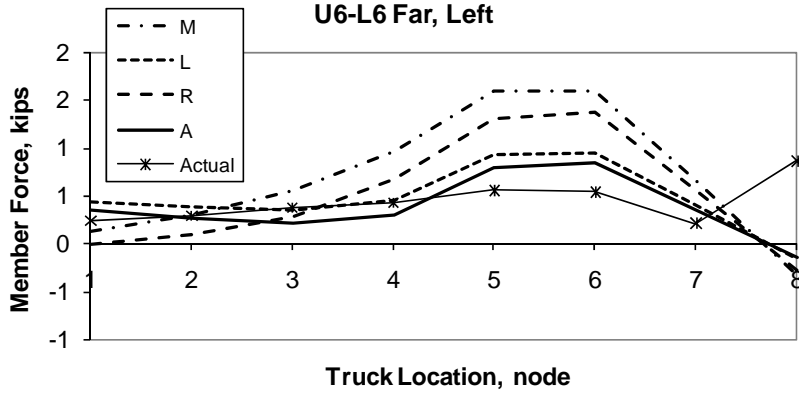
U6-L6 Far, Center



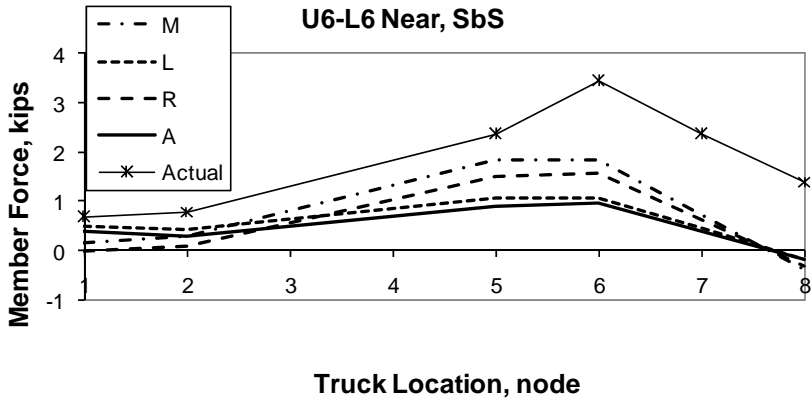
U6-L6 Near, Left

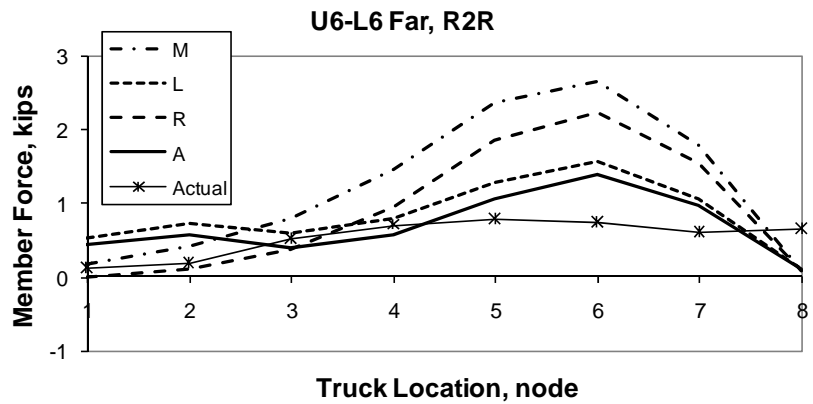
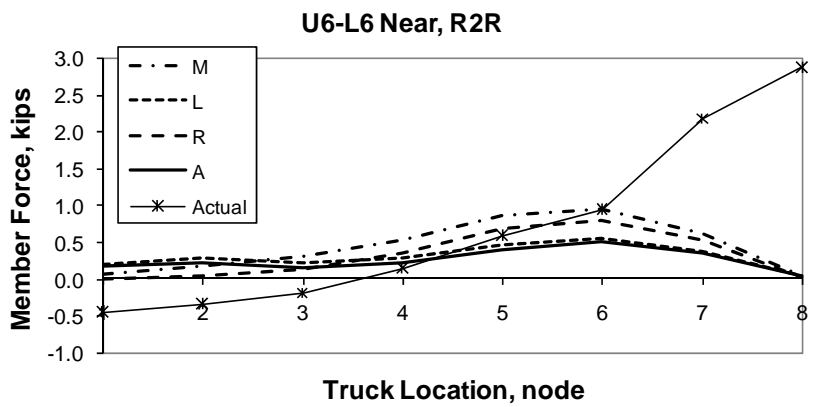
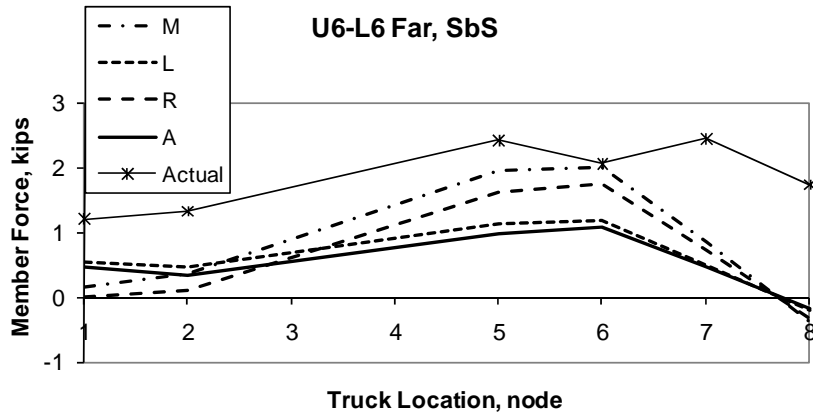


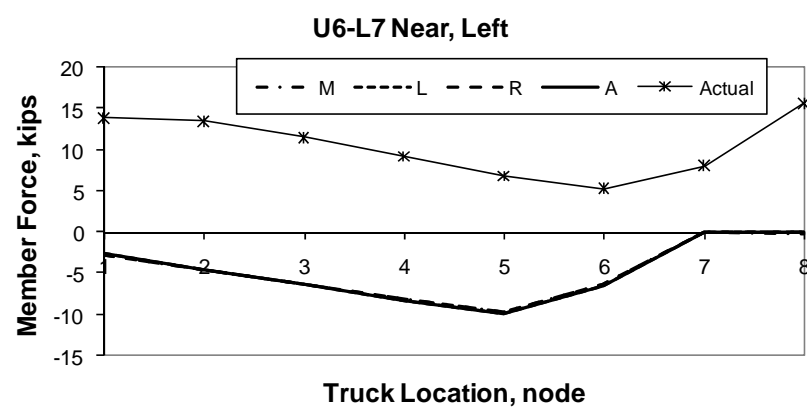
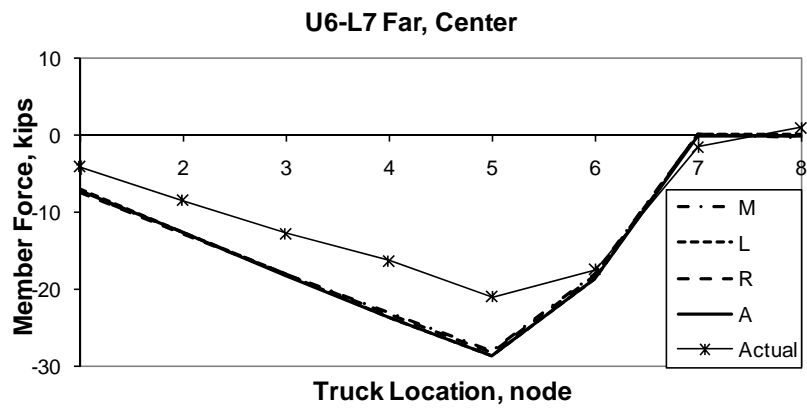
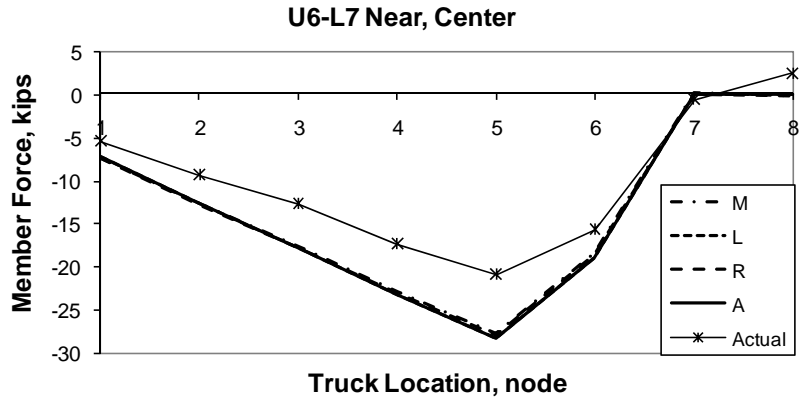
U6-L6 Far, Left

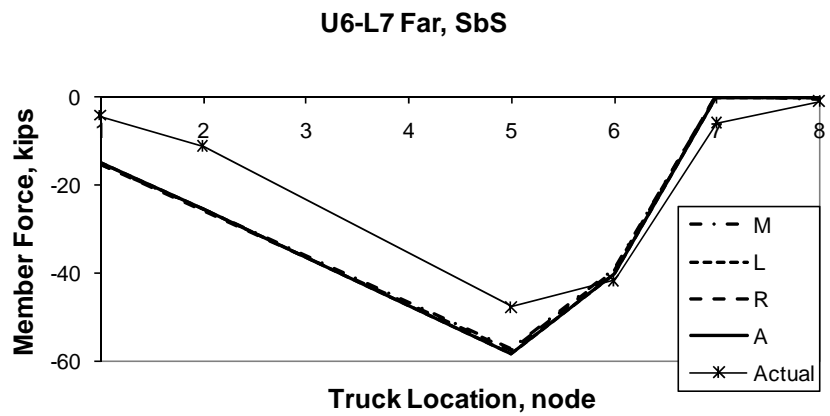
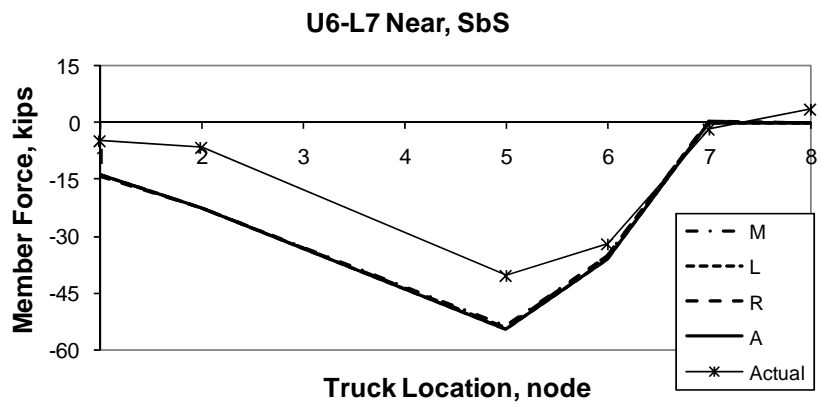
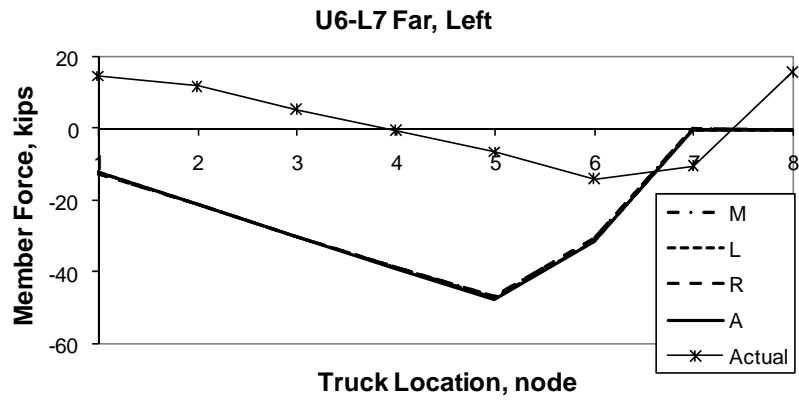


U6-L6 Near, SbS

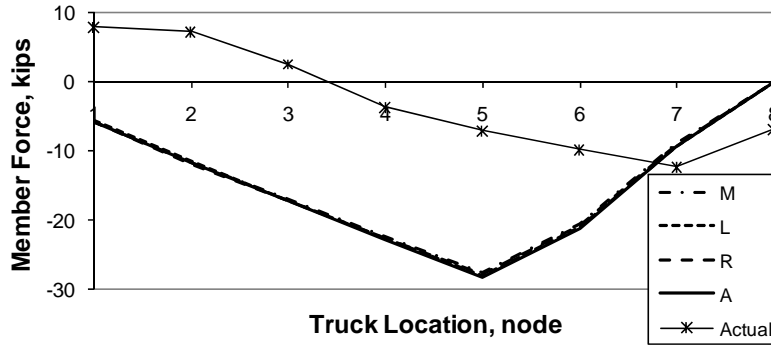




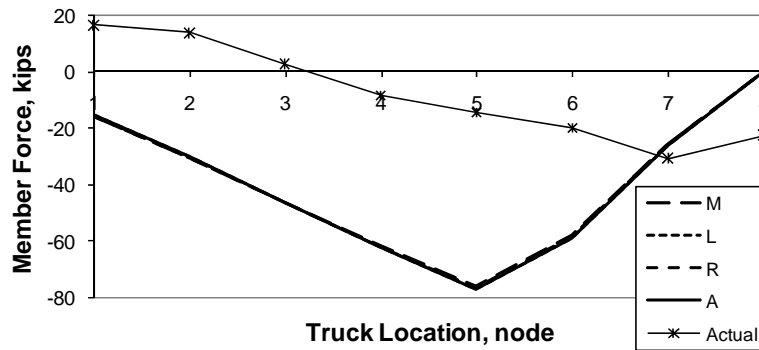




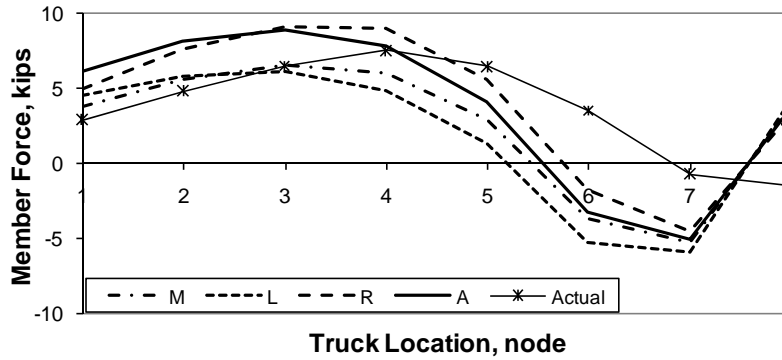
U6-L7 Near, R2R



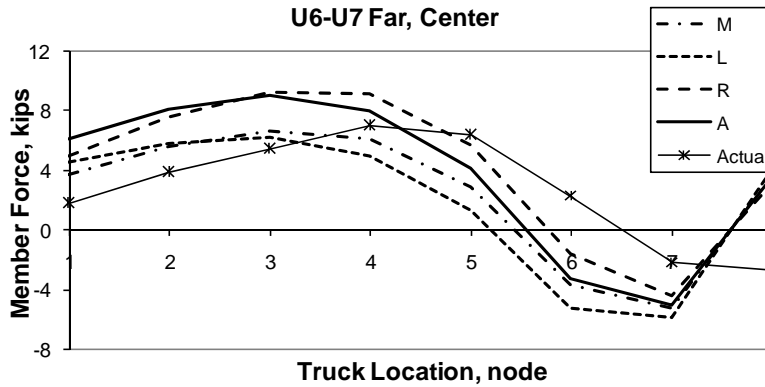
U6-L7 Far, R2R

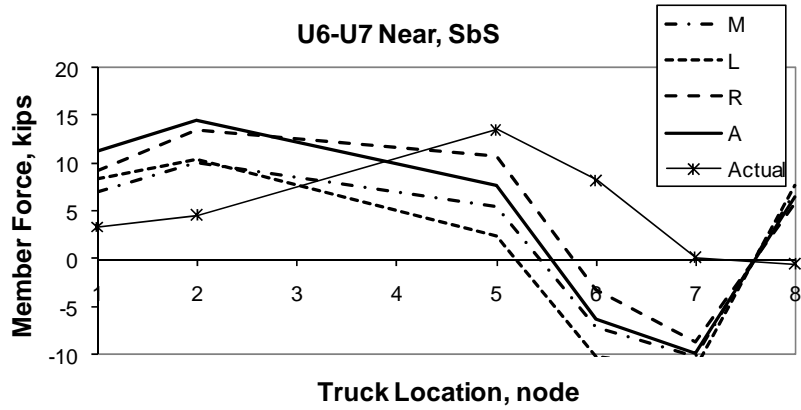
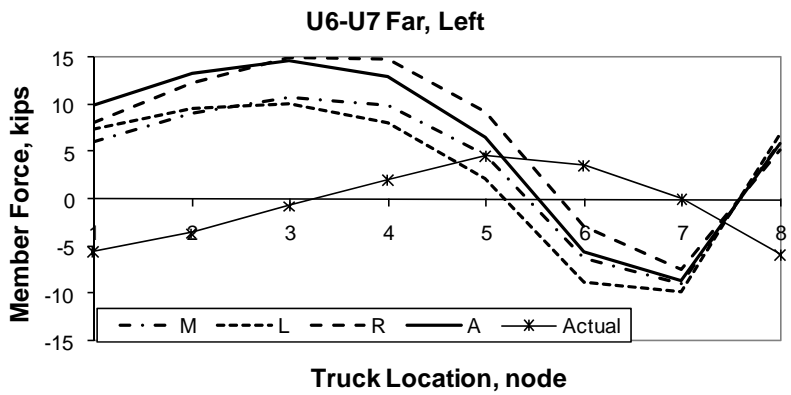
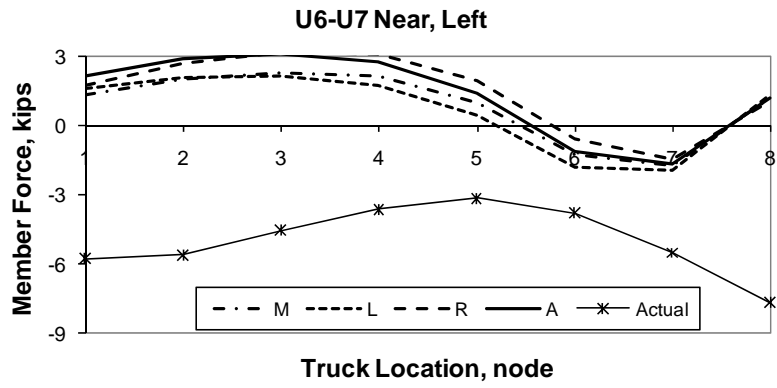


U6-U7 Near, Center

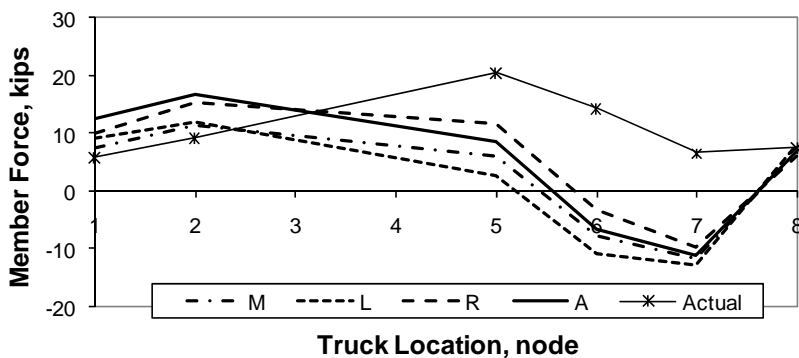


U6-U7 Far, Center

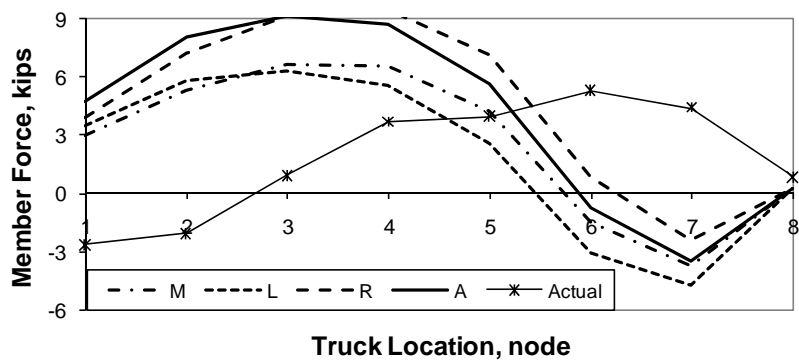




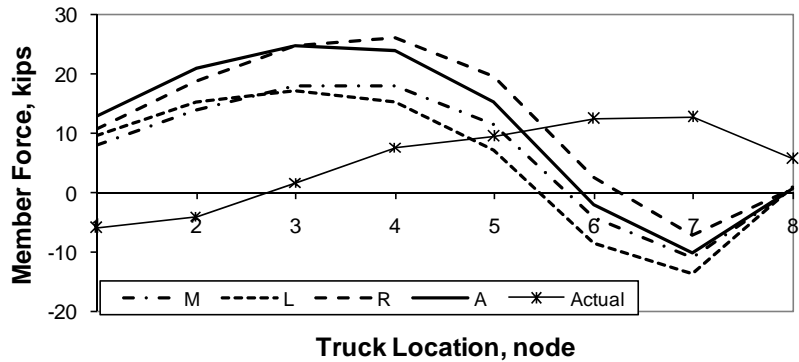
U6-U7 Far, SbS

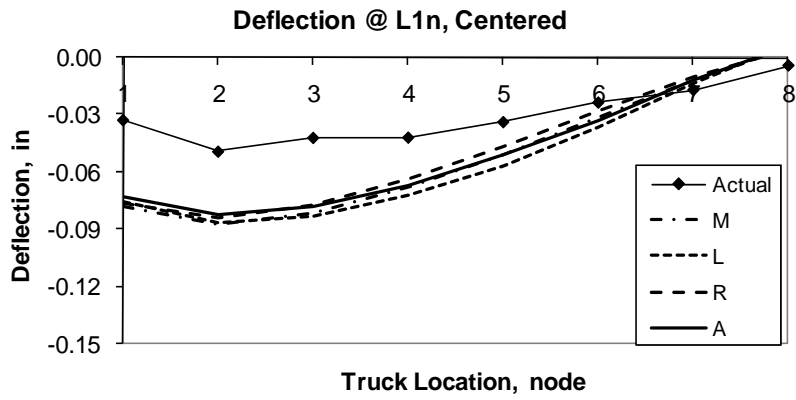
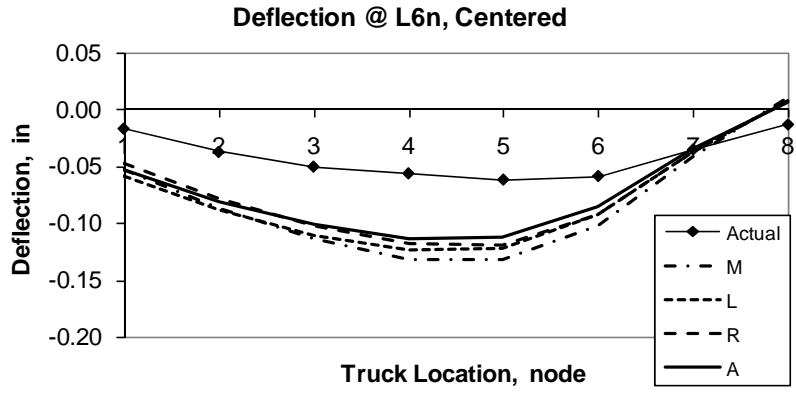


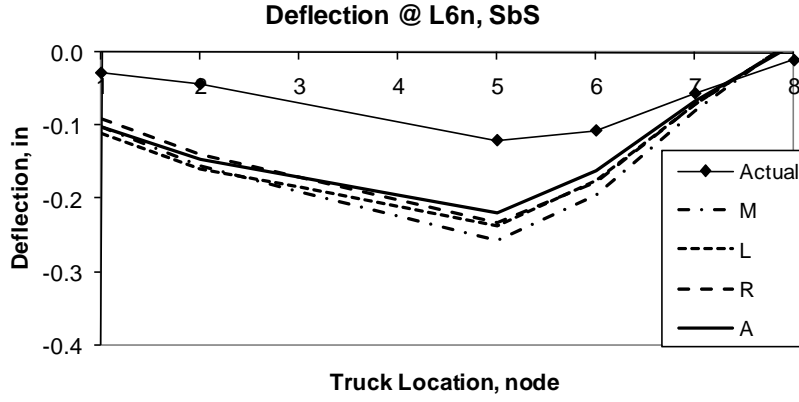
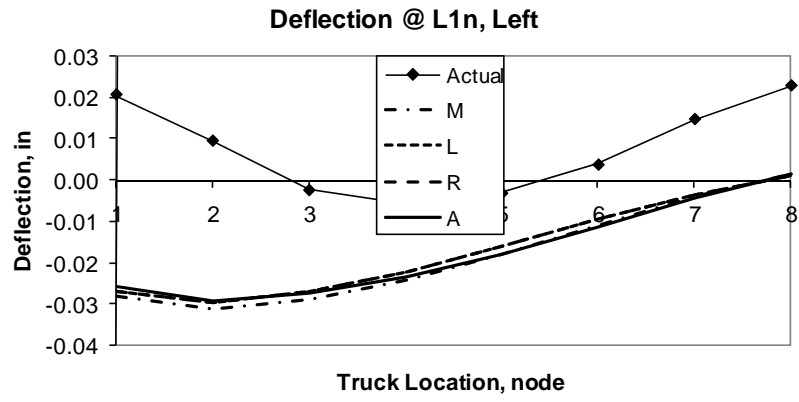
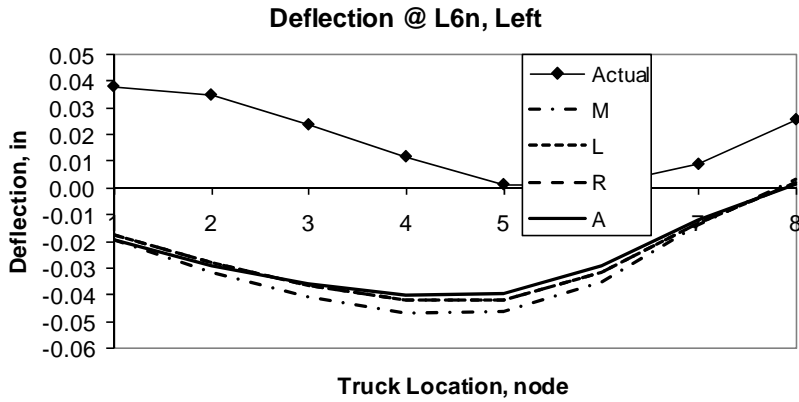
U6-U7 Near, R2R

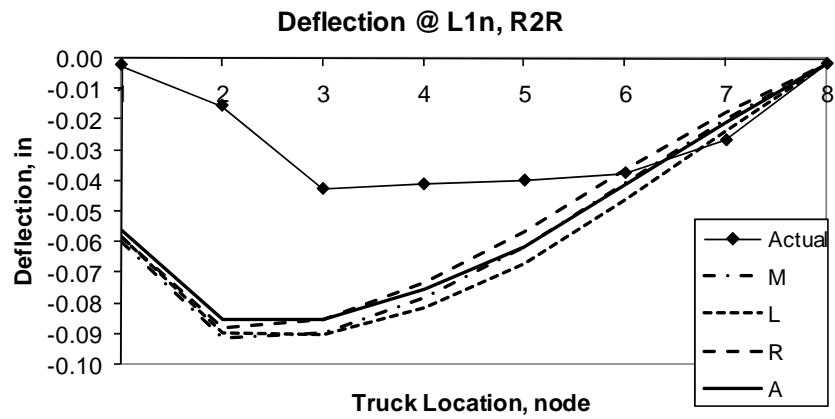
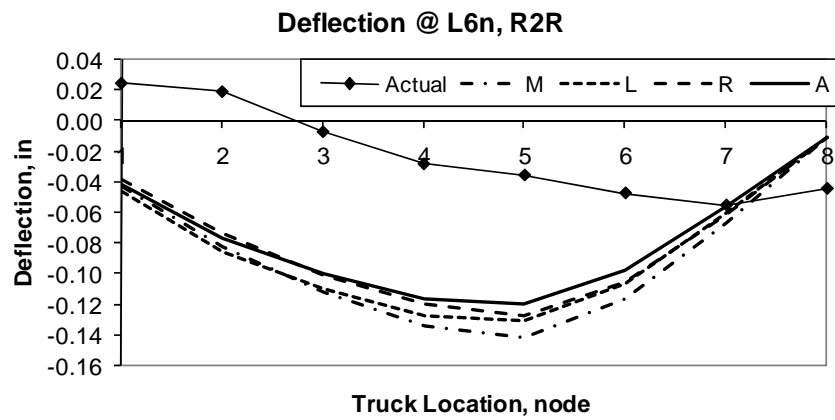
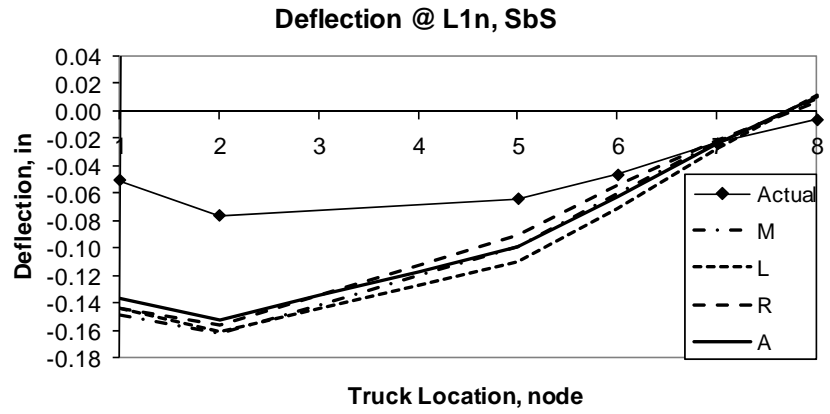


U6-U7 Far, R2R

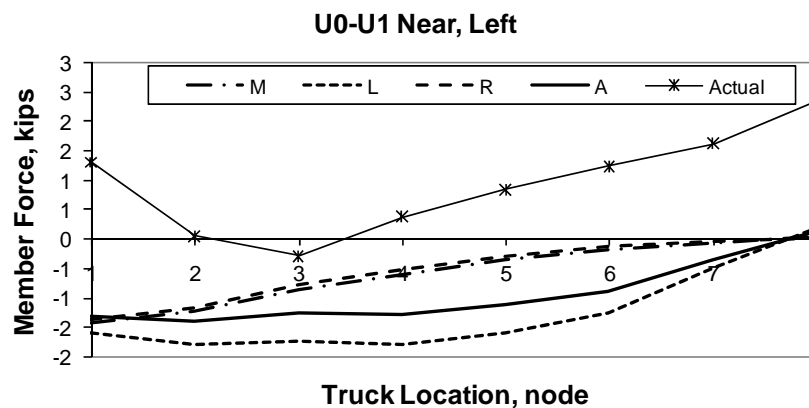
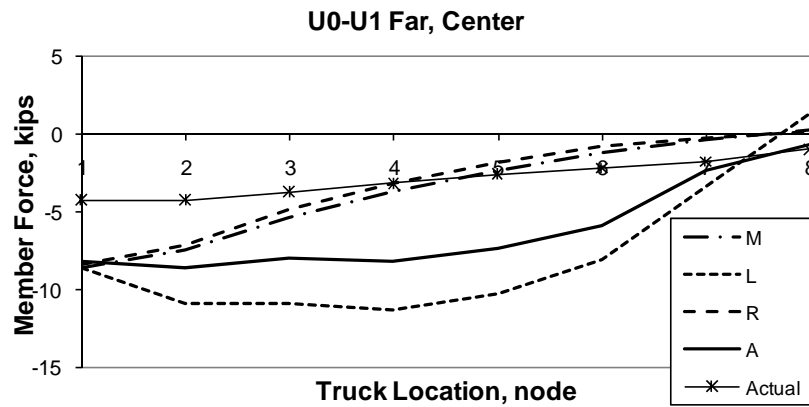
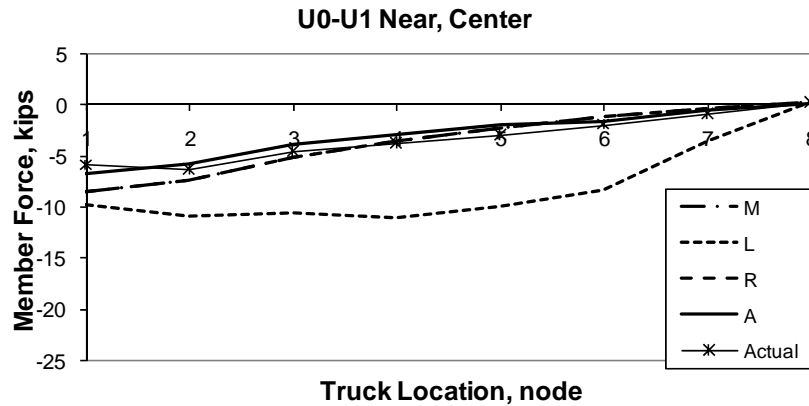




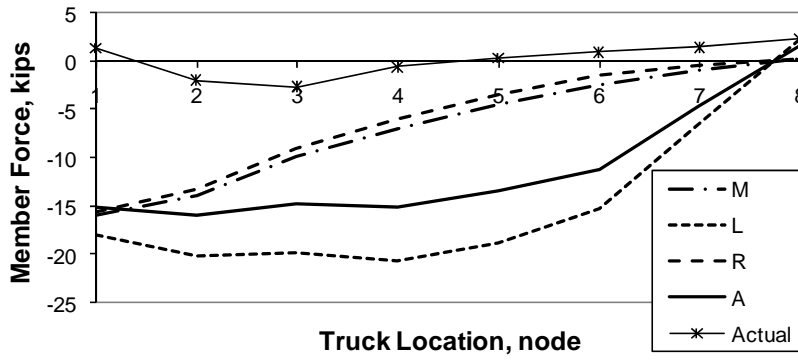




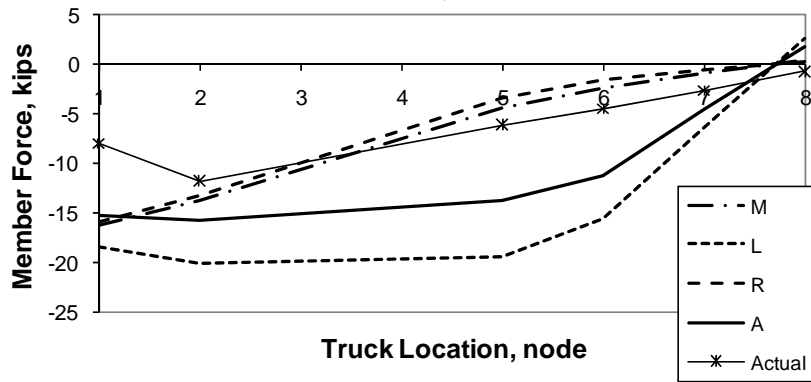
The following pages contain the member force plots for all monitored members and the member forces predicted by the stringer frame model for all four load regimes. They are organized by member. Node deflection plots are included, and the deflections predicted by the stringer frame model for all four load regimes follow. They are organized by node.



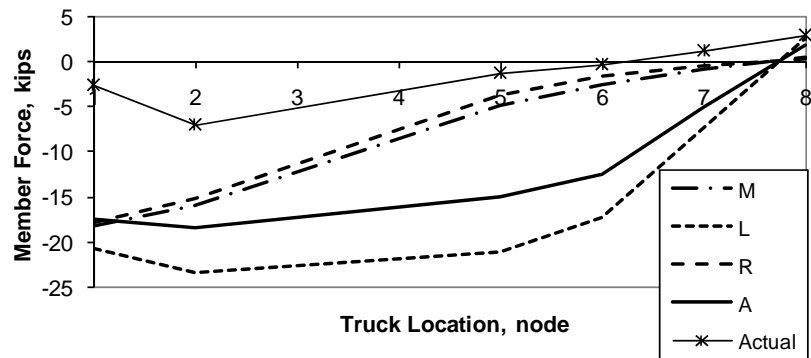
U0-U1 Far, Left



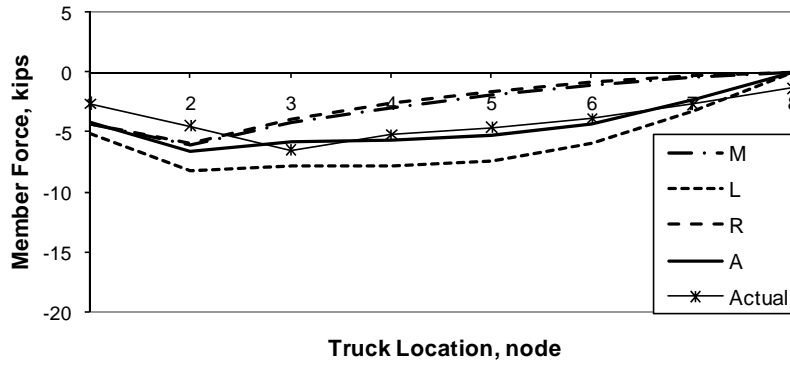
U0-U1 Near, SbS



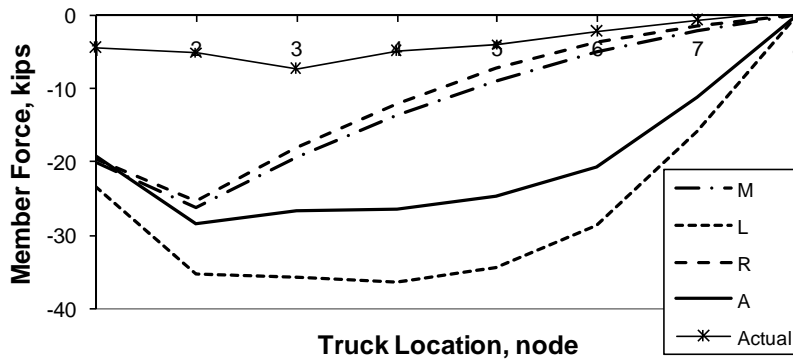
U0-U1 Far, SbS



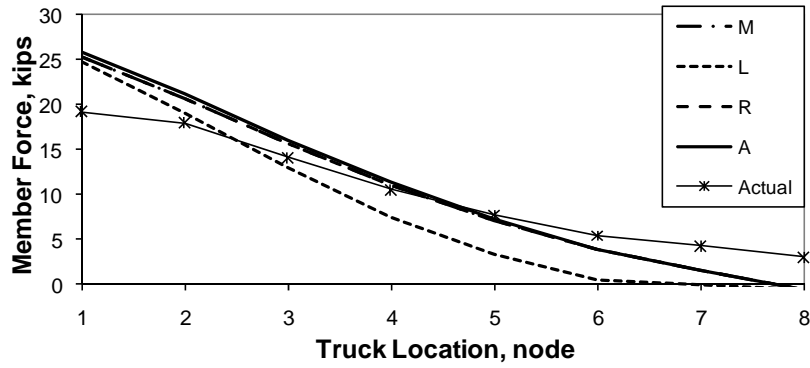
U0-U1 Near, R2R



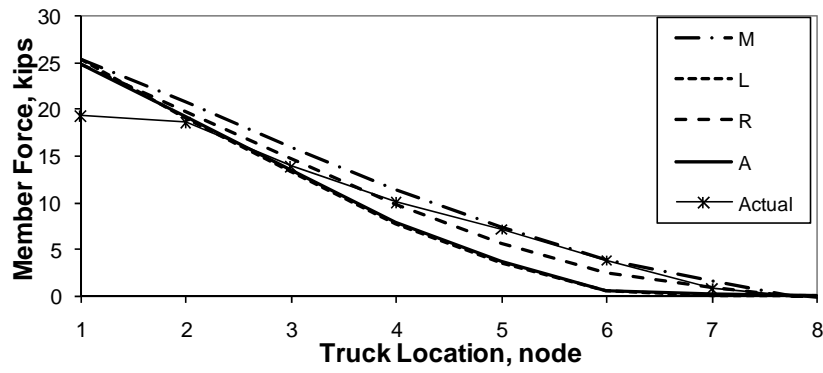
U0-U1 Far, R2R



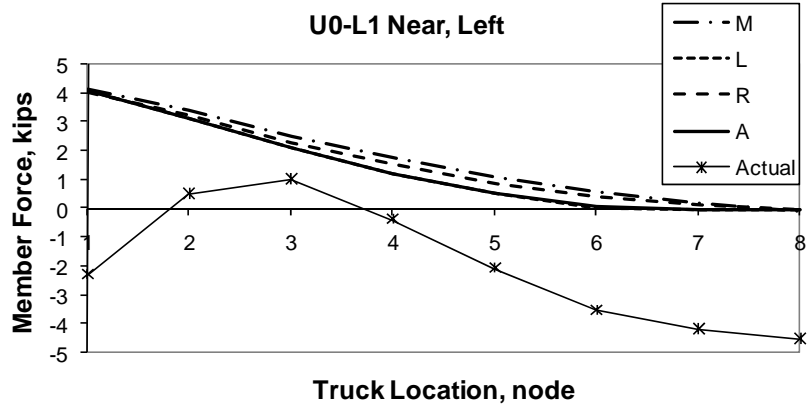
U0-L1 Near, Center



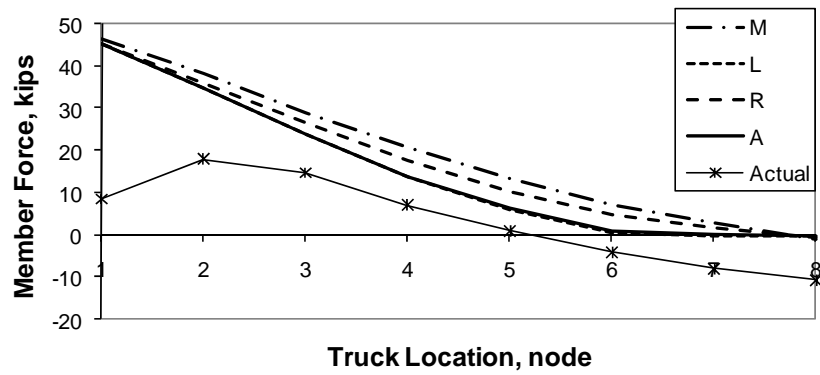
U0-L1 Far, Center

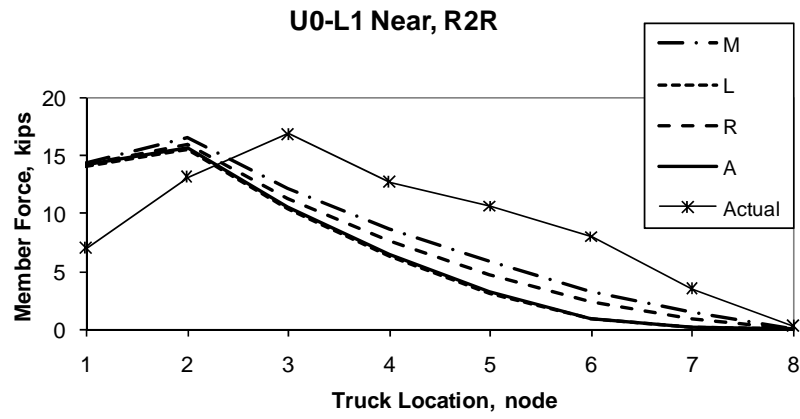
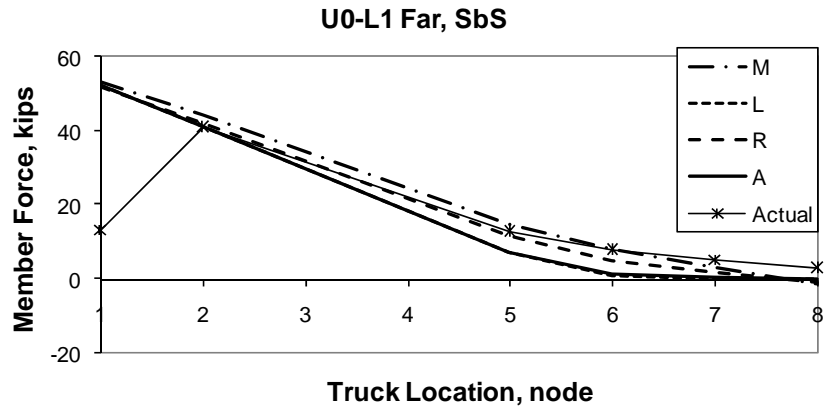
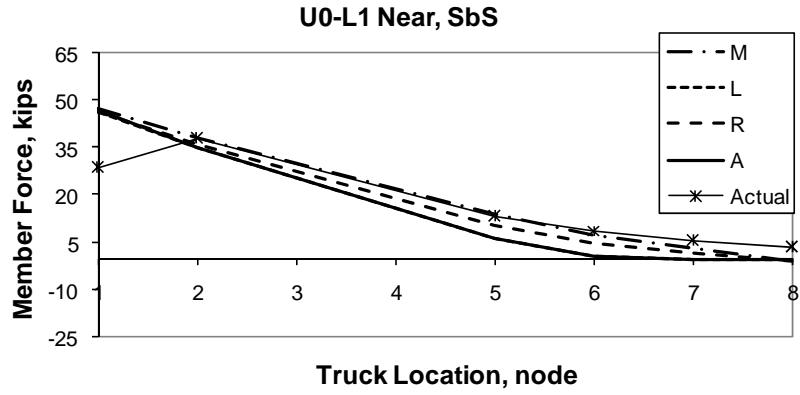


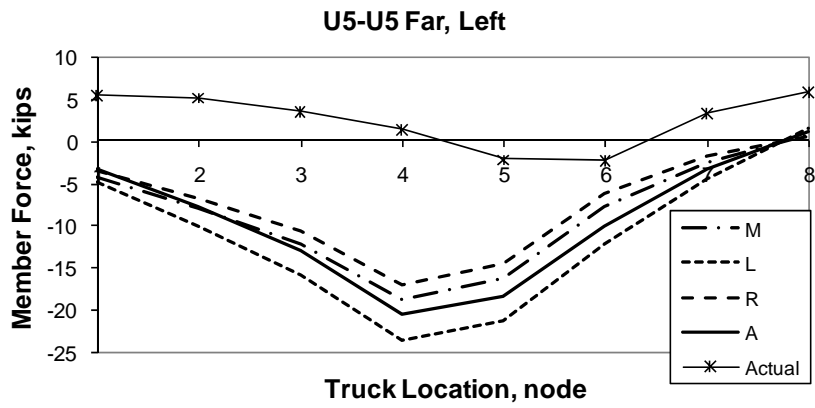
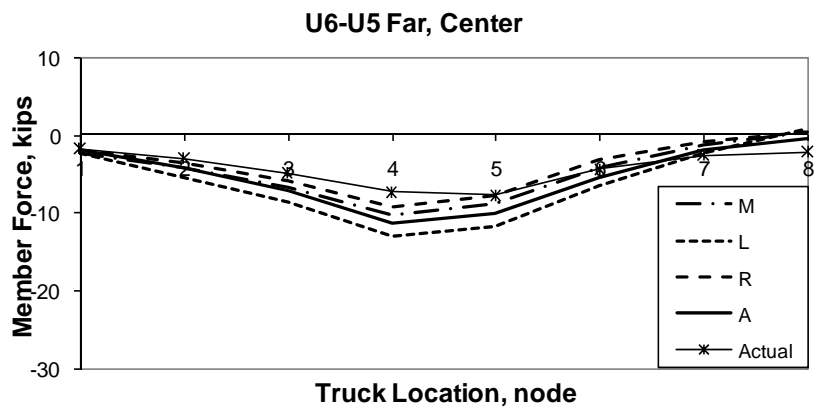
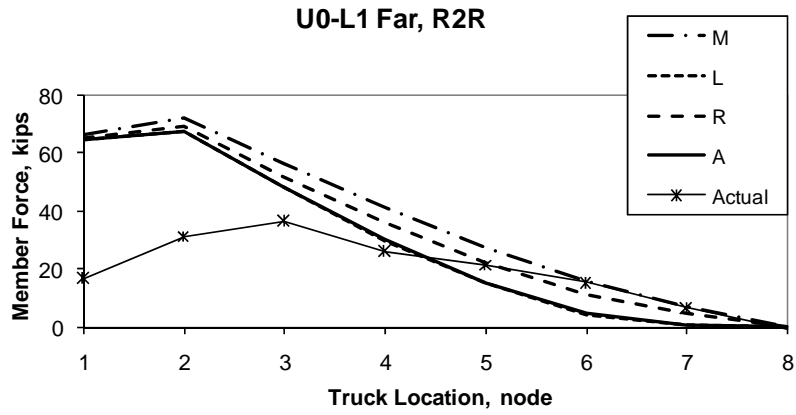
U0-L1 Near, Left



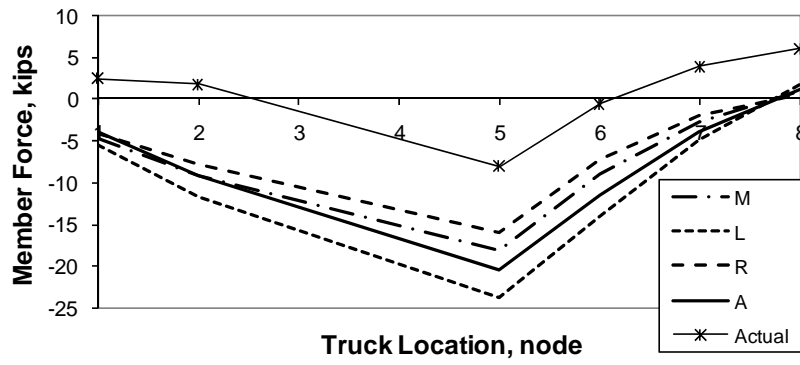
U0-L1 Far, Left



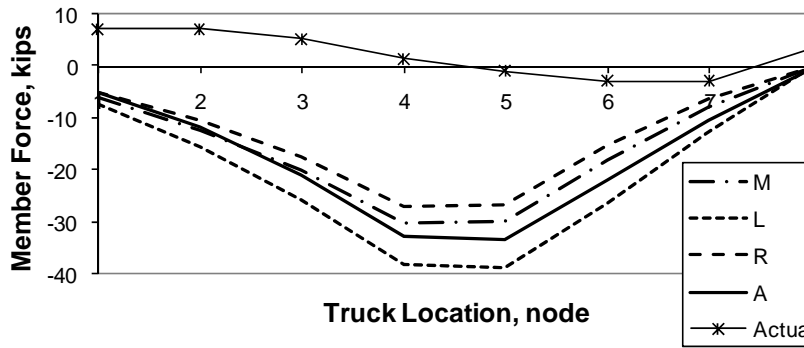




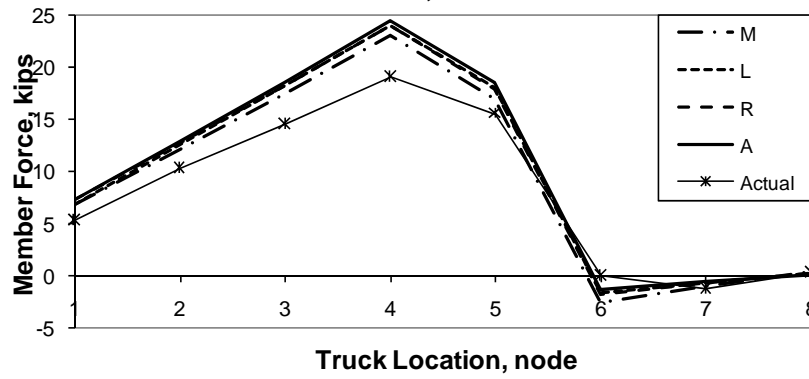
U6-U5 Far, SbS

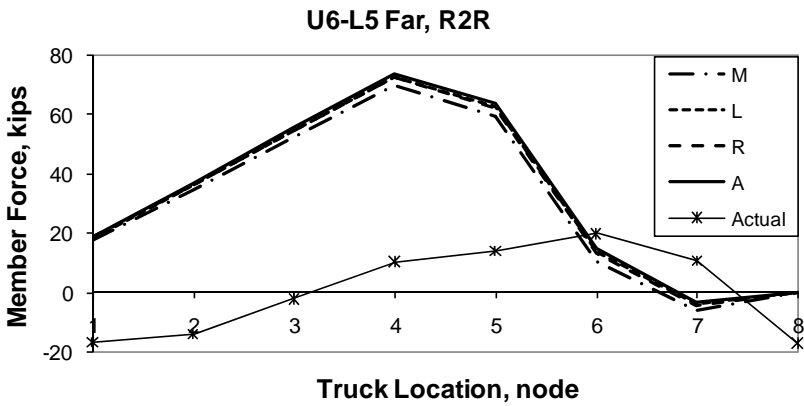
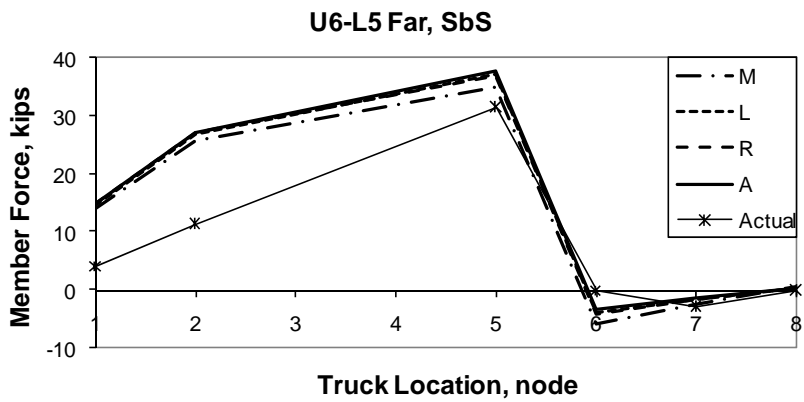
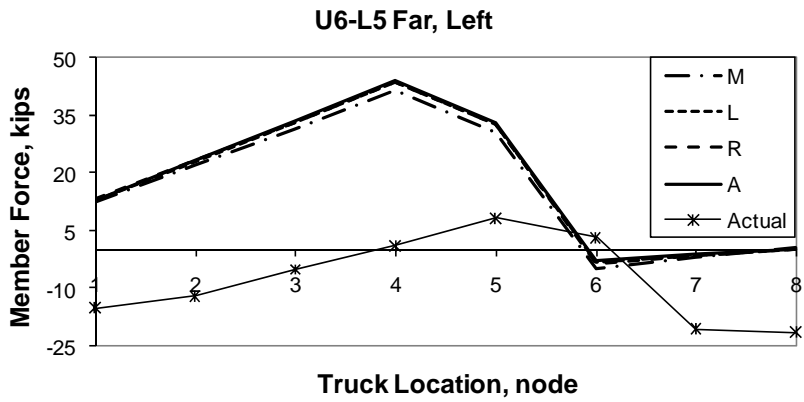


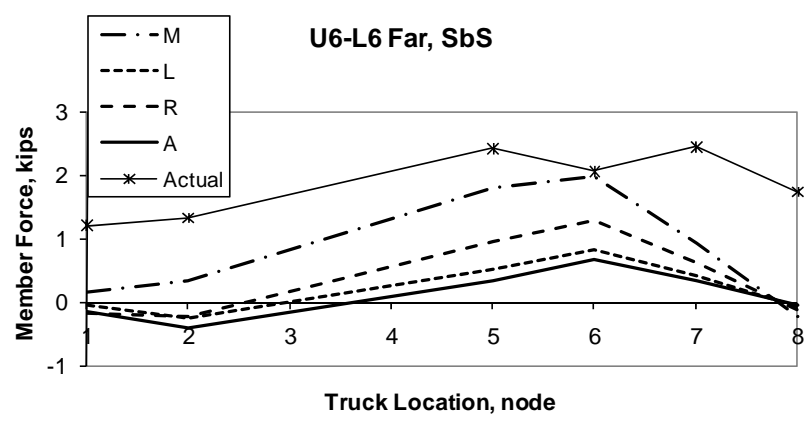
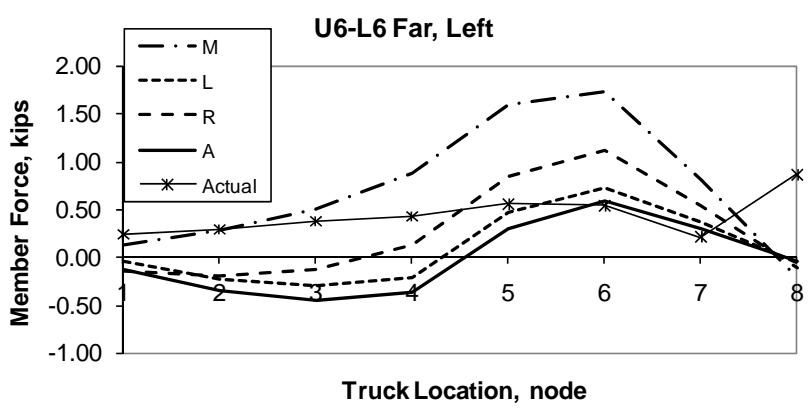
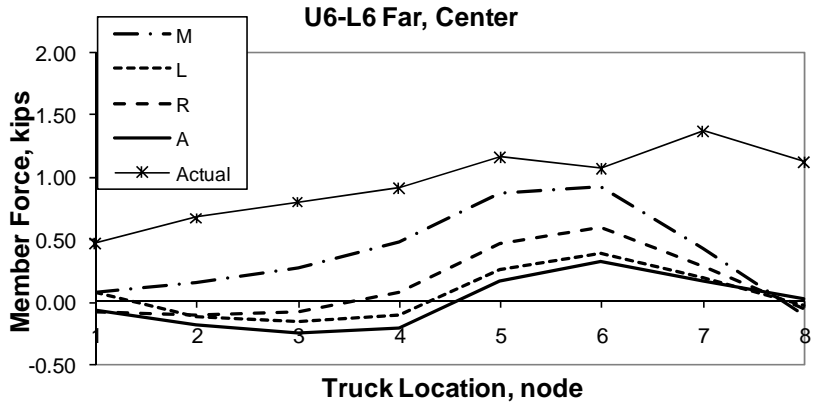
U6-U5 Far, R2R

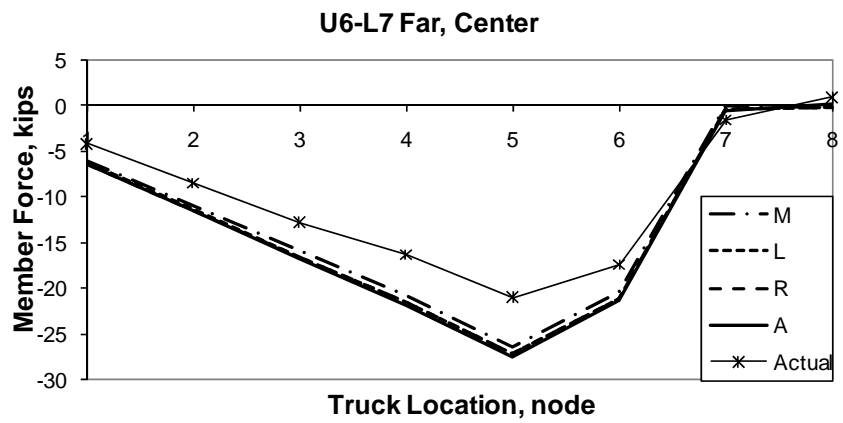
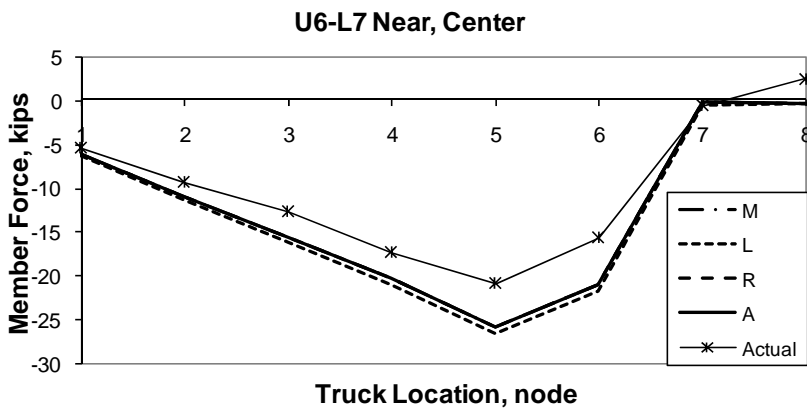
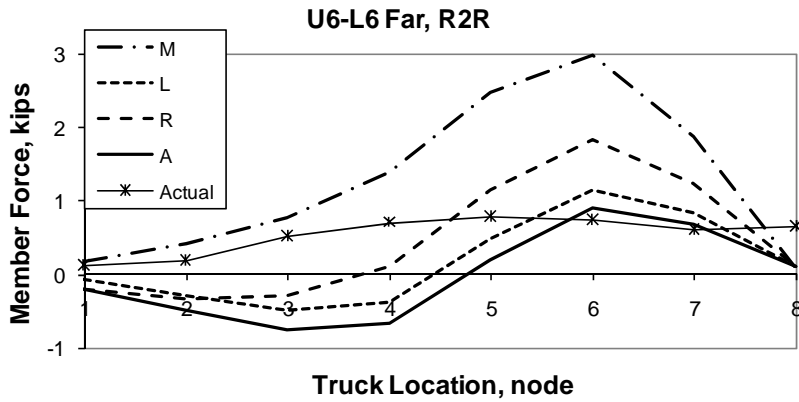


U6-L5 Far, Center

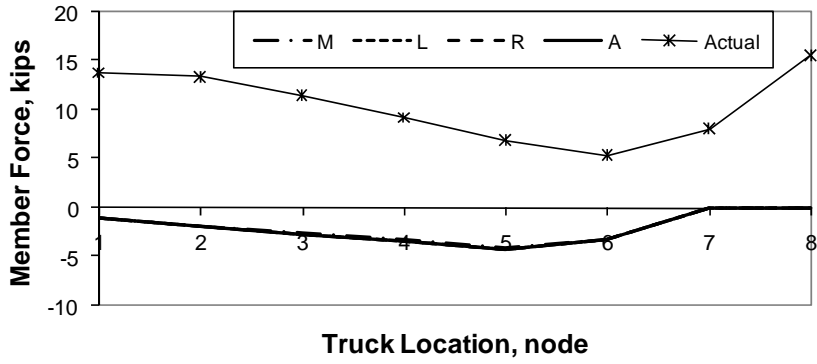




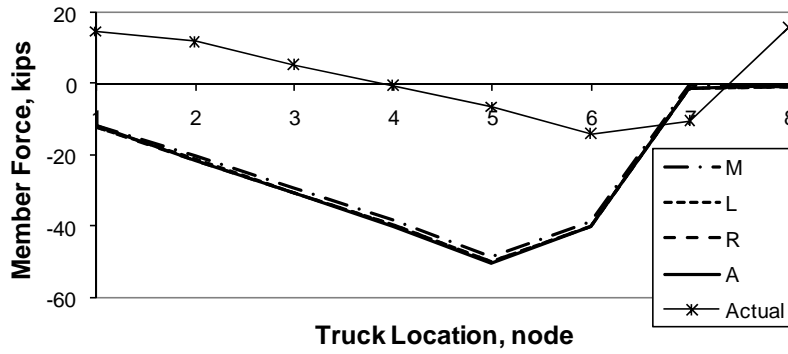




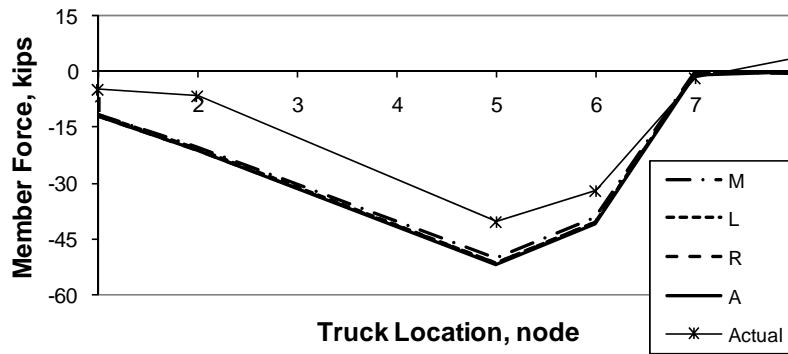
U6-L7 Near, Left



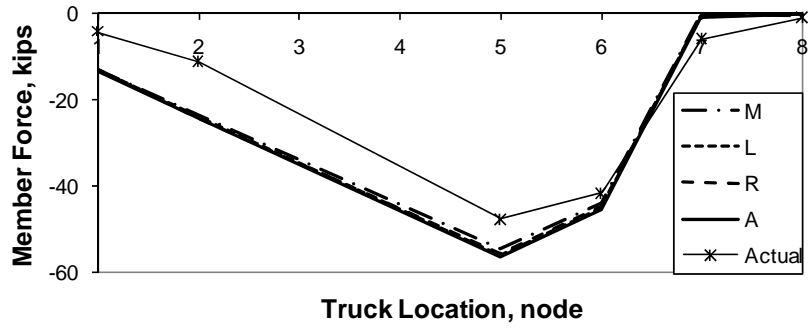
U6-L7 Far, Left



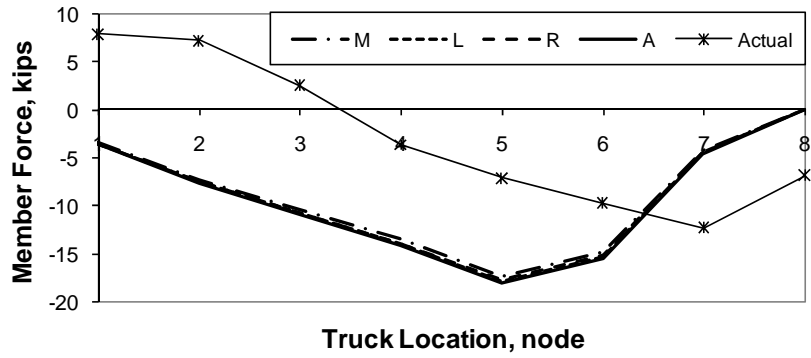
U6-L7 Near, SbS



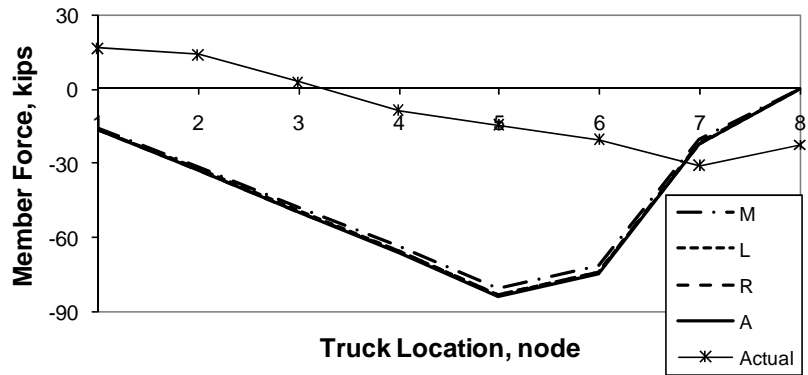
U6-L7 Far, SbS

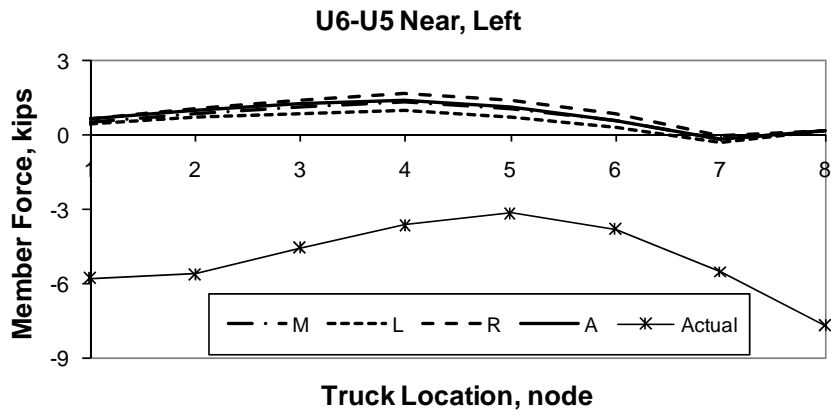
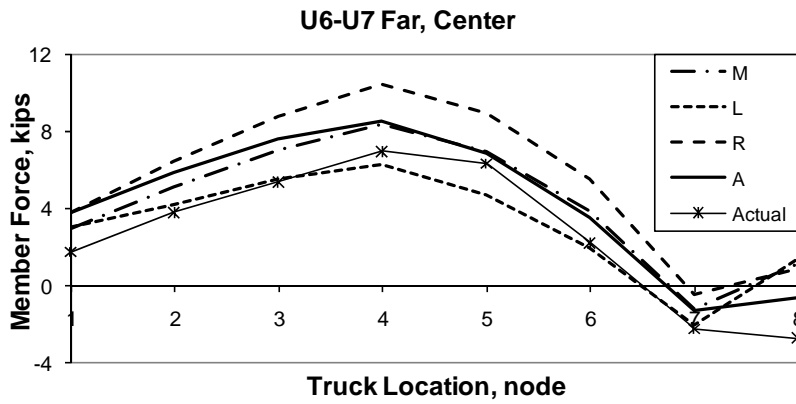
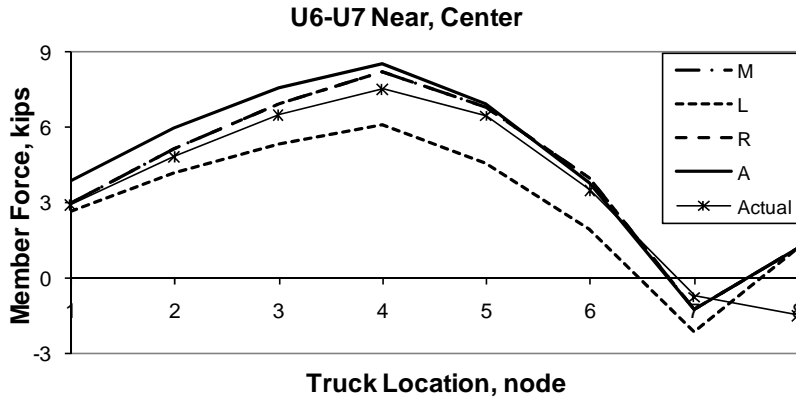


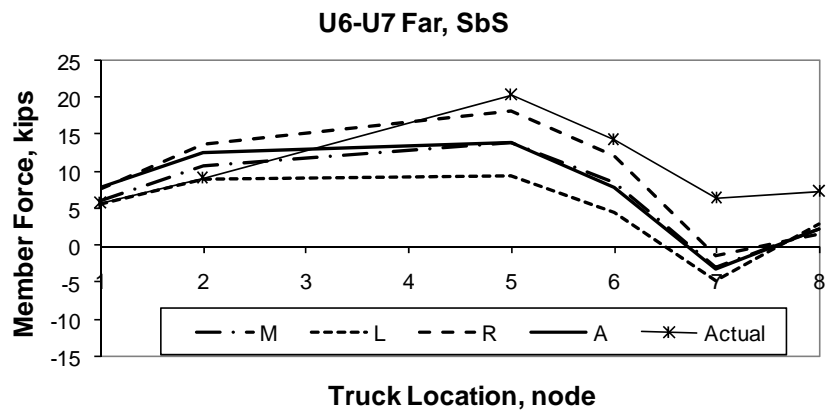
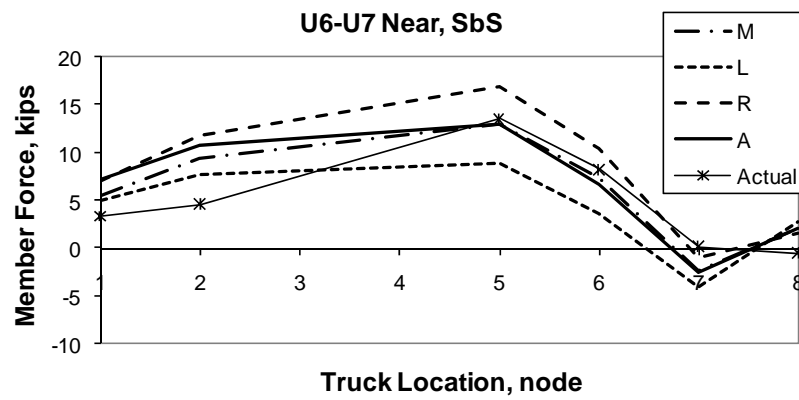
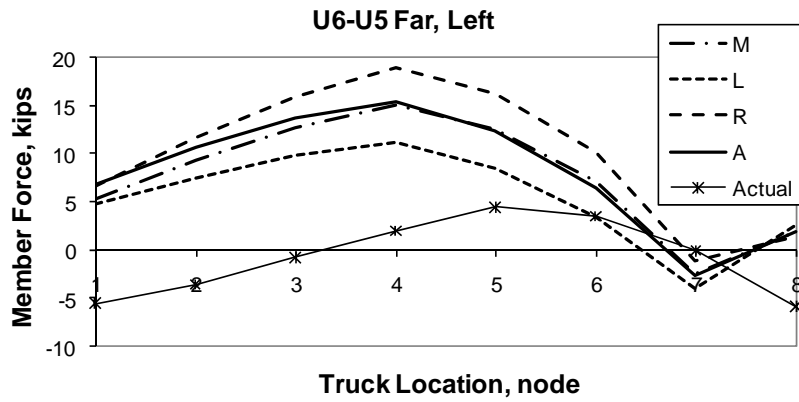
U6-L7 Near, R2R



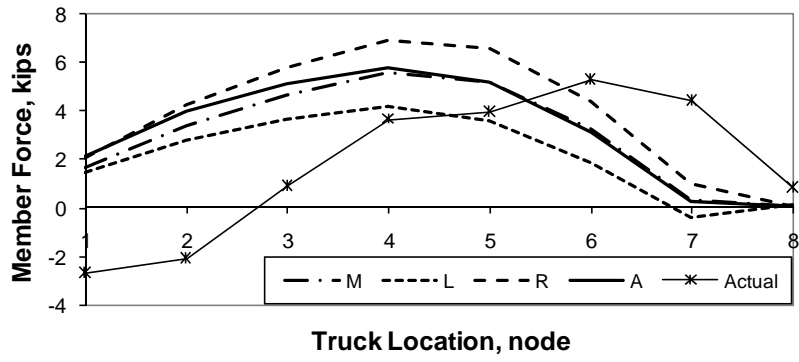
U6-L7 Far, R2R



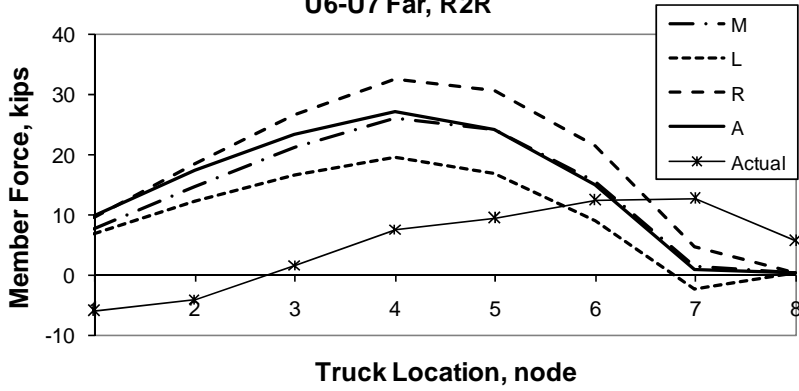




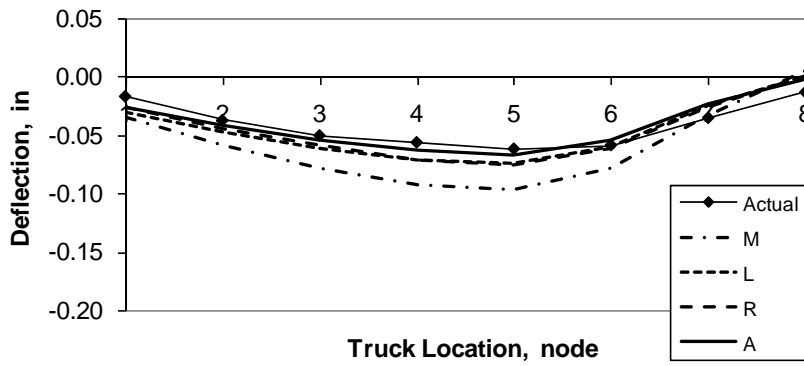
U6-U7 Near, R2R

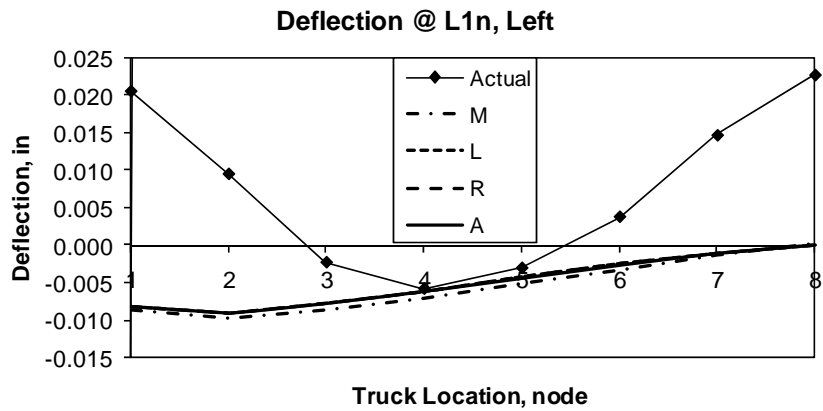
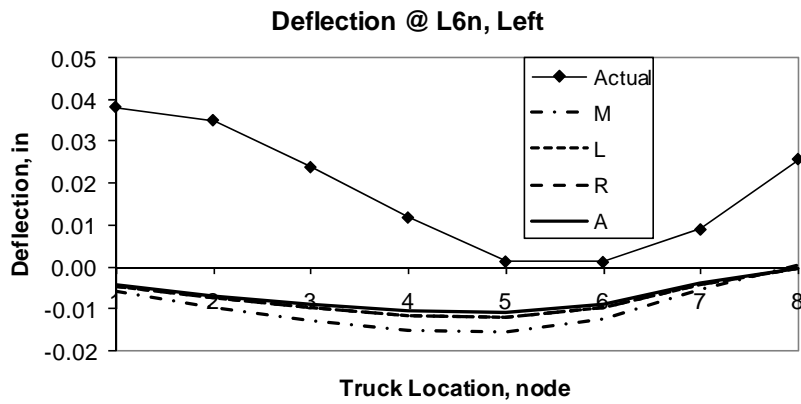
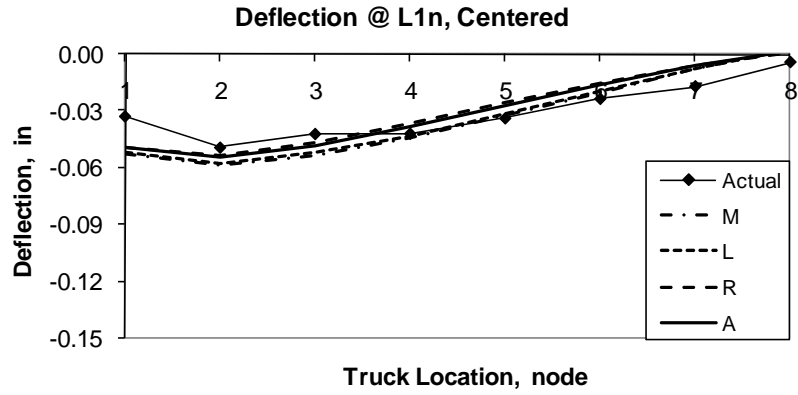


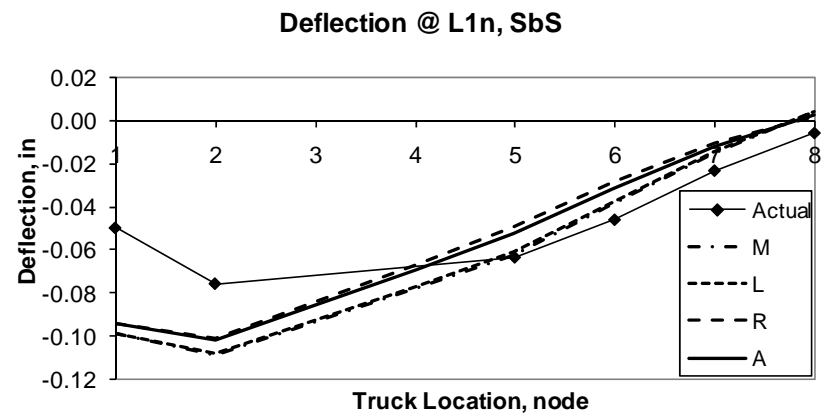
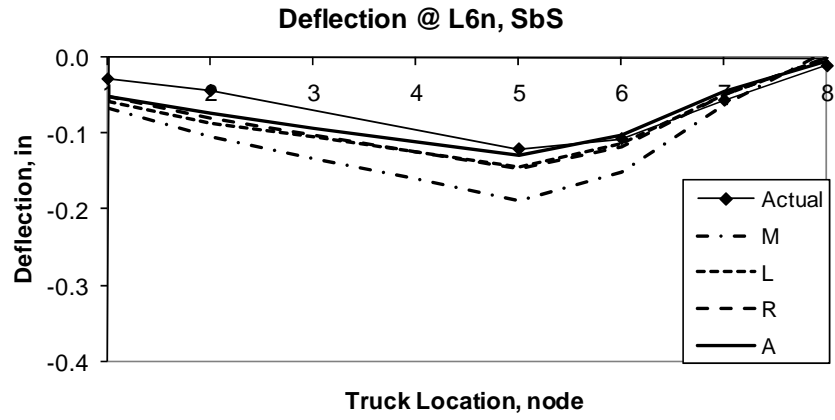
U6-U7 Far, R2R



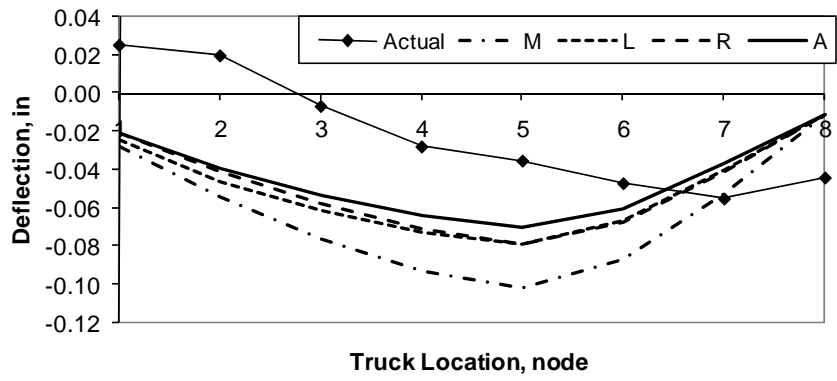
Deflection @ L6n, Centered







Deflection @ L6n, R2R



Deflection @ L1n, R2R

